Identification, purification and characterisation of bacterial amyloids

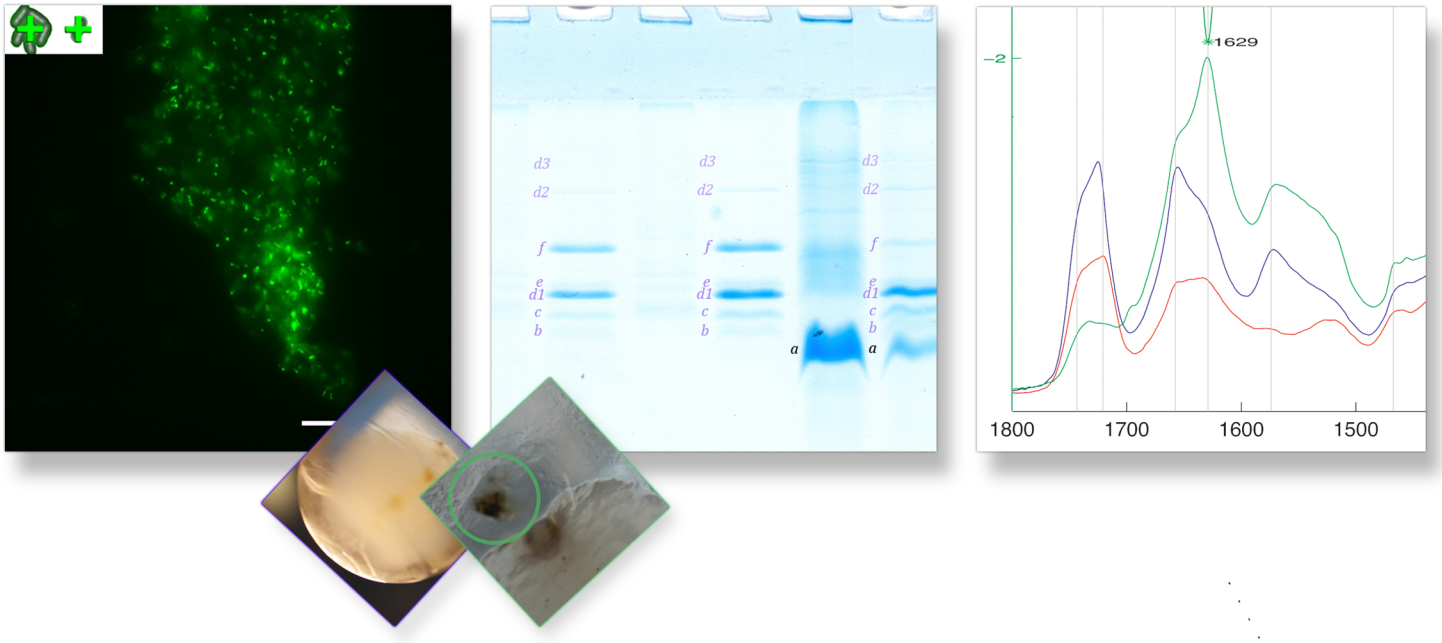

Master Thesis
2010

Rico Nielsen

Department of Biotechnology, Chemistry and Environmental Enginnering
AALBORG UNIVERSITY

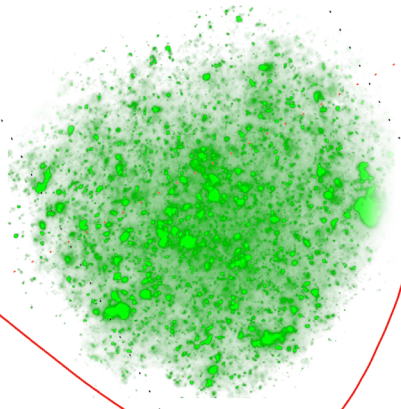

Table of Contents

Preface

This report documents the work performed by Rico Nielsen during the Master's in Science and Engineering project covering the 9-10th semester. The work was done within the period September 1st, 2010 to Oktober 1st, 2010, at the Section of Biotechnology in the Department of Biotechnology, Chemistry and Environmental Engineering, Aalborg University.

The supervisor of the project had been Professor Per Halkjær Nielsen.

Co-supervisors was Postdoc Morten Simonsen Dueholm and Associate Professor Allan Stensballe.

I would like to thank Per Halkjær Nielsen for his patient guidance and understanding and Morten Dueholm for his guidance in the lab. Thanks should also be given to the members of the Network for Functional Bacterial Amyloid for their contributions. I would also like to thank laboratory technicians Susanne Bielidt, Marianne Ahrenfeldt Stevenson and Jane Ildal for for being cheerful and helpful with lab-stuff ;-) Also I would like to thank Søren B. Nielsen for assistance with performing fourier transform infrared spectroscopy at Århus University.

Finally I would like to thank all members of the enviromental biotechnology group for making my stay enjoyable, including Marta Nierychło, Ihab Bishara Lolas and Sarita Singh.

Aalborg University
Department of Biotechnology, Chemistry and Environmental Engineering
Sohngaardsholmsvej 49, 9000 Aalborg, Denmark

Project title:	Identification, purification and characterisation of bacterial amyloids
Alternative title:	Identification, purification and characterisation of extracellular bacterial proteins such as amyloids
Student:	Rico Nielsen
Supervisor:	Professor Per H. Nielsen, Ph.D.
Co-supervisors:	Post doc Morten S. Dueholm, Ph.D & Associate Professor Allan Stensballe, Ph.D
Semester period:	9th-10th semester
Completet:	October 1th *
Copies printet:	6
Number of pages	69

‘

Abbreviations

AB	Antibody
ALF	Amyloid-like fimbriae
ATR-FTIR	Attenuated total reflectance- Fourier transform infrared spectroscopy
FA	Formic acid
FTIR	Fourier transform infrared spectroscopy
FuBA	Functional bacterial amyloid
P_FuBA	'Purified functional bacterial amyloid' or 'potential functional bacterial amyloid'. Refers – in each case - to the *purified material* than is the outcome of attempts to purify FuBA within this project.
SE	*Staphylococcus epidermidis*
ThT	Thioflavin T

Abstract

The aim of these studies is to screen for expression of functional bacterial amyloids (FuBA) among environmental isolates, and detect purified FuBA. The motivation for this aim is the overall realisation that FuBA have great and widespread impact on human endeavours and human health, in beneficial as well as bad ways. The characterisation of new FuBA and the way the affect bacterial life contribute to the understanding and tailoring of FuBA and the bacteria expressing them. Within this project bacterial biofilms are found to express FuBA based on the binding of a conformationally specific antibody that targets the amyloid motif. In a handful of cases there is evidence that FuBA has been purified, but contaminations hamper the validations. It is clear that for further studies the purification protocol must be optimised to allow successful screening among a broader range of bacteria, although is it almost certainly impossible to find one universal method to purify FuBA. Within the project initial experiments offering proof of concept for a novel method to detect surface exposed functional bacterial amyloids using ATR-FTIR on hole bacteria is presented shortly. The final conclusion is that the quest to purify and understand FuBA remains – and it remains as an intriguing challenge!

Synopsis

Formålet med dette projekt er at søge og bestemme for ekspression af funktionelle bakterielle amyloider blandt bakterielle isolater fra miljøet, og dernæst at detektere oprenset amyloider. Motivationen for dette mål er en overordnet forståelse af at bakterielle amyloider har stor og bredtfavnende indvirkning på vores gøremål og menneskers helbred, på godt og ondt. Karakterisering af nye bakterielle amyloider og måden hvorpå de påvirker bakterielt liv, vil bidrage til forståelsen og tæmningen af bakterielle amyloider, samt bakterierne som udtrykker dem. Inden for rammerne af dette projekt, er det påvist for bakterielle biofilm, at de udtrykker bakterielle amyloider baseret på bindingen af et antistof til det amyloide struktur. I en håndfuld af tilfældende er der indikation på at FuBA blev oprenset, alt imens kontaminanter dog gør billede noget uskarpt. Det er klart at med hensyn til fremtidige studier må oprensnings-protokollen optimeres, med henblik på at muliggøre succesfuld oprensning blandt en bredere vifte af isolater, selv om det også er forståelsen, at der ikke findes en universel oprensnings-metode som virker for alle bakterier. Inden for rammerne at projektet har indledende forsøg vist lovende udsigter for en ny måde at detektere overflade eksponeret bakterielle amyloider baseret på fourer transform infrarød spektroskopi med hele bakterie-celle, og de resultater er gengivet her. Den endelige konklusion er, at udfordringen med at oprense og forstå naturen af amyloider består – og den består som en spændende udfordring!

Introduction

Amyloid fibril – an ordered fibrillar protein aggregate with a defining cross β–structure was for long recognised as Pandora's box of being alive – the trousseau that only brought, and only could bring, ailment to man, including 20 or so neurodegenerative diseases. But, along with the discovery that mature amyloid fibrils in diseases, actually may be a save heaven from the real threats, namely the (intermediate) oligomer forms, and the recognition that all polypeptide chains may form amyloids (but with different propensity) arose another paradigm shift from looking outside man: Amyloids are not only formed as misfolded entities in a unregulated manner *in vivo* in man, but is found widespread in Natures biological setups, where they are formed to serve a purpose. Thus, after a lag phase in the understanding of the true nature of amyloids for over a century, functional amyloids are now found in humans, invertebrates, insects, fungi and, not least, bacteria where they play important and diverse roles (D. Otzen & P. Nielsen 2008)(Hammer et al. 2008).

Different bacteria utilise amyloids – or FuBA for functional bacterial amyloids – for different purposes. Since the late 1980's FuBA with different roles have been found and characterised. This includes the production of amyloid-like fimbriae (ALF) by enteric gram negative *E. coli* that express ALF called curli, strains of *salmonella* that express ALF known as tafi, a *Pseudomonas* strain of the *P. fluorescens* group (MS Dueholm et al. 2010), and the gram negative *Bacillus subtilis* (Romero et al. 2010). Other kinds of FuBA include chaplins from the gram positive *Streptomyces coelicolor* that are involved in production of aerial hyphae and dispersal of spores (Claessen et al. 2003), pili with adhesive properties from *Mycobacterum tuberculosis (Alteri et al. 2007)*, harpins from *Xanthomonas axonopodis* that induce cell death in plants, and Microcin 492 from *Klebsiella pneumoniae* that is cytotoxic towards certain bacteria (D. Otzen & P. Nielsen 2008).

Amyloid fibrils are pliable, but with a yield strength comparable to steel, and have excellent protease and detergent resistant. Thus its may not be surprising that amyloids are harnessed by various organisms, including bacteria. The taming and harnessing of amyloids occur through regulation. The way that *E. coli* protects itself from the cytotoxic intermediates forms of amyloids (protofibrils and/or oligomers) are through a two-component formation system with spatial (and temporal) regulation. In vivo the major curli subunit, the protein CsgA is secreted out of the cell, and only starts to form curli fibrils if exposed to the homologues protein CsgB, the minor curli subunit. Attached to the surface it may form a nucleating structure that can be elongated to form curli fibres. Six proteins encoded by two operons are involved in expression, transport and assembly of curli. Expression of the components is regulated by several environmental conditions in a complex manner, including temperature, salt and nutrient availability. When formed curli are 4 nm to 12 nm wide and 0.1 to 10 μm long (Matthew R. Chapman et al. 2002)(Hammer et al. 2007). It is expected that many other mechanisms are used by bacteria to tame and tailor FuBA (D. Otzen & P. Nielsen 2008).

FuBA are best known from their structural role in bacterial biofilms, where bacteria live in sessile communities enclosed by self-produced extracellular polymer substances (EPS). Multiple constituents contribute to biofilm development and maintenance, and their relative abundance in a biofilm varies depending on environmental conditions. The major components of EPS are generally polysaccharides and protein in addition to lipids and eDNA (Austin et al. 1998)(P Larsen et al. 2008)(A. Jain et al. 2007). Although there is no evidence that FuBA is a prerequisite for biofilm formation, they are suggested to affect the properties of biofilms, when present (Jordal et al. 2009). FuBA have shown to attain architectural

complexity in biofilms. Surface exposed FuBA, as the ALF types, facilitate surface adhesion, colony formation, and maintain colony-architecture trough cell-cell interactions and increased hydrophobicity, while extracellular FUBA in the EPS play a similar role (Romero et al. 2010). Apart from these amyloid adhesins FuBA that only occur in the cellular capsule have also been indicated (Jordal et al. 2009). And FuBA is indeed not a commodity in bacterial biofilms, but found to be widespread among bacterial phyla from different habitats and abundant. For example 5-40% of all prokaryotes within biofilms from habitats as activated sludge treatment plant, drinking water reservoir and seawater produced surface exposed FuBA (Poul Larsen et al. 2007).

The finding of FuBA as important functional components of biofilms and the realisation that the great majority of bacteria in different habitats grow in biofilms (Poul Larsen et al. 2007), have enormous implications. In technical systems, biofilm may cause biofouling, biodeterioration and biocorrosion (H. Gibson et al. 1999)(Kjellerup et al. 2005), but they are also useful in several biotechnology processes and serve a purpose in water and wastewater treatment (the latter recognised as one of the biggest environmental problems facing our world today) (Lens et al. 2003)(Poul Larsen et al. 2007). In the medical field, bacteria in biofilm may colonize mucosal surfaces as well as invasive devices and implants, causing serious infections that show diminished sensitivity to antibiotics, host defences and external stresses (J. Costerton et al. 2005)(Ryu & Beuchat 2005)(Silverstein et al. 2006). In addition FuBA (curli) have been shown to play a role in pathogenesis, as they mediate bacterial attachment and internalization of host cells (Gophna et al. 2001), and their are various studies that indicate that FuBA might act as a seed for formation of amyloids in humans, and thereby contribute to the propagation of neurodegenerative disorders, directly (cross-seeding) and indirectly (D. Otzen & P. Nielsen 2008). Given the widespread abundance of FuBA, and the effect these are believed to impose on human endeavour and health, good as bad, there is enormous stipulation to understand the formation and actions of FuBA.

Central to the effort to understand and tailor the formation and actions of FuBA is an ability to identify, purify and analyse FuBA from different bacteria. As expected, these efforts take advantage of the unique properties central to all amyloids. Amyloid can be defined as orderly repeats of protein molecules arranged in a fibre with a cross β structure, in which the β-strands runs perpendicular to the fibre axis. This distinct structure constitutes the core two the excellent stability of amyloids and its tinctorial properties. To identify FuBA producing bacteria or purified FuBA two dyes, Congo red and Thioflavin T (ThT), have been used in combination with different analytical methods, in particular. The drawbacks of these dyes are their specificity, as they have been found to bind to other organic molecules (polymers), including cellulose, DNA, and, for Congo red, certain non-amyloid proteins in addition. Conformation specific antibodies are considered to be more reliable in the detection of amyloids. The antibodies WO1 and WO2 have been raised against amyloids of Alzheimer's disease (Aβ), and binds to a generic amyloid epitobe present in all amyloids, without binding to the constituent monomers. According to (D. Otzen & P. Nielsen 2008) the real proof for the presence of FuBA is purification in hot/boiling SDS, with a verification of the cross β-structure using Fourier-transform infrared spectroscopy, circular dichroism, and X-ray fibre diffraction in combination, and also ThT fluorescence (of purified FuBA and refolding fibrils). Furthermore to indicate the presence of FuBA (and obtain the monomer) treatment with strong acid such as 90-100% formic acid have been observed to release FuBA monomers that can be detected in SDS-PAGE (and sequenced by MS/MS). Finally transmission electron microscopy images of bacteria with FuBA and of purified FuBA can help to verify the agreement between the fibrils, and establish their coincident biological significance (in particular in the case of extracellular FuBA). To

discovery and investigate FuBA as described requires pure cultures, vigorous expression of amyloids and an efficient purification protocol.

FuBA have only been described in detail for a relatively few bacterial strains in terms of structural and functional properties, including their regulation of expression (four cases of ALF have been characterised in detail, as mentioned). Identification and characterisation of FuBA from other bacteria will aid in the understanding of FuBA and the many roles they play.

The aim of this study is to screen for FuBA production among environmental isolates, and detect purified FuBA.

To identify putative producing strains environmental isolates will be grown on Congo red identification plates and subject to a immunofluorescence assay with a conformational specific antibody that targets the amyloid fold. To investigate if FuBA is purified formic acid will be used to releases FuBA monomers for detection by SDS-PAGE, and ATR-FTIR will be used to indicate the presence of the amyloid motif.

Materials & Methods

Organisms and Growth Conditions

Strains used in this study are listed in Table 1. Positive control for FuBA production *E. coli* MG1655 mutant SM2258 producing curli and negative control *E. coli* MG1655 mutant SM2257 unable to produce curli were grown in colonization factor antigen (CFA) medium at 200 rpm or on CFA agar plates at 37°C. 44% (V/V) glycerol stocks of SM2257 and SM2258 were prepared from bacteria incubated with 35mg/ml kanamycin and 10mg/ml tetracycline, respectively. CFA medium was made of 1% casamino acids, 0.15% yeast extract, 0.005% $MgSO_4$, 0.0005% $MnCl_2$ (Evans et al 1977). pH was adjusted to pH 7.4 with NaOH. *S. epidermidis* were grown in tryptic soy broth (TSB) medium without shaking or on TSB agar plates at 37°C. TSB medium was made of 3% (W/V) tryptic soy broth (Oxoid) and 0.3% (W/V) yeast extract (MP Biomedicals) with pH adjusted to pH 7.1 with HCL. All agar plates were solidified with 2% agar.

To obtain putative FubA producing bacteria strains were isolated as pure cultures from environmental samples by growth on Congo red indicator plates at 26°C. The origins of the environmental samples are listed in Table 1. More elaborately, environmental samples were collected in 10ml greiner tubes. Next dry samples were resuspended in filtered tap-water and homogenised with a sterile tissue grinder. An eight-step 1:10 serial dilution was carried out for all samples. Samples were inoculated on Congo red indicator plates, spread by sterile glass beads and incubated at 26°C for 42 hours sealed in parafilm. Congo red indicator plates were made of CFA agar supplemented with 20µg/mL of Congo red (Sigma) and 10µg/mL Coomassie brilliant blue G-250 (AppliChem) (M Hammar et al. 1995). Single colonies of various colours and morphology were wetted in sterile filtered tap-water using a sterile inoculation loop, and then the isolates were inoculated on CFA agar plates at 26°C for 56 hours. Next single colonies were inoculated in 10 ml CFA in greiner tubes and incubated at 26°C and 200 rpm for 20 hours. 44% glycerole stocks are prepared, left at room temperature for 30 minutes and stored at ÷80°C. The isolates, along with UK1-UK11 were grown in colonization factor antigen (CFA) medium at 200 rpm or on CFA agar plates at 26°C from glycerol stock crystals.

Antibody Assay

Immunofluorescence labelling of FuBA were performed using protocols with 1% (W/V) BSA as blocking agent or 1% (V/V) gelatine, according to X. BSA and AB suspension were prepared within 1 hour of use. All buffer solutions were sterile filtered after preparation.

Antibody Assay A: Bacterial samples were homogenised and diluted to OD_{600} of 1 in PBS. Next bacteria were pelleted (10,000 rpm, 5 min.), resuspended in 1% (W/V) BSA in PBS and incubated at 37°C and 200 rpm for 1 hour. Tween 20 were added to 0.05% (V/V), and subsequently diluted WO2 primary AB was added to 10nM. Samples were mixed thoroughly by vortexing and incubated at 37°C and 200 rpm for 2 hours. Controls of secondary AB were without addition of WO2. Samples were pelleted (10,000 rpm, 5 min.), and the pellet were washed twice in 1% (W/V) BSA in PBS with 0.1% (V/V) Triton X-100. Next pelleted sample (10,000 rpm, 5 min.) was added secondary AB (F9259 FITC fluorophor-labeled µ-chain specific, Sigma-Aldrich) using 50.5 µl of a 1:256 working dilution of AB in PBS with 1% (W/V) BSA and 0.025% (V/V) Tween 20. Samples were mixed thoroughly by vortexing and incubated at 37°C and 200 rpm for 1 hour. Pelleted sample were then washed three times in 0.1% (V/V) Triton X-100, and the washed pellet was resuspended in PBS (50 µl).

Antibody Assay B: Bacteria was PFA fixated prior to antibody labelling of FuBA using Assay B. Initially bacteria from 2 ml culture was pelleted and washed in 1 ml ice cold PBS (16,162×g, 5 min.). Washed pellet was resuspended in 1 ml ice cold 4% paraformaldehyde (PFA) in PBS, and fixation occurred at 4°C for 3 hours. Fixated sample was pelleted (16,162×g, 5 min.) and PFA waste discarded. Next pelleted sample was washed twice in sterile filtered tap-water (filter pore size was 0.2 µm). Washed pellet was resuspended in 500 µl ice cold PBS, added an equal volume of ice cold EtOH and then mixed briefly by gentle vortexing.

Table 1: List of strains used.

strain	short name	origin of isolate	relevant genotype	source or reference
Escherichia coli K-12 SM2257	SM2257		MG1655 csgA::uidA-kan malT54::Tn10	(C Prigent-Combaret et al. 2001)
SM2258	SM2258		MG1655 ompR234 malT54::Tn10	(O Vidal et al. 1998)
Streptococcus epidermidis SMH100	SE			(Schaudinn et al. 2007)
Chloflexi EU25	CHL	slude sample		(Kragelund et al. 2007)
Aeromonas spp.	UK1 / UK1r			Dueholm et al. (unpublished)
Aeromonas spp.	UK2			Dueholm et al. (unpublished)
Paenibacillus spp.	UK3			Dueholm et al. (unpublished)
Pseudomonas spp.	UK4			(MS Dueholm et al. 2010)
	UK5-UK11			Dueholm et al. (unpublished)
	SL[c]	sludge sample [a]		This study
	PH[c]	sink plug hole [b]		This study
	TC[c]	toilet cistern tank (stirred up) [b]		This study
	HR[c]	plastic shower head, ring (rubber) [b]		This study
	HA[c]	shower head fusion to hose (metal) [b]		This study
	HE[c]	shower head entrance (plastic) [b]		This study
	WA[c]	wall in shower enclosure [b]		This study

[a] LimoTee KA Oedinhause 21.10.2008 BB.

[b] within the bathroom of apartment 83, Borgmester Jørgensensvej 5, 9000 Aalborg, Denmark.

[c] the prefixes of these isolates short name reflect their origin, and is followed by a suffix, an integer, for each specific isolate.

To perform WO1 staining of FubA 200µl of fixated sample was pelleted (16,162×g, 5 min.) and washed in 1 ml PBS. Unspecific AB binding sites were blocked by incubating pelleted samples (16,162×g, 5 min.) with 1% (W/V) gelatin in PBS at 37°C for 1 hour. After blocking each sample was split in two to use one sample as control of the secondary antibody. Then samples were pelleted and added a WO2 primary AB solution of 1 nM WO2 primary AB in PBS with 0.98% (W/V) gelatin and 0.05% (V/V) Tween 20 or a secondary AB control solution of 98% (W/V) gelatin and 0.05% Tween 20 in 98% (V/V) PBS. Samples were thoroughly mixed by vortexing and WO2 primary antibody was allowed to bind at 37°C for 2 hours. After WO2 binding samples were pelleted (16,162×g, 5 min) and washed threefold with 1% gelatin in PBS with 0.1% Triton X-100 to remove unbound WO2. Washed pellet was added secondary AB (F9259 FITC fluorophor-labeled µ-chain specific, Sigma-Aldrich) using 100µl of a 1:256 working dilution of AB in PBS with 0.99% (W/V) gelatin and 0.025% (V/V) Tween 20. Samples were thoroughly mixed by vortexing and incubated at 37°C for 1 hour. After binding of secondary AB samples were pelleted (16,162×g, 5 min) and washed in 0.1% Triton X-100 in PBS. Washed samples were resuspended in PBS (100µl).

Analysis of AB-labeled samples was done within two days of staining using epi-fluorescence on an Axio Imager.A1 microscope equipped with a Photometrics Coolsnap™ Cf intensity camera with FITC filter settings (excitation at 490 nm and emission at 494-520 nm). AB labeled sample were spotted on a glass slide and subsequently covered by cover glass before sample drying. Exposure time was kept constant at 50 ms, and images were obtained within 1 second of exposure to limit photobleaching of the fluorephor.

FuBA purification

FuBA were isolated using two similar versions of a protocol designed by Dueholm et al. (unpublished). The protocols were a modification of the one developed for isolation of FuBA from UK4 (Morten S. Dueholm et al. 2010), which was originally based on a protocol by (COLLINSON et al. 1991) for FuBA isolation from *Salmonella enteritidis*. The one utilised protocol was a version that required smaller sample volumes and was used for screening for FuBA production. Bacteria were grown on one agar plate or in liquid media. Next bacteria were harvested by centrifugation (24.000 g, 20°C, 30 min) and suspended in 15 ml (*/900 µl*) of 10mM Tris-Hcl, pH 8.0 (tris buffer). Cell suspension were homogenised using a tissue grinder or vortexed until no clumps remained. Freshly prepared enzyme mix were added to 0.1mg/ml RNase, 0.1mg/ml DNase I, (*0.1mg/ml alginate lyase),* 1mg/ml lysozyme, 1mM $MgCl_2$ with 0.1% (V/V) Triton X-100 and samples were incubated at 37°C for 30 minutes. Cells were broken by three freeze-thaw cycles using a dry ice/ethanol bath and a water bath *(/heating block)* at 37°C. Suspensions were incubated at 37°C for 2 hours. After incubation samples were adjusted to 1% SDS and boiled for 20 min *(/5 min)*. Insoluble material was collected by centrifugation (28.000 g *(/20.000)*, 20°C, 30 min), resuspended in 20 ml *(/1.2 ml)* tris buffer, and boling in 1% SDS was repeated. Insoluble material was washed twice in 25 ml (*/1.4 ml*) tris buffer (28.000 g (*/20.000g*), 20°C, 30 min). The purified material was resuspended in tris buffer and subject to formic acid (FA) treatment and SDS-PAGE, as well as ATR-FTIR measurements.

Electoforeces

Sodium dodecyl sulphate-polyacrylamide gel electrophoresis (SDS-PAGE) was performed according to the method of Laemmli (Laemmli 1970). To perform SDS-PAGE with FuBA two samples with purified FuBA was frozen in liquid nitrogen and freeze dried to dryness (12-24 hours). The resulting powder of one sample was resuspended in 98-100% (V/V) formic acid (200 µl) by pipetting, frozen once again in liquid nitrogene and freeze dryed to dryness. Samples were mixed with 1×SDS-PAGE loading buffer and 15µl were loaded onto a 15% (W/V) acrylamide gel with a 5% (W/V) stacking gel. Stacking of protein bands were carried out at a constant

voltage of 70 for 20 minutes followed by protein separation at 130V. Proteins were visualised by staining with a solution of 0.25% (W/V) Comassie brilliant blue R-250 (Sigma) in 45% (V/V) ethanol and 10% (V/V) acetic acid. Destaining was carried out with a solution of 45% (V/V) ethanol and 10% (V/V) acetic acid.

Fourier Transform Infrared Spectroscopy

FTIR was carried out using a Tensor 27 (Bruker) FTIR spectrophometer equipped with a DTGS Mid-infrared detector and a Golden Gate single reflection diamond attenuated total reflectance (ATR) cell (Specac). 2 µl of purified FuBA was dried on the ATR crystal using dry nitrogen. Spectra were recorded from 4000-1000 cm^{-1} using a nominal resolution of 2 cm^{-1} and 64 accumulations. To compensate for atmospheric gases, such as water vapour and carbon dioxide, atmospheric compensation of the spectra was performed in the OPUS 5.5 system (Bruker). To identify absorbance peaks in the interferogram the second derivate was computed in OPUS 5.5 using 17 fitting curves, and local minima were identified using the matlab function peakdet (http://www.billauer.co.il/peakdet.html).

Results & Discussion

Within the global goal to understand and tailor the effects of functional bacterial amyloids – FuBA – on human health and endeavour, the aim of this study was to screen for FuBA production among environmental isolates, and verify the presence of purified FuBA. To verify – or at least indicate - that FuBA was purified two approaches were used, both based on the structural properties of the amyloid fold. SDS-PAGE of formic acid (FA) pre-threaded *purified material* (referred to as *p_FuBA* for purified/potentially FuBA) was used to detect the release of FuBA monomers. And ATR-FTIR was used to detect if structures with the amyloid fold was present in the *p_FuBA*. As part of the isolation of the bacteria, the bacteria were grown on Congo red identification plates that can be used to indicate putative FuBA producing bacteria. Staining of the bacterial isolates with a conformationally specific antibody targeted towards the amyloid epitope was also performed to probe the extent of FuBA expression.

Summary of Results

In total 50 isolates were subject to purification and estimation of FuBA expression (including UK4 that is known to produce amyloids (Morten S. Dueholm et al. 2010), three morphotypes, and excluding curli positive *E. coli* mutant SM2258, curli negative mutant SM2258 and a ethanol fixated *Chloroflexi* that was included in the antibody assay only). 37 of the strains were isolated within this study. In Table 2 many of the findings from the above-mentioned experiments are summarised. Thus for each isolate are listed the evaluation of:

- **Antibody Assay:** Expression level of FuBA
- **SDS-PAGE:** Potential FuBA monomer – Presence and Size in kDa.
- **ATR-FTIR:** Presence of amyloid motif – Peak location of Amide I band
- **+** Image of a colony when grown on Congo red identification plates (only the bacteria isolated within this study)

Taken together these findings indicate for each isolate its ability to express FuBA (at the utilised growth conditions), and whether FuBA might had been purified for that isolate. In overall it was found that the majority of the isolates forms biofilms and also express FuBA, some of them extensity (antibody assay). In about 15 cases putative FuBA monomers are identified, some better candidates than others. FTIR of *p_FuBA* identified about 29 isolates that showed absorption (a peak) in the region associated with amyloid fibrils. If a few candidates should be mentioned where FuBA purification seems to be successful, according to both SDS-PAGE and FTIR, UK1, UK5, TC1 and PH15 could be put forward. It should be stated, however, that although it might be indicated that FuBA are purified in certain cases, the presence of FuBA must be verified by other methods as well. Also the interpretation of the SDS-PAGE and possible the FTIR results is somewhat hampered by protein contaminants. It is clear that for each strain deviations from the ideal situation described in Fig. 1, is the background for the results. In the following the results will be discussed in more detail, in order to draw out more information and in the quest to understand the background for the results.

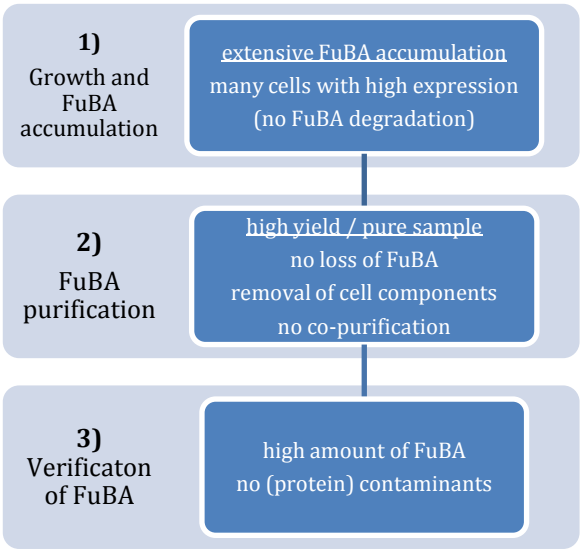

Fig. 1. Purification of FuBA from a bacterial isolate and validation of its presence is a 3 step process, with a few important parameters of success. In practice it might be difficult to meet these criteria, but failure to do so might interfere with the interpretation of the outcome of purification in the validation step of FuBA.

Table 2. Summary of experimental results

	whole cells	purified material/FuBA (*p_FuBA*)					
Strain	**Coloni on Congo red identifiaction plate**	**AB Assay[1]**	**SDS-PAGE of ±FA pre-threated *p_FuBA* [2]**		**FTIR of *p_FuBA* [3]**	**peak in amide I region (cm^{-1})**	
						> 1630	**≤ 1630**
SM2258	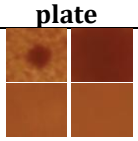			15.3 kDa [D]		1663	1623
SM2257							
SE	-						
UK1	-			*d1:* ~21 kDa [D] f: ~28 kDa *		(1658)	1629
UK1r	-			*d1:* ~21 kDa f: ~ 28 kDa			
UK2	-			~29 kDa			
UK3	-			~22 kDa		1652	1626
UK4	-			25 kDa			
UK5	-						?
UK6	-						
UK7	-						1641
UK8	-						
UK9	-						
UK10	-			~25 kDa [D] ~50 kDa			
UK11	-			~22 kDa ~52 kDa			
CHL	-		-	-	-		-
SL2				~34 kDa *		1651	1627
SL3				~20 kDa *		1652	1623
SL4a						1651	?
SL4b							
SL4c				~13 kDa		1651	1624
SL5				~15 kDa		?	1627
SL6						1653	1623
SL7						1652	1622
SL8							
SL10						1652	1623
SL11							1627
SL12				~33 kDa *		1651	1621
SL13			-	-		1658	1621
PH1a							
PH1b						1652	1623
PH2						1657	

Table 2 *continued*: Summary of experimental results

	whole cells		purified material/FuBA (*p_FuBA*)					
Strain	**Coloni on Congo red identifiaction plate**	**AB Assay[1]**	**SDS-PAGE of ±FA pre-threated *p_FuBA* [2]**		**FTIR of *p_FuBA* [3]**	**peak in amide I region (cm^{-1})**	
						> 1630	**≤ 1630**
PH3							
PH4							
PH7						1657	1626
PH8							
PH9				19 kDa		1653	1625
PH10							
PH11							
PH12						1651	1631
PH13							
PH14							
PH15				~19 kDa *		1656	1628
TC1				~19 kDa		1652	1626
TC2				~19 kDa		1653	1626
TC3						1653	1624
TC4						1652	1626
TC5						1652	1623
TC6						1656	1626
HA1						1656	1627
HE1							
HE2							
HE3							
Summary - presence of FuBA (÷controls and UK4)			~15 candidates identified		~21 candidates identified		

[1] The symbols are explained in detail in Fig. 8.

[2] Fig. 8		no or very little binding of WO1		intermediate binding of WO1
		strong binding of WO1		no microcolonies formed
		FuBA monomer proteins has been purified		
		Potential FuBA monomer proteins have been identified. A contaminant in the non FA pre-threaded sample have roughly the same size		
		Potential FuBA monomer proteins has been identified		

[3] The symbols are explained in Table 4. A symbol with an integer signifies that a Amide I peak was identified in the interval ϒ1611 cm^{-1}:1630 cm^{-1}], charactistic for amyloid fibrils (G Zandomeneghi et al. 2004)..

Antibody Assay: What was seen

To evaluate the extent to which each strain expresses surface exposed FuBA, staining was performed with a conformationally specific antibody that targets the amyloid epitope. *E. coli* mutants with and without FuBA (curli) expression served as controls. Controls with no WO1 primary antibody (but only FITC labeled secondary antibody) were included. The results from the immunofluorescence assay are shown in appendix A, and include evaluation of the presence of microcolonies for each isolate and their binding of the conformationally specific antibody. The premise for sufficient accumulation of FuBA is high expression of FuBA pr. cell (as determined by emission intensities) and a large fraction of cells that perform the task.

If microcolonies of any size and abundance are considered, X out of 53 bacterial isolates bound WO1 strongly, X bound WO1 intermediate, 2 isolates bound WO1 very limited, 2 isolates did not form microcolonies, and the microcolonies of two strains showed very high fluorescence emissions from the control without primary AB, including *S. epidermidis*. This seemed to be an effect of increased autofluorescence for these strains at the available filter, as the emmison of *S. epidermidis* in PBS was measured and found comparably high (results not shown). For strains that bound WO1 strongly, microcolonies down to two cells showed representation of the strong binding, while surrounding single cells could not be detected, as was evident in all cases. The fluorescence emission from stained cells was found to photo-bleach very rapidly (See Fig. 10 **Appendix A**) and therefore emission was recorded within 1 second of exposure.

It was found that single cells of SM2258 and SM2257 both with and without primary antibody had similar fluorescence emission (displayed for Assay A, but confirmed for Assay B as well, using a longer exposure time, results not shown). Also it can be seen that SM2258 microcolonies binds the antibody strongly, when stained by protocol B (See Fig. 9 **Appendix A**). In contrast artificial cluster of SM2257 created by cornered cells was found to emit florescence with similar or slightly less intensity that unstained SM2258 in PBS and SM2258 without primary AB.

Antibody Assay: FuBA expression - nil, a little, or a lot; the latter it is

That the majority of the strains express FuBA (to some extend) is in accordance with the findings by Larsen et al. (2007), Larsen et al. (2008) and Jordal et al. (2009) who all used conformation specific antibodies combined with others methods to detect widespread abundance of FuBA producing bacteria within various habitats, including freshwater lakes, brackish water, drinking reservoirs and waste water treatment plants. That only microcolonies were observed to bind WO1 (after 5 days of incubations), while single (platonic) cells did not bind in any case, indicates the role of FuBA in mediating not only biofilm formation, but possible also maintaining biofilm architecture. On the other hand, while FuBA was detected as part of most microcolonies, FuBA seems not to be a requirement for floc formation, as was found for example isolate TC2 that remained unstained. Jordal et al. (2009) suggest that where FuBA are expected to affect the properties of biofilms the may not be a prerequisite for flocculation.

Antibody Assay – Thread carefully

That SM2258 overexpressing curli was observed to bind WO1 very strongly is an important validation of the antibody assay. However, the inability of curli negative to form microcolonies oppose the evaluation of any unspecific primary antibody binding, as single cells in no case were found to be indicative of binding. WO1 specificity for amyloids has, however, been tested with several proteinasceous aggreagres (O'Nuallain & R Wetzel 2002). Besides it does not bind to monomers of fibril structures as well (Hrncic et al. 2000) (O'Nuallain & R Wetzel 2002). It was confirmed that the measured emission from the samples (SM2258 and *S. epidermidis*) without

primary antibody was a autofluorescence background signal, that is strain dependent at the available filter. This finding also confirmed that the FITC-conjugated pentameric secondary antibody binds only WO1, and is not trapped within the microcolonies or binds to cell- or EPS components. In fact it seems that the antibodies binds majorly at the surface of microcolonies, and penetration is limited (See for example UK 5 in **Appendix B**). This was also found by Larsen et al. (2007) who also showed that the small dye ThT in contrast to WO1 also bound within microcolonies. Thus the observed binding of WO1 to the surface of microcolonies does not indicate preferential FuBA expression at the surface of microbial flocs, but rather the in penetration of one or both of the antibodies (ironically this may in part be due to surface exposed FuBA).

SDS-PAGE: FuBA monomer: I'm blue and single

Purification of FuBA was carried out using two version of a protocol developed by Dueholm et al. (unpublished), based on the protocol used to purify FuBA from UK4 (MS Dueholm et al. 2010). The one protocol version involves smaller samples volumes, and is used for screening of FuBA by purification. The method relies on cell disruption by freeze-thaw cycles, enzymatic degradation of cell wall component and nucleic acid, and removal of contaminating proteins by boiling in 1% hot SDS. The premise is that FuBA is very stable, and indeed FuBA (curli and tafi) has been shown to be extremely resistant to mechanically and chemically denaturation, and do not depolymerize in 5M NaOH, 8M urea or boiling in 2% SDS (COLLINSON et al. 1991)(COLLINSON et al. 1992). To investigate for the presence of FuBA, the p_FuBA was threaded with 98-100% FA to release FuBA monomers and lyophilized SDS (COLLINSON et al. 1991)(COLLINSON et al. 1992). After resuspension in 1×loading buffer the material was analysed by SDS-PAGE, and compared to a non-FA pre-threaded sample, both stained with coomassie. The premise is that the large and stable FuBA cannot enter the gel matrix in SDS-PAGE, while the release of monomers by FA can be detected. 50 strains were subject to FuBA purification (See Table 3 for an overview of the purification attempts). The overall results from SDS-PAGE analysis of *p_FUBA* from the strains (excluding SM2258, SM2257 and UK4) is that a number (~15) of potential FuBA monomers are identified, where some are more promising than others.

SDS-PAGE: Controls show the way

Curli positive SM2258 and curli negative mutant SM2257 were included in the purification attempts. This was done to investigate the ability of each purification attempt to purify FuBA, and, as part hereof, to observe the criteria for identifying putative FuBA monomers from SDS-PAGE. Fig. 3 displays the outcome of SDS-PAGE of *p_FuBA* from SM2258 and SM2257 that had been

Table 3. An overview of FuBA purification attempts

Strains included in purification	**Growth conditons (see also material and methods)**	**Purification protocol**	**SDS-PAGE of ± FA pre-threaded *p_FuBA***	**FTIR with *p_FuBA***	**SDS-PAGE and FTIR result summarised in table X.**
SM2258 and SM2257	3.5 or 4.5 days	large vol	Fig. **2**	Fig. 3	yes
37 isolates of this study and SE	agar plates 4.5 days	screening protocol	Fig. 16 app. B	Appendix C	yes
37 isolates of this study	liquid culture 3.5 days	screening protocol	Fig. 14 App. B	no	no
UK1-11 (12 isolates)	liquid culture 2.5 or 4.5 days	large vol	**Fig. 12**	Appendix C	yes
UK1	agar plates, 4.5 days	large vol	Fig. 6 gel B1	Appendix C	
UK1	liquid culture 3.5 days	screening protocol	Fig. 6 gel B2	-	
UK1	liquid culture 7 days	large vol.	Fig. 6 gel B3	-	
UK1	liquid culture, 2.5 days	large vol	Fig. 5	pooled: Fig. 7	yes
UK1	liquid culture, 1-7 days	large vol	**Fig. 13**	pooled: Fig. 7	

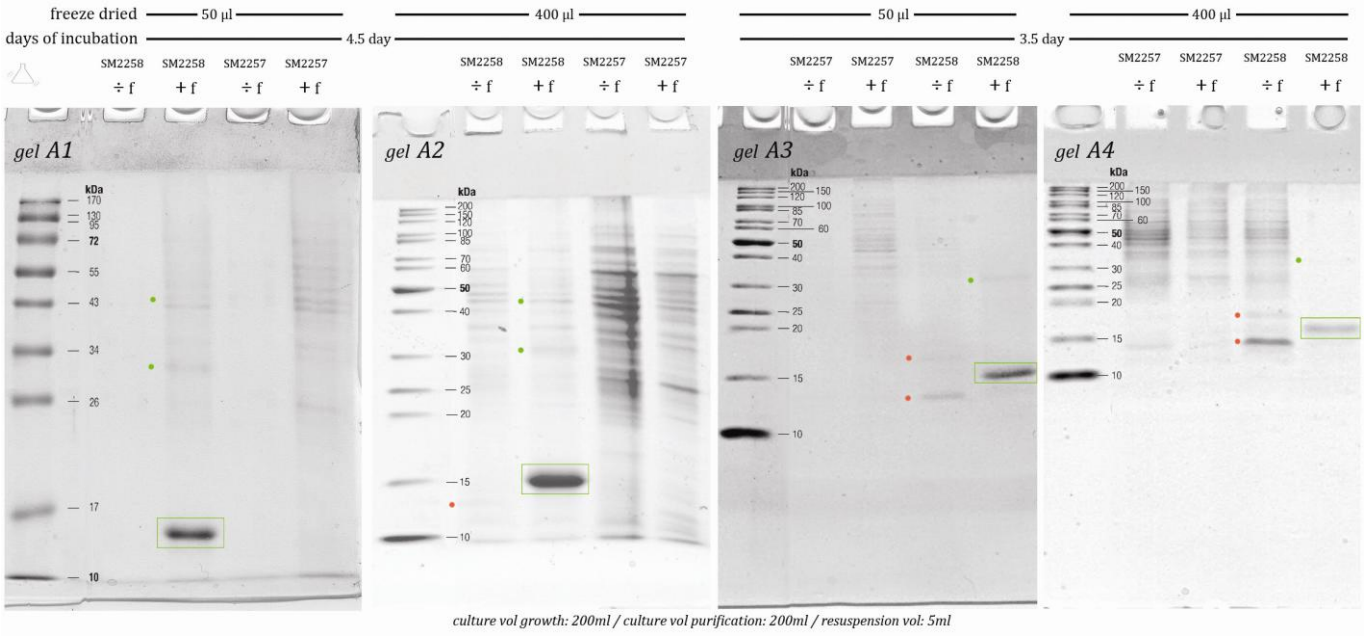

Fig. 2. SDS-PAGE of 50 µl and 400 µl of +/÷ FA pre-threated FuBA purified from SM2258, as well as SM2257.

incubated for 4.5 day and 3.5 days. At both incubation conditions SDS-PAGE of the purified material from SM2258 resulted in an intense band around 15 kDa for the FA pre-threaded sample, a band that was not present for SM2257. For SM2258 two additional proteins bands were observed, a faint band around 30 kDa and an even fainter band around 45 kDa (See Fig. **2 gel A1**). In one case in particular several bands were visible from the *p_FuBA* of SM2257 (See Fig. **2 gel A2**).

The band around 15 kDA corresponds to the CsgA monomer of curli (15 kDa) (Arne Olsen et al. 1989), and indicates strongly that FuAB (curli) was successfully purified from SM2258, in contrast to SM2257 that do not express curli. The additional bands at ~30 kDa and ~45 kDa are believed to be a dimer and trimer of CsgA (or potentially a heterodimer of CsgA and minor curli subunit CsgB). This is analogous to the dimers observed for other FA depolymerised FuBA (White et al. 2001)(MS Dueholm et al. 2010). In Table 2 FuBA monomer candidates with potential dimer-formation have been marked with a *, indicative of the possibility, that this protein existed at a higher polymerisation state prior to FA treatment, i.e. as FuBA. The presence of several contaminating proteins for both the FA pre-threaded samples and the non FA-threaded samples indicates cell lysis upon resuspension of lyophilized sample in 1×loading buffer. Thus, as disused in more detail later, contamination of *p_FuBA* with cytosolic proteins (after formic acid treatment and/or resuspension of lyophilised *p_FuBA* in 1×SDS-PAGE loading buffer) must be expected, both when the bacteria are gram negative (E. coli) and gram positive. This can give rise to both false positives and negatives in SDS-PAGE, and give (additional) misleading structure information in for example FTIR. That lysis of cells is a general problem can be approached from the SDS-PAGE results (See for example **Appendix B**). In the appointment of putative FuBA monomers, the criteria of 'only visible' in the FA pre-threaded sample have been respected, to limit the identification of false-positive.

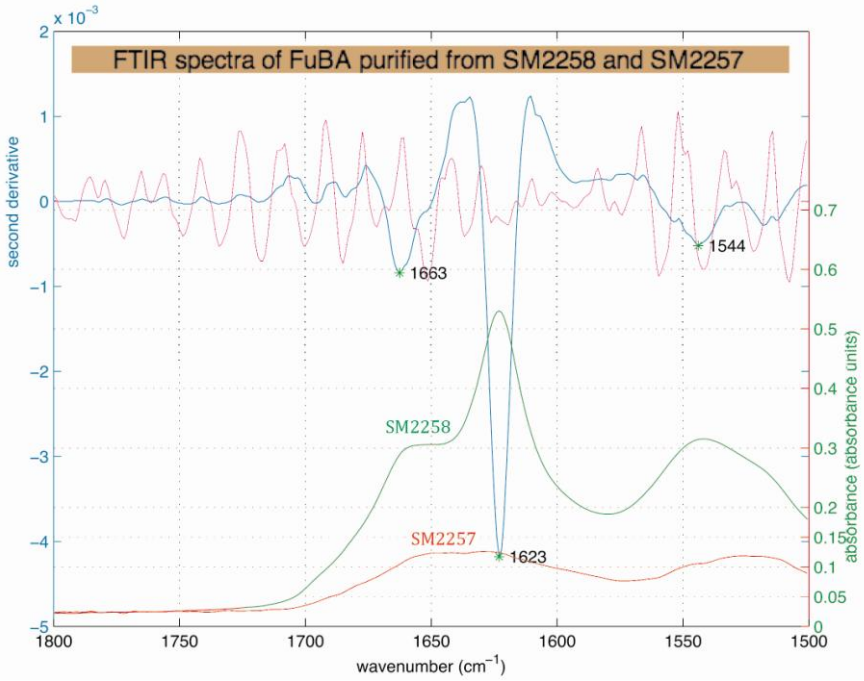

Fig. 3. Amide I region of the FTIR spectra of FuBA purified from SM2258 and SM2257. For SM2258 the absorbance peak position are found from local minima of the second dirivative, graphed in blue. The purified material is identical to that analysed by SDS-PAGE on gel A1/A2 in Fig. **2**.

ATR-FTIR – FuBA or not FuBA

The amyloid-like nature of the purified material for all isolates was investigated by ATR-FTIR. Proteins absorption gives rise to an Amide I, II, and III band (1500-1800 cm^{-1}), and Amide I is used as a marker for protein secondary structure in particular. The Amide I band (within the region 1600-1700 cm^{-1}) is assigned to C=O stretching vibrations of the amide group of the peptide main chain (Jackson & Mantsch 1995) (Cheatum et al. 2004). Thus amyloid fibrils can be identified by FTIR by their distinct cross β-motif (Giorgia Zandomeneghi et al. 2004)(Nilsson 2004). To locate peak positions in the interferograms obtained from ATR-FTIR second derivative analysis was utilised. FTIR spectra of all the isolates can be observed in **Appendix C**, and the results of the peak position analysis are summarised in Table 2 by use of symbols. The symbols categorises the FTIR spectra, as explained in Table 4 **Appendix C**. Spectra that represents the results of FTIR are curli positive mutant SM2258, curli negative mutant SM2257, PH1b, UK7, and HE1 Second derivative analysis of the amide I band of *p_FuBA* from SM2258 (1) showed two very intense peaks, one at 1623 cm^{-1} and one at 1663 cm^{-1}. The intensity of the peak at 1623 cm^{-1} was 177% of the peak at 1663 cm^{-1}. For purified material from PHb1 (2) two intense bands were observed in the Amide I band, one at 1623 cm^{-1} and one at 1652 cm^{-1} (2). Different variations of this theme, a peak in the range 1621-1629 cm^{-1} and a higher frequency peak between 1651-1658 cm^{-1} were observed from the *p_FuBA* of the isolates. *p_FuBA* from X isolates showed the higher frezuency peak in the interval 1651-1653 cm^{-1}, while *p_FuBA* from X isolated had the peak at 1656-1658 cm^{-1}. For X samples the intensity of the low frequency peak in the amide I band was higher than that of the higher frequency peak (2), while for X samples it was the other way around (4). For X sample the peaks identified by second derivative analysis was part of the same local maxima on the interferograms (3). For all the samples within this theme (2 3 4) the intensity maxima between the two peaks in the amide I band was never more than ±15%. In addition many spectra with this theme had (less intense) peaks around 1684 cm^{-1} and 1695 cm^{-1}, although they are not always assigned on the spectra with a * and a value. The *p_FuBA* for X isolates, including UK7 (÷), had a single peak in the amide I region above 1631 cm^{-1}. Almost all samples where the maximum intensity of the amide I band was above 0.2 absorbance units had a peak at 1539-1545 cm^{-1}, and in some cases one at 1512-1518 cm^{-1} within the Amide II band.

For *p_FuBA* with a absorption maxima in the amide I and II region below 0.2 absorption units (÷A) no peaks could be assigned: For *p_FuBA* from SM2257 (÷A) it was not possible to identify any peaks from the noisy second derivative. *p_FuBA* from HE1 (÷A) resulted in similar

absorption intensity as that of *p_FuBA* from SM2257, but for HE1 the fluctuations in the second derivative was negligible. Thus it was not possible to assign any peak positions. Finally it was observed that X samples, including PHB1, had a intense peak around 1740 cm^{-1}.

Amide I – What are you telling me, its is FuBA I see

Amyloids have shown to produce narrow amide I' (measured in D_2O) bands with peaks from 1611 cm^{-1} to 1630 cm^{-1}, whereas native β-sheets cluster between 1630 cm^{-1} to 1643 cm^{-1} (Giorgia Zandomeneghi et al. 2004). That ATR-FTIR measurements on amyloids in the unhydrated state at first hand are expected to produce peaks in the same range (1611 cm-1 to 1630 cm-1) may be appreciated from a study by (Fraser et al. 1991) where air-dried amyloid fibril samples were nearly identical to those of deuterated samples. This is probably an indicating of little change in the fiber conformation upon drying, and reflects the strong hydrogen bonding in amyloid fibrils.

The purified *FuBA* given the symbols 2 3 4 all have a peak in the interval at 1621 cm^{-1} to 1629 cm^{-1}, which is within the range of peak positions displayed by amyloids fibrils. According to (Nilsson 2004) there is currently no amyloid criterion for the amount of β-sheet secondary structure necessary to qualify a sample as (containing) amyloid fibrils, i.e. any percentage is acceptable. Thus based on these results it might be sufficient to say, that many of the samples with *p_FuBA* properly does include FuBA. But it might be possible to say more, that can help explain the origin of the spectra - perhaps not any conclusive in each case, but still something that can point out certain possibilities, and perhaps give hints on where to next with the investigations.

Amide I – β-sheet structures

According to Cerf et al. (2009) it is possible to distinguish amyloid fibrils (or generally β-sheet structures) in FTIR, whether the β-sheets are parallel or anti-parallel. This is based on experimental studies on well defined amyloid fibrils, as well as theoretical studies. In antiparallel β-sheet structures two components are present. The major component has an average wavenumber located at ~1630 cm^{-1}, whereas the minor component is characterised by an average wavenumber at 1695 cm^{-1}. Moreover the minor component in β-structures is found to be approximately 5. fold weaker than the major component around ~1630 cm^{-1}. For parallel β-sheet structures the amide I is not split, but display only the major component around 1630 cm^{-1}. It should be mentioned that (Uversky & Longhi 2009) claim that there is no experimental evidence for a difference between the frequencies of parallel and antiparallel β-sheets, in disagreement with the finding of Cerf et al. (2009).

Amide I – SM2258 and SM2257

The narrow and intense peak at 1623 cm^{-1} of FuBA purified from curli positive mutant SM2258 is characteristic for the cross β-motif with its stable and/or long β-strands with many hydrogen bonds (Cerf et al. 2009). For β-plated structures the minor component at 1663 cm^{-1} has been proposed to result from a splitting of the main β-sheet component, indicative of an anti-parallel arrangement of the β-strands (López de la Paz et al. 2002). However, Cerf et al. (2009) performed studies on a well defined amyloid fibril from Aβ-(1-42) with parallel β-sheets Aβ-(1-42), and in this case a peak around ~1660-1665 cm^{-1} seems to originate from a combination of random coil/helixes (1650-1660 cm^{-1}) and β-turns (1670cm^{-1}). Shewmaker et al. (2009) find from solid state NMR that curli is not a parallel in register β-structure, but may be a α-helix-like structure. In any case, the spectra of purified FuBA from SM2258 is very similar to published spectra of purifed curli (Morten S. Dueholm et al. 2010), confirming along with the SDS-PAGE results that the utilised purification procedure does result in curli purification (MS Dueholm et al. 2010). The circumstance that no peaks could be assigned for *SM2257pm* is in accordance with the inability of the mutant to produce curli.

The Amide I bands of the isolates (2 3 4) all have additional features that may set them apart from that expected for amyloid fibrils, namely the broadness of the amide I band and the intense peak at 1651 cm^{-1} to 1658 cm^{-1}, which seems to diminish the 'amyloid' peak. Potential explanations for the observed ATR-FTIR spectra of the samples with symbol 2 3 4 include:

Amide I – Amorphous aggregates

According to Zandomeneghi (2004) inclusion bodies and thermally induced nonfibrillar aggregates can gives rise to a similar absorption in the region around 1611 cm-1 to 1630 cm-1, like amyloid fibrils. This demonstrates that is important to probe the structure elements within the *p_FuBA* with other methods, for example circular dichroism.

Amide I – FuBA contaminated with other (cellular) proteins

Potentially the two peaks in the Amide I band could arise from FuBA together with contaminating proteins. If so, the higher frequency peak at 1651-1658 cm^{-1} may be ascribed to contribution from proteins with significant α-helixes or disordered structures (Jackson & Mantsch 1995)(Uversky & Longhi 2009). This explanation may be valid for *p_FuBA* from strains that are not efficiently lysed by the freeze-thaw cycles upon purification. Contaminating proteins alone are not belived to explain the peaks in the Amide I region below 1630 cm^{-1}, as even all-β-proteins have peaks no lower than 1630 cm^{-1} (G Zandomeneghi et al. 2004) (Cerf et al. 2009).

Amide I – Bacteria with FuBA

SDS-PAGE of *p_FuBA* from a great number of the isolates indicated that bacteria are present, and probably lysed in the preparation of the samples for SDS-PAGE. If (non-lysed) cells are present in the samples with purified material it is possible that cells with surface exposed FuBA give rise to the observed ATR-FTIR spectra. This interesting explanation is elaborated on in the following. Its inspired from a comparison between ATR-FTIR spectra of fixated SM2257 and SM2258 bacteria, along with the obtained spectra of curli from SM2258, as depicted in **Fejl! Henvisningskilde ikke fundet.**. The spectra of fixated SM2258 bacteria show an intense peak at 1624 cm^{-1}, whereas fixated SM2257 show no similar component in the Amide I band. That the intense peak around 1623 cm^{-1} is shared between the

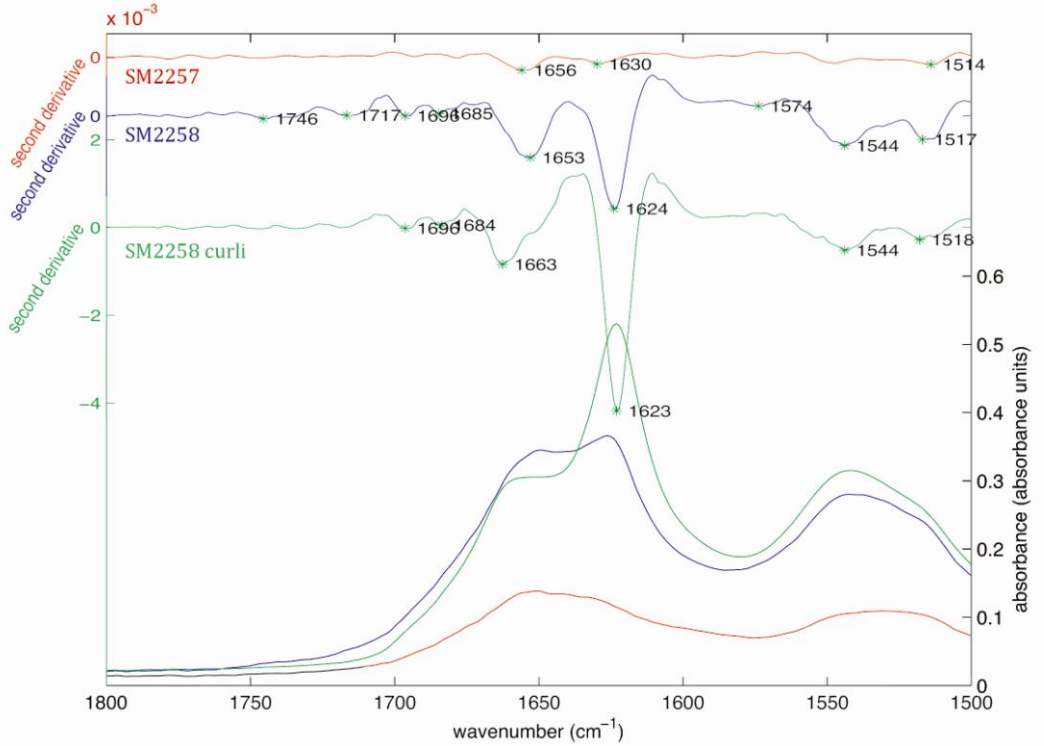

Fig. 4. Amide I region of the FTIR spectra of RED: PFA fixacted SM2257 BLUE: PFA fixacted SM2258 GREEN: FuBA (curli) purified from SM2258. The absorbance peak positions are found from local minima of the second dirivative. 2 µL fixed bacteria was used.

spectra of fixated SM2258 and curli, along with the agreement of the spectra's shape, suggest that surface exposed curli are detected on the fixated cells. The apparent sensetivity of ATR-FTIR to surface exposed proteins have previously been utilised by Kamnev (2008). Kamnev (2008) used the general rules of thumb for secondary structure assignments to infer a predominance of α-helices at normal growth conditons for bacterial cellular proteins, and to detect an enhanced proportion of β-structures upon nutritional stress. Thus, the peak around 1654 cm^{-1} of fixed SM2258 and SM2257 is probably due to helical cellular proteins, while the small peaks at 1630 cm^{-1} for SM2257 likely is due to outer membrane proteins with a extensive β-sheet structure.

The apparent finding that curli of SM2258 can be detected on cells by ATR-FTIR might not be surprising. TEM microscopy has shown that curli are extensively surface exposed as a mesh of long (up to 300nm) projections in SM2258 biofilms (and in addition, SM2258 does not produce flagella) (MS Dueholm et al. 2010) (Claire Prigent-Combaret et al. 1999). According to the antibody assay, many of the isolates seemed to produce extracellular FuBA extensively, and these surface exposed FuBA may also be detected in ATR-FTIR, as seems to be the case for *E. coli*. Thus, as implicated from the results displayed in **Fejl! Henvisningskilde ikke fundet.**, the ATR-FTIR spectra of purified material from the isolates with a peak in the amyloid amide I band (2 3 4) may very well be due, at least partly, to the presence of cells with surface exposed FuBA in many cases. If so, the relative intensity of the two major components in the amide I band may represent the proportion of surface exposed secondary structure elements, primarily between α-helixes/random coil and (amyloid) β-sheet structures, as indicated by the observed peaks (1651-1658 cm^{-1} and 1621-1629 cm^{-1}). The peak locations at 1653 cm^{-1} for many of the isolates might reflect a contribution from unstructured proteins. Although protein denaturation in SDS have shown to produce non-native proteins, but not necessarily unordered polypeptide chains (Daniel E. Otzen 2002), is it possible that the combined effect of the purification strategy (freeze thawing and hot SDS) will affect protein composition and structure on the surface of the present bacteria, even if not lysed. The (potential) ability of ATR-FTIR to detect FuBA on bacteria is very interesting, and might constitute a new method to probe the expression of FuBA by bacteria. If so the approach is very rapid, can directly complement the finding from antibody staining, and generally be used to screen for conditions where FuBA expression is favourable.

PH12 has a very intense peak at 1631 cm^{-1}. Considering the harsh purification protocol (boiling in 1% SDS) it is possible, that it is the signature of amyloid, perhaps one where the hydrogen bonding in the fibrils is comparable to that for all-β proteins. An amyloid fibril studied by (Fraser et al. 1991) using ATR-FTIR had its peak at 1631 cm^{-1}. But then again, observing the SDS-PAGE of *p_FuBA* from PH12 (See Fig. 17 **Appendix B**), the peak at 1631 cm^{-1} may originate from cytosolic proteins, or (if the bacteria are not significantly lysed) surface exposed proteins, possible all-β proteins (like porins). A feature of the FTIR spectra that indicates the presence of cells is the peak at 1740 cm^{-1}. According to (Legal et al. 1991) a small absorption band around 1740 cm^{-1} can be ascribed to stretching of ester carbonyl groups (C=O ester), when measuring on bacteria. More specifically, intact cells are found to display a peak at 1745 cm^{-1} while collapsed cells walls peak at 1736 cm^{-1}. Thus, strictly speaking, could a band at 1740 cm^{-1} signify partial cell ruption of the population in suspension. All FTIR spectra that display a peak at 1740 cm^{-1} also show many bands in SDS-PAGE, indicating that its meaningful to link the peak at 1740 cm^{-1}, with the (relatively abundant) presence of cells in *p_FuBA*.

UK1 FuBA purification – Try again, you might succeed

Several attempts to purify FuBA from UK1 were commenced within this project. The outcome of purification was generally plentiful of a white/transparent to pale brownish fluffy precipitate, often in addition to a smaller amount of some brownish and black material that had pellet first (See Fig. 7 **B**). Analysis of purified material from UK1 by SDS-PAGE led to the identification of a number of potential FuBA monomers (See Fig. 6 **gel B3**), where the abundance of each was dependent on incubation conditions (with no obvious pattern). Initially purification attempts had focus on the protein named *UK1-f* of approximately 29 kDa. The

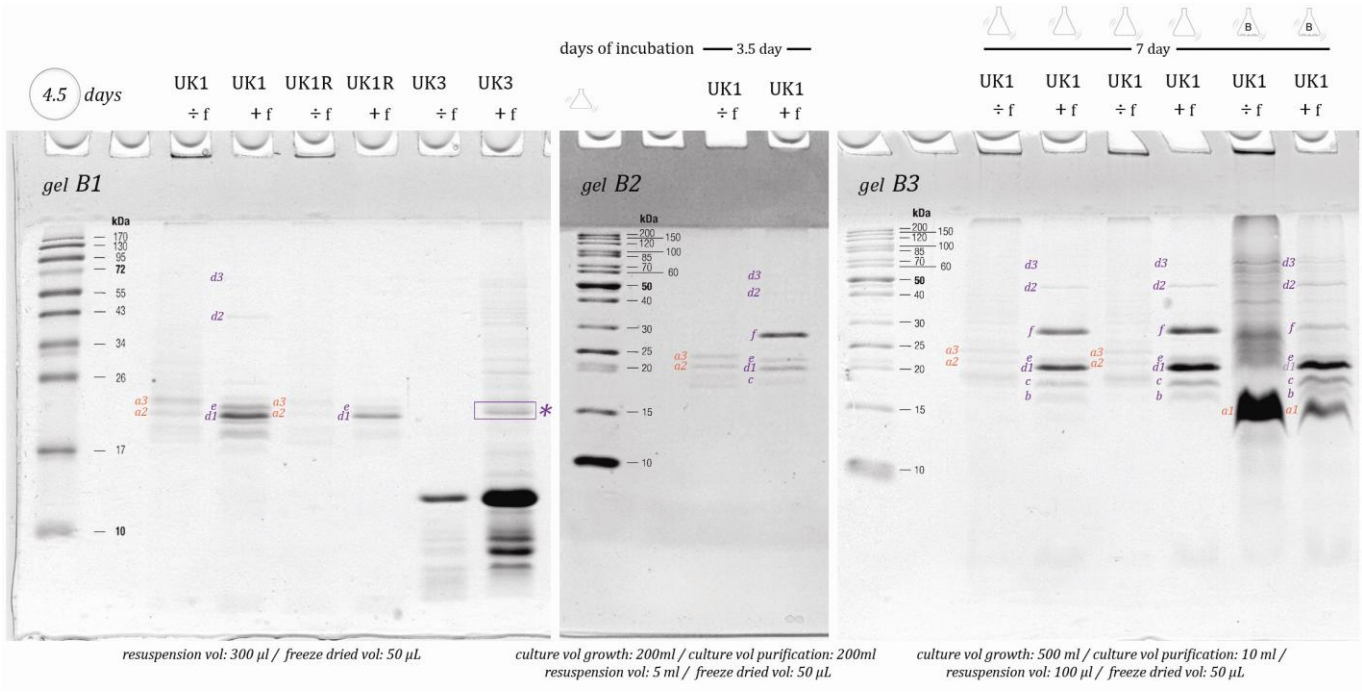

Fig. 6. SDS-PAGE of +/÷ FA pre-threated FuBA purified from UK1 at different growth conditons. SDS-PAGE of FuBA purified from UK1R and UK3 are included.

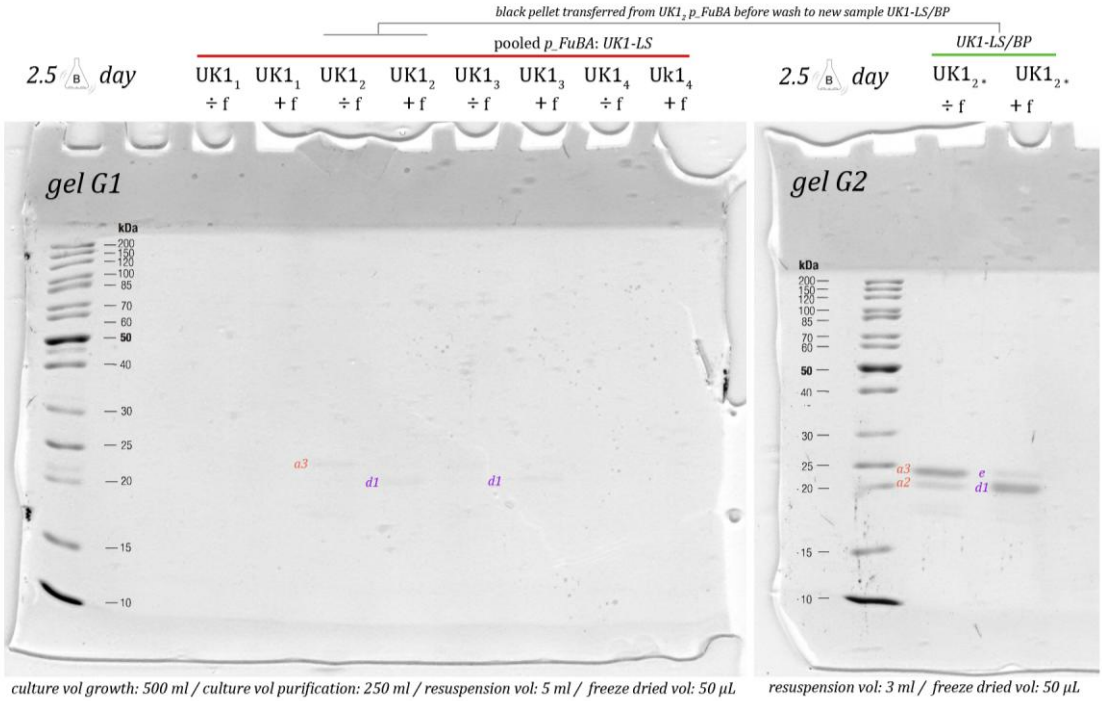

Fig. 5. SDS-PAGE of +/÷ FA pre-threated FuBA purified from UK1. Doing purification from $UK_{1\text{-}4}$ the larger part of some blackish pellets were removed. One of these, from UK_2 was resuspended in 3 ml buffer and analysed by SDS-PAGE (right panel).

observation that the amount of *UK1-f* observed in SDS-PAGE was significantly decreased when incubation was prolonged from 3.5 to 4.5 days, pointed towards the possibility of FuBA degradation. Thus to examine accumulation of FuBA, purification was made from cultures with prolonged incubations (See **Fig. 13**). The yield of *UK1-f* on SDS-PAGE, as well as *UK1-d1,* was overall found to be limited in this semi-quantitative purification study: The apparent accumulation of *UK1-f* and U*K1-d1* rose and fell several times over the period of 7 days with no seemingly pattern. After 7 days the yield of *UK1-f* and *UK1-d1* was limited, while in another purification attempt with seven days incubation the yield of these proteins, as well as other FuBA monomer candidates, were significantly more pronounced (See Fig. 6 **gel B3**). In particular, the presence of potential FuBA monomer *UK1-d1* (approximately 21 kDa) was obvious, as was also the case when purification was done from UK1 grown on CFA agar plates for 4.5 days (See Fig. 6 **gel B1**). Initially *UK1-d1* was thought to be a contaminant that was present in both the samples with and without FA pre-treatment. This view came from a early large shale purification attempt with UK1, in which the larger part of some black/brownish pellets had been removed prior to the final washing steps (believing them to be contaminants). SDS-PAGE of such a pellet in suspension, displayed two proteins bands that seemed to be present in both the FA pre-threaded sample, as well as the non-threaded (See Fig. 5 **gel G2**). But a closer look on the results from SDS-PAGE of other purification experiments (see Fig. 6 **gel B1**, **B2** and **B3**) indicated that *UK1-d1,* as well as *UK1-e*, appeared as potential FuBA monomers, as the contaminants named *a2* and *a3* were of slightly larger size than *UK1-d1* and *UK1-e,* respectively, and only appeared in the non-FA pre-threaded sample. Noticing *UK1-d1* of approximately 21 kDa it is possible that the fainter bands *UK1-d2* band are dimers of *UK1-d1*, and the even fainter *UK1-d3* band are timers (See Fig. 6 **gel B3**, as well as gel **B1** and **B2**).

***UK1-d1* – A diamante in the rough, potentially**

UK1-d1 is interesting as a potential FuBA

A)

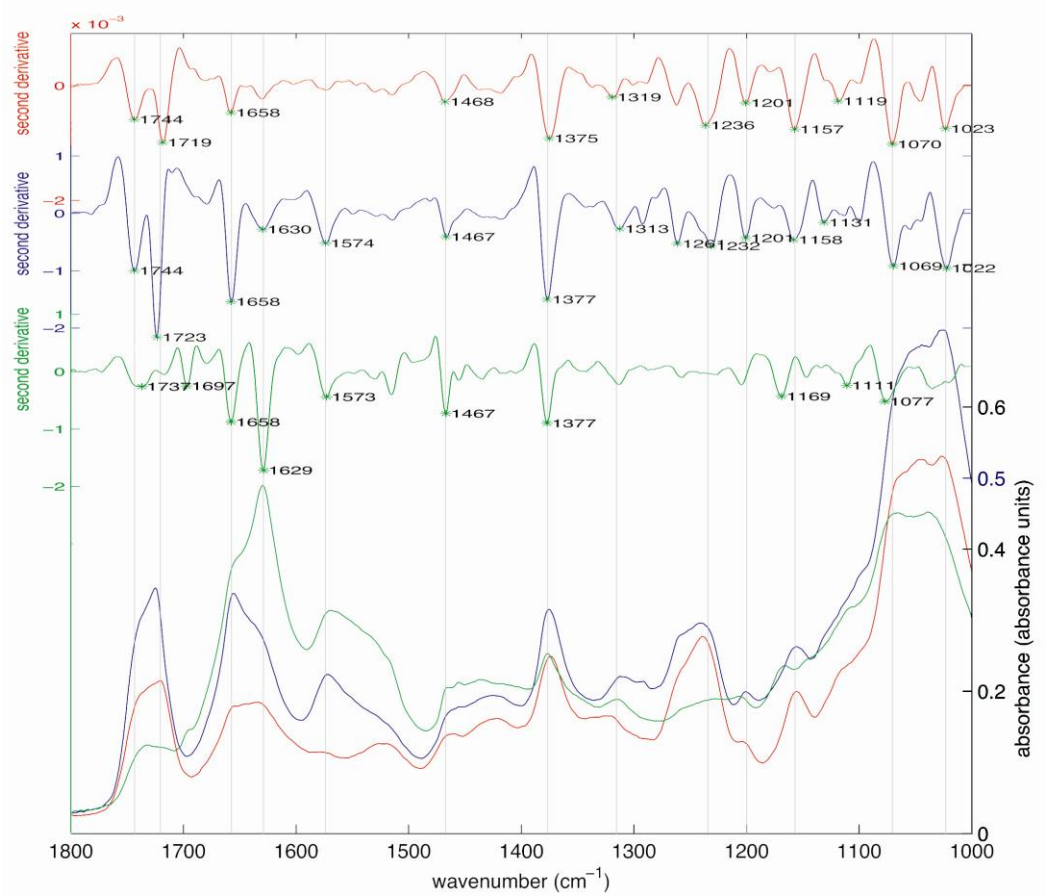

B)

Fig. 7 FTIR of *UK1-LS/BP, UK1-TS* and *UK1-LS.*

monomer, first of all because it is often abundant in SDS-PAGE of the FA pre-threaded sample, including when FuBA was purified from CFA agar plates (in which case *UK1-f* was undetectable). Secondly, the putative oligomers of *UK1-d1* (named *UK1-d2* and *UK1-d3*) might indicate that *UK1-d1* existed as a higher polymerisation state prior to FA treatment, as it is the case after FA treatment of FuBA from E. coli, Salmonella spp. and *P. fluorescens*, as well as SM2258 within this study (White et al. 2001)(Matthew R. Chapman et al. 2002)(MS Dueholm et al. 2010). The existence of seven protein bands (including UK1-d2 and *UK1-d3*) in the FA pre-threaded sample (See Fig. 6 gel B3) is not believed to be due to cell lycis, as more cytoplasmic proteins bands would be expected in that case.

The amyloid-like nature of *p_FuBA* from UK1 was investigated by FTIR. The first spectra on purified material from UK1 (See SDS-PAGE on **Fig. 12** gel D1) had to low absorbance intensity to detect protein (See ATR-FTIR spectra in Appendix C). To increase the concentration of FuBA several samples with *p_FuBA* UK1 was pooled. Sample *UK1-TS* (time series) constituted all insoluble material from the 1-7 days incubations (See SDS-PAGE on **Fig. 13**). Sample *UK1-LS* (large shale) was pooled from the *p_FuBA* of the large shale FuBA purification (See SDS-PAGE on Fig. 5). And sample *UK1-LS/BP* was a black pellet, with a small amount of white/bronish material sticking to it (See SDS-PAGE on Fig. 6 **gel B3**). It had been transferred from one of the samples ($UK1_2$) from the large shale FuBA purification experiment before the final washing steps. Photographs of sample *UK1-TS* , *UK1-LS* and *UK1-LS/BP* can be seen in Fig. 7 **B**. Prior to FTIR the material was washed once in 1.5 ml 10mM Tris-HCL buffer, PH 8.0 (10.000g, 5 min.) and then resuspended in just enough tris-buffer to be able to pipette it. The interferograms from FTIR with sample *UK1-TS*, *UK1-LS* and *UK1-LS/BP* can be observed in Fig. 7 **A** (range 1000-1800 cm^{-1}). The interferograms have very similar shapes, and second derivative analysis of the FTIR spectra showed that several peaks were shared among the samples, including intensive peaks around 1658 cm^{-1}, 1467 cm^{-1} and 1377 cm^{-1}. Peaks around 1744 cm^{-1}, 1721 cm^{-1} and 1234 cm^{-1} were only identified for sample *UK1-TS* and *UK1-LS*. For sample *UK1-TS* and *UK1-LS/BP* two unique peaks were found around 1629 cm^{-1} and 1574 cm^{-1}.

The results of FTIR indicate that FuBA is potentially detected in sample *UK1-LS/BP*, and that *UK1-TS* and *UK1-LS* primarily constitute one or several non-protein compounds. This view is discussed in the following. The narrow peak at 1629 cm^{-1} for sample *UK1-LS/BP* is indicative of amyloid-fibrils, or β-pleated sheets with strong hydrogen bonding at least. A less intense peak around 1629 cm^{-1} for sample *UK1-TS,* and an even smaller component for *UK1-LS,* might indicate that these samples include the same β-pleated sheet structures, but to lesser extends. A peak at 1658 cm^{-1} can origin from α-helix. But if the peak at 1658 cm^{-1} is solely due to α-helix, or any secondary structure of a protein, a peak of larger intensity within the amide II band might be expected in sample *UK1-LS*. The peaks at 1744 cm^{-1}, 1721 cm^{-1}, 1234 cm^{-1} and perhaps also that at 1658 cm^{-1} is believed to originate from one or several non-protein compound readily present in sample *UK1-TS* and *UK1-LS*, and only to a limited extend, in sample *UK1-LS/BP*. It was speculated if the non-protein part of UK1 *p_FuBA* might be cellulose, as UK1 produces cellulose at 26° when grown on Congo red identification plates (Dueholm, unpublished). But (micro)cellulose has peak absorbances in the 1033-1164 cm^{-1} region, and does not absorb significantly at the observed bands (Hori & Sugiyama 2003). Instead the peaks at 1721 cm^{-1} and 1744 cm^{-1} is indicative of a mixture of crystalline and amorphous (from boiling) PHA, that can be produced in high amount as a storage compound by some Aeromonas strains (S. Reddy et al. 2008)(Kichise et al. 2002), although the positions of the lower frequency peaks of *UK1-LS* does not coincide fully with those of PHA (Xu et al. 2002)(Arcos-Hernandez et al. 2010).

SDS-PAGE (Fig. 6 **gel B3**) and FTIR (*UK1-LS/BP* on Fig. 7) of the sample with black pellet purified from UK1 indicated that its correct to point out *UK1-d1* as a FuBA monomer candidate, as part of the black pellet, or the material sticking to it, potentially consist of FuBA. It also showed that the white viscous material purified from UK1 seems to consist mostly of non-protein material. In comparison purified FuBA from *G. obscurus* was black (Jordal et al. 2009), while Dueholm et al. (2010) isolated UK4 FuBA from prepative SDS-PAGE as a white precipitate. Thus, in the case of UK1, it seems that the purification protocol co-purify some compound, that can mask the detection of FuBA in FTIR. This masking may come about both due to diluting effects of the purified FuBA, trapping of FuBA in the viscous material, and due to overlap of absorption bands (around 1658 cm^{-1}). It may also alter the properties of the FuBA.

Success of Purification: Many small brooks make a strong river

One interesting case, is UK4 that bound WO1 intermediate, significantly less than curli positive SM2258. UK4 (a *Pseudomonas* strain) have been shown to express surface exposed FuBA, as stated by (Morten S. Dueholm et al. 2010). The stained sample was grown at conditions (CFA medium, 26°C, 200 rpm, 5 or 2.5 days, respectively), at which FuBA was also produced and purified, according to SDS-PAGE. Thus the relatively poor staining of UK4 may lower the barrier when candidates for FuBA purification are chosen from staining experiments, or it may simply remind us that FuBA expression is very sensitive to incubation conditions. If the overall amount of produced FuBA is not the detrimental factor for success of purification, then it may indicate that the property of the FuBA itself, its stability, that are the most important factor (potentially in combination with the property of the bacteria expressing the FuBA).

Optimisation of purification – some options

That *E. coli* evidently resisted lysis upon the harsh FuBA purification treatment indicates that the freeze thawing cycles has not been efficient in disrupting the cells. Loss of viability due to freeze thawing occur through ice formation, hyperosmotic stress as well as other factors, and whether bacteria survive the treatment is among other things dependent on nutrial status, growth phase, colling rate, and prior exposure to stresses (Sleight et al. 2006). According to Packer et al. (1965) the effect of freeze thawing is most dependent on cell protection by spent growth medium, and heating the medium in the presence of alkali abolished this effect. In any case its evident that loss of viability due to freeze thawing is proportional to the number of freeze thaw cycles (PACKER et al. 1965) (Sleight et al. 2006). So a strategy to increase cell lysis in this step may be to combine several approaches, in addition to enhancing the effect of lysozyme.

For many bacteria the effect of lysis by lysozyme is dependent on an initial disruption of the (outer) membrane: Gram-negative bacteria are almost always resistant to lysis by lysozyme, due to the protection of the peptidoglycan layer by an outer lipopolesaccaride layer (Bøgh-Sørensen 2003), and, as in the case of e. coli, lysozyme inhibitors (Deckers et al. 2004). Many gram-positive bacteria are also resistant to lysozyme, often due to modifcations in their peptiglycan layer (Hebert et al. 2007). Among the bacteria that resist lysozyme treatment and freeze thawing are gram-positive bacteria expected to resist the hot/boiling SDS treatment in particular, due to their thicker peptidoglycan layer. Poor lysis of gram positive cells upon freeze thaw cycles and hot SDS treatment have been reported by others (Gothwal et al. 2007). Thus all in all it must be expected that both gram negative and many gram positive bacteria may contribute with contaminating cytosolic proteins in SDS-PAGE of p_FuBA. This is in accordance with the findings that many isolates show additional bands in SDS-PAGE, and point out the need for additional means to lyse cells upon purification, or, as in Dueholm et al. (2010), additional purification steps like preparative SDS-PAGE. As discussed for UK1, non-protein contaminants in p_FuBA, may also be a problem upon purification (and subsequent detection of FuBA). And it is likely that more efficient cell lysis may remove such contaminants as well (if their origin are intracellular).

To improve lysis by lysozyme many suggestions have been put forward, including adding various compounds to the growth medium (Bøgh-Sørensen 2003) (CHASSY & GIUFFRIDA 1980). Another approach is to add Achromopeptidase, that has shown effective in lysing gram postive bacteria that are not efficiently lysed by lysozyme, or adding a cocktail (Ezaki & Suzuki 1982).

Finally the use of bead beating or grinding has proven useful for lysis of gram positive cells, that are not lysed easily by freeze thaw cycles and hot SDS threatment alone (Gothwal et al. 2007).

Conclusion

The aim of this study was to screen for FuBA production among environmental isolates, and detect purified FuBA.

Using a conformational specific antibody that targets the amyloid epitope, it was found that the majority of the isolates formed biofilm at the utilised growth conditions and also expressed FuBA. Expression of FuBA seemed, however, not to be a prerequisite for biofilm formation.

In a number of cases (about a handful) FuBA seems to be purified, according to a SDS-PAGE assay where FuBA monomers are detected and FTIR measurements that probe the amyloid-motif. The verification of that FuBA is purified, however, is not crystal clear, and is in many cases hampered by the presence of cells and their cellular proteins in the purified samples. In one case, for the Aeromonas strain referred to as UK1, it is very likely that FuBA is purified, along with major amounts of some non-protein contaminant. In all cases the presense of FuBA must be verified by others techniques. In future studies the purification protocol should be optimised to provide improved lysis of bacteria to minimise contaminants.

In the course of the project a possible novel approach to identify FuBA producing bacteria showed potential proof of concept with FuBA/curli positive *E. coli* mutant SM2258 and curli negative mutant SM2257. The approach is based on ATR-FTIR on hole bacteria, and detection of surface exposed FuBA.

Perspective

If the majority of bacteria (readily) express FuBA, as implied by the antibody assay, the attempts to purify FuBA may move in two directions using the existing protocol. Either the task is to identify (another) bacteria that will work with the current protocol, or the task is to identify the particular set of conditions that will work for at given bacteria using the protocol. The former implies screening many different isolates with different properties at identical or similar growth conditions, and the latter involves working with one bacteria and varying growth conditions. Perhaps the strength of the purification screening protocol (utilising small culture volumes) lies in its ability to fathom both approaches. Maybe the best approach is to use identical global conditions (as done within this project majorly) in the first run with a diverse set of isolates. And then, after haven identified some promising candidates, chose the best ones, and thereafter apply the screening protocol again, this time using one or few isolates but with different incubation conditions to further narrow down the set of conditions (The Holy Trinity: bacteria - growth conditions – protocol) until the yield of FuBA is acceptable. This approach also limit the resources spent on one bacteria that might never be compatible with the fundamentals of a certain protocol – for example if the FuBA of one bacteria for one reason or another are degraded in the cause of purification, using a protocol that is based on the general high stability of FuBA, then its bad luck. It also possible to use different purification strategies on one isolate off cause, but it must be obvious, that its easier to find a new target/bacteria, than it is to invent a new protocol, although slight chances might always be incorporated in the protocol (here the use of controls can be very nice to have, but also delusive – bacteria don't behave the same, evidently).

But, in any case, a good place to start would be to optimise the protocol based on current knowledge. For example, the current protocol used within this project, should be optimised to increase efficiency of cell lysis. Its important that cells, cell component, cellular proteins, and any other compound does not end up in the final purified material (are co-purified). Suggestions to increase lysis efficiency have already been given.

In addition is will be exciting to see if ATR-FTIR really can predict/detect surface exposed FuBA, and if so, how sensitive the technique is. A starting point would be an attempt to see if measurements with FTIR on bacteria would coincide with the results from the antibody assay (semi-quantitatively). Using fixed cells will ensure that they results are directly comparable. And off-cause it need to be ensured that the fixating does not affect the outcome (in a unpredictable way). According to Legal et al. (1991) DNA can infer with assignment (the bases absorbs near the amide region), so addition of DNase and RNase for degradation of any extracellular nucleotides may be tried out in addition. If the FTIR approach on hole cells have any predictive effect, it might be an excellent tool for quick accessing optimal growth conditions for FuBA expression/production, verifying the antibody assay, and also, together with transmission electron microscopy, contribute to the verification that FuBA on cells and purified FuBA have similar structural properties.

Appendix A

Antibody Assay on bacteria using W01 targeting the amyloid structure

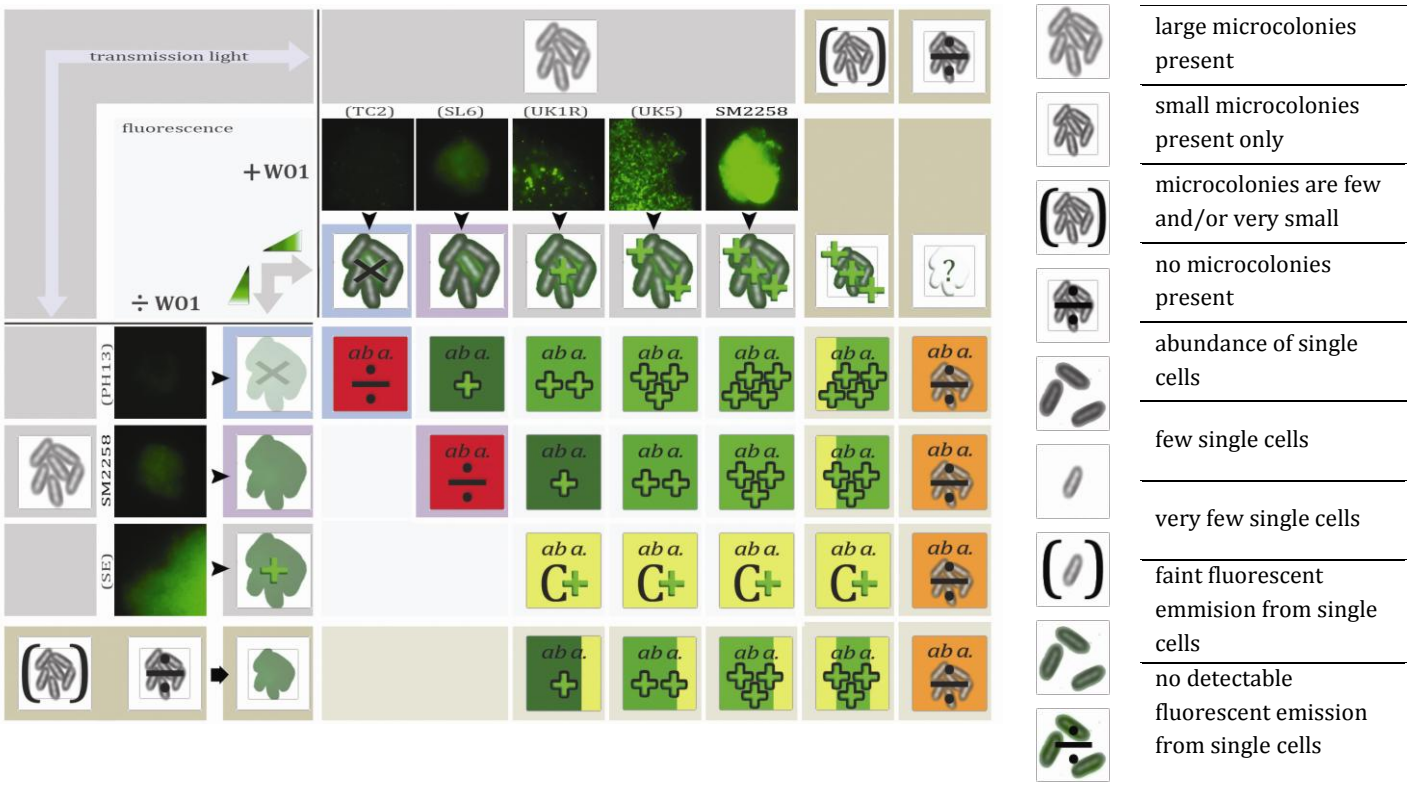

Fig. 8. To estimate binding of W01 the strains are catogorised, i.e. awarded an icon, as explained in the above figure. The catogorisation of each strain is based on the grouping of the recorded fluorescense emmision (intensity) from the samples with and without W01. The fluroscense emmision from 2258 are used as reference. For the samples with W01 added five groups of fluroscnese emmision are made, where the fluroscense emmison from 2258 is the most intense. Three groups of fluorescense emmison are made for the samples without W01, and 2258 defines the intermediate level of secondary AB background fluorescense. A yellow icon is given to strain where the secondary AB background flurescense is significantly higher than that of SM2258. The icon 'no microcolonies' with a orange background is given to strains where no microcolonies are detected in the sample with W01 added. If no microcolonies are present in the sample without W01 or the microcolonies consist of only few cells the background level for this strain is set to be equalent to that of SM2258. The presense of yellow bars in the awarded icons signifies that the colonies in the primary sample (with W01) and/or the control are very small (and few), and that the estimation of the fluroscense emmison may be made on poor grounds. See figure for further explanation.

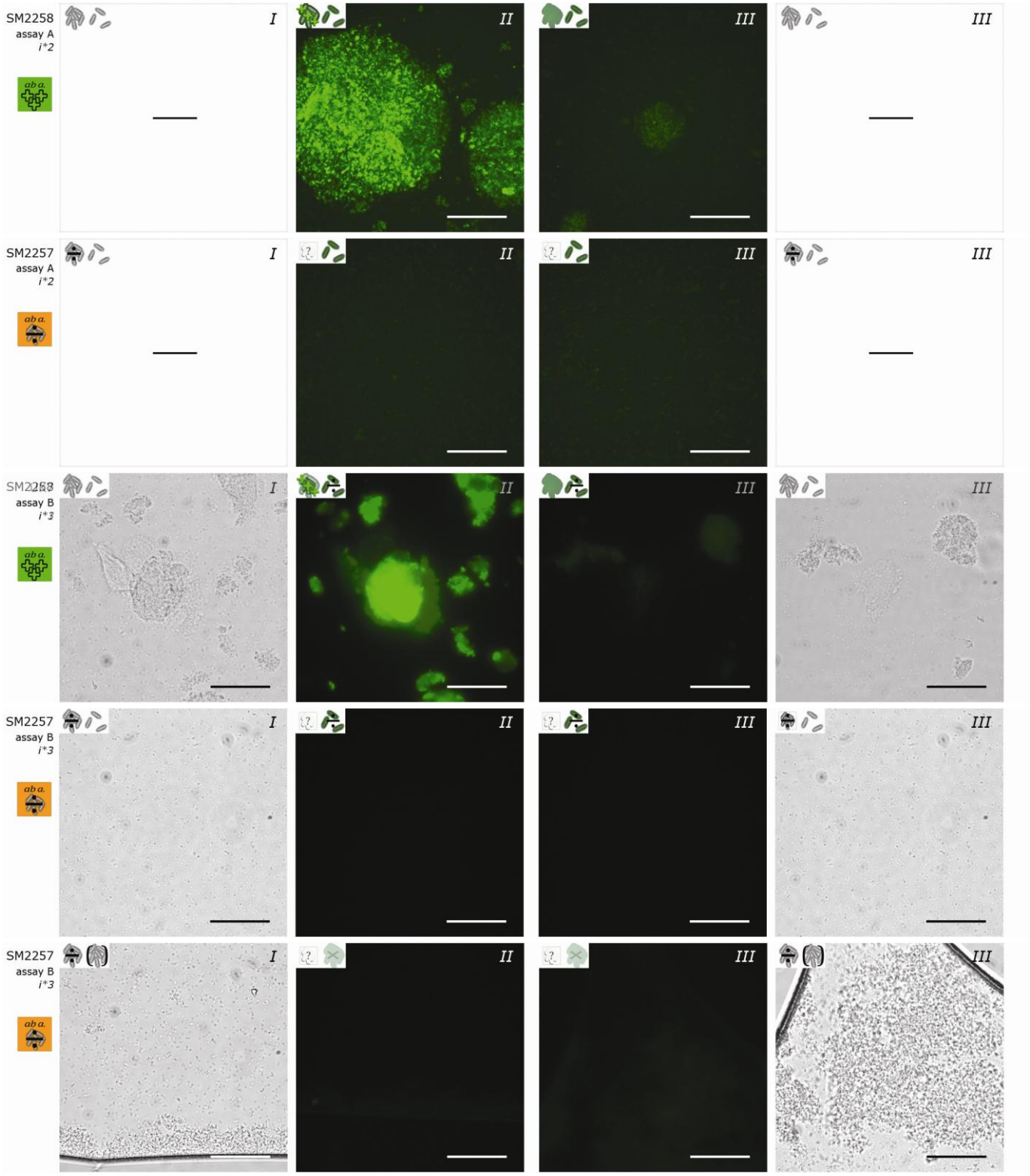

Fig. 9. The fluroscense emmison of curli positive e. coli mutant 2258, and curli negative mutant 2257 stained using Antibody Assay A and B, respectively. The four downmost images display artifical microcolonies of SM2257, i.e. cells that are cornered together after microscopy sample preparation. Scale bar, 10µm

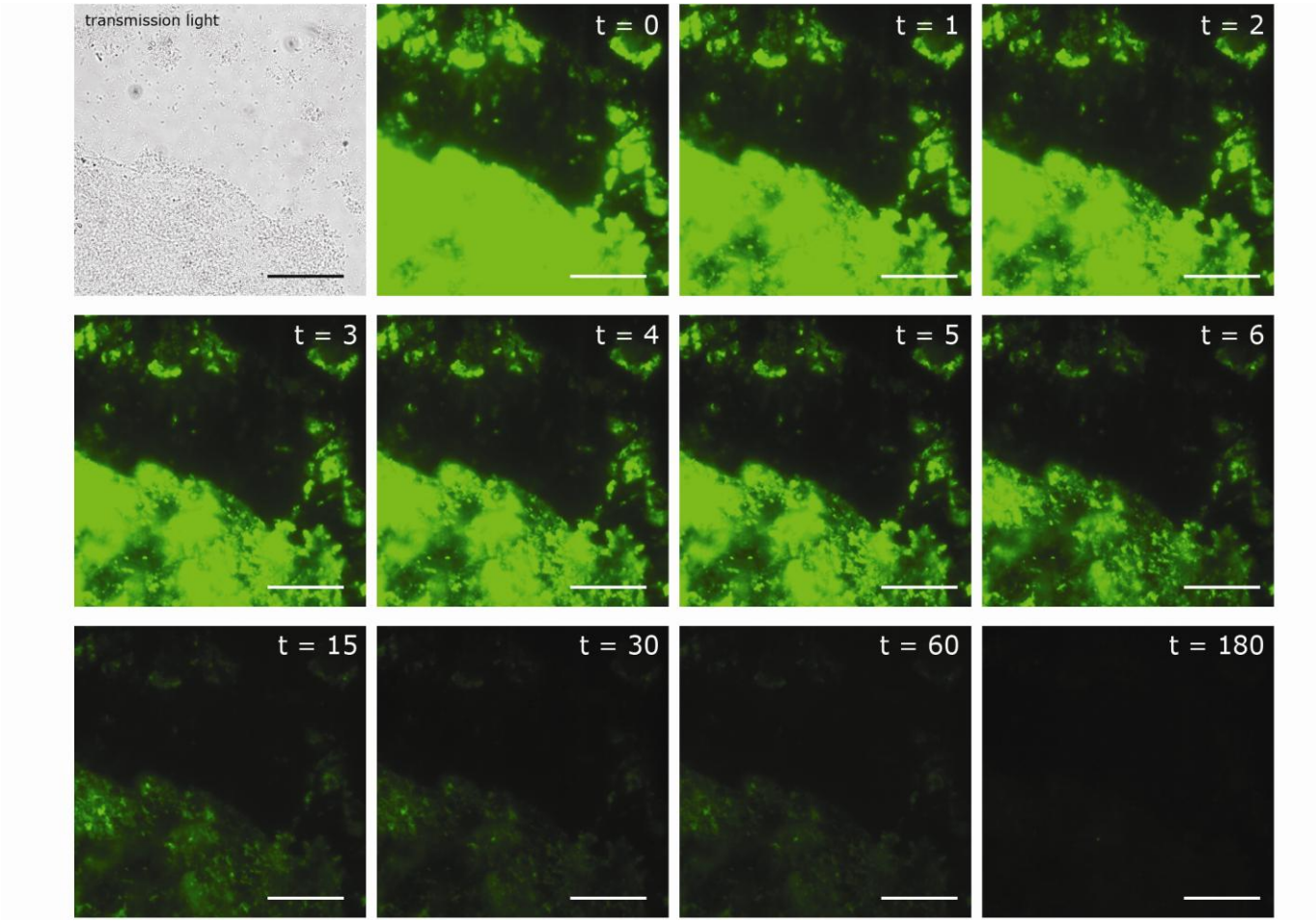

Fig. 10. Recordings of fluorescence emmision from antibody stained SM2258 after t seconds of exposure. SM2258 had grown for 48 hours. Protocol Antibody Assay B were used. Scale bar, 10µm

Immunofluroscense Assay A and B on bacteria using WO1 conformational specific antibodies that targets the amyloid epitobe.

Incubation conditions of bacteria: i*1: 5 days in 10 ml CFA medium (50 ml greiner tube), i*2: 5 days in 10 ml CFA medium with antibotics (50 ml greiner tube), i*3: 2 days in 10 ml CFA medium with antibotics , i*4: 5 days in 20 ml TSB medium (50 ml erli er meyer flask), i*5: 5 days in 10 ml TSB medium (50 ml greiner tube), i*6: unknown.

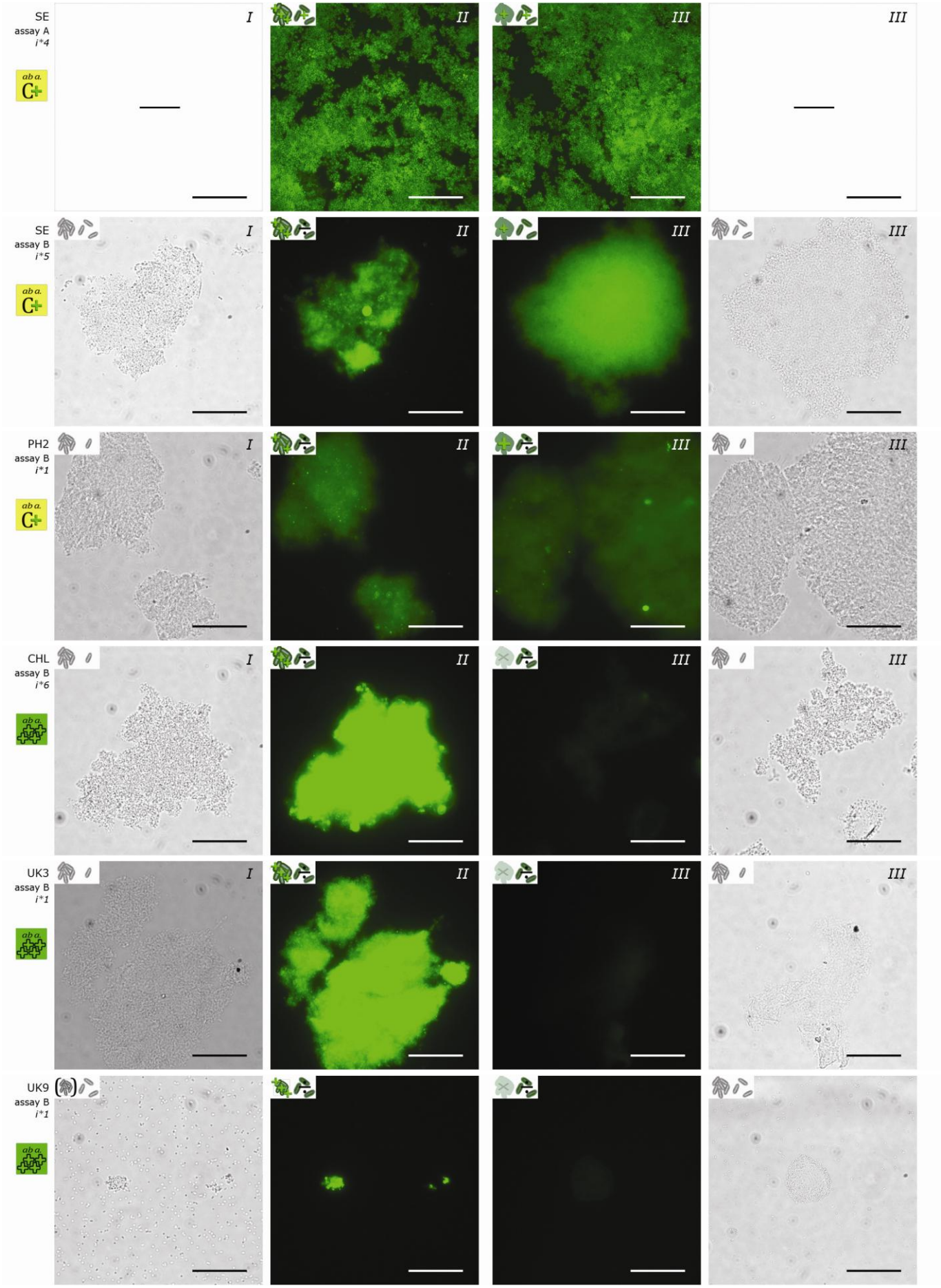
SE
assay A
i*4
I
II
III
III
SE
assay B
i*5
I
II
III
III
PH2
assay B
i*1
I
II
III
III
CHL
assay B
i*6
I
II
III
III
UK3
assay B
i*1
I
II
III
III
UK9
assay B
i*1

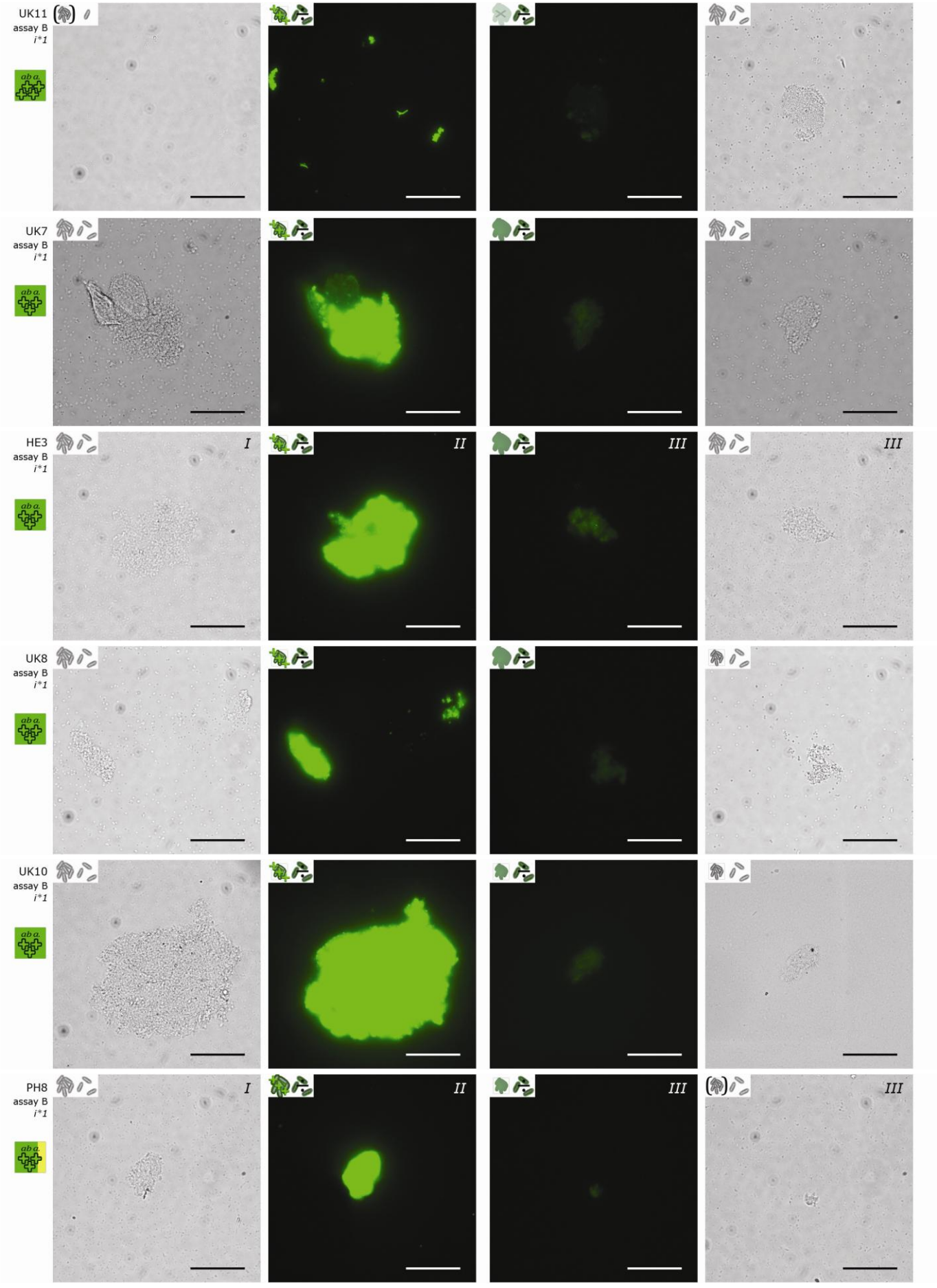
UK11
assay B
i*1
UK7
assay B
i*1
HE3
assay B
i*1
I
II
III
III
UK8
assay B
i*1
UK10
assay B
i*1
PH8
assay B
i*1
I
II
III
III

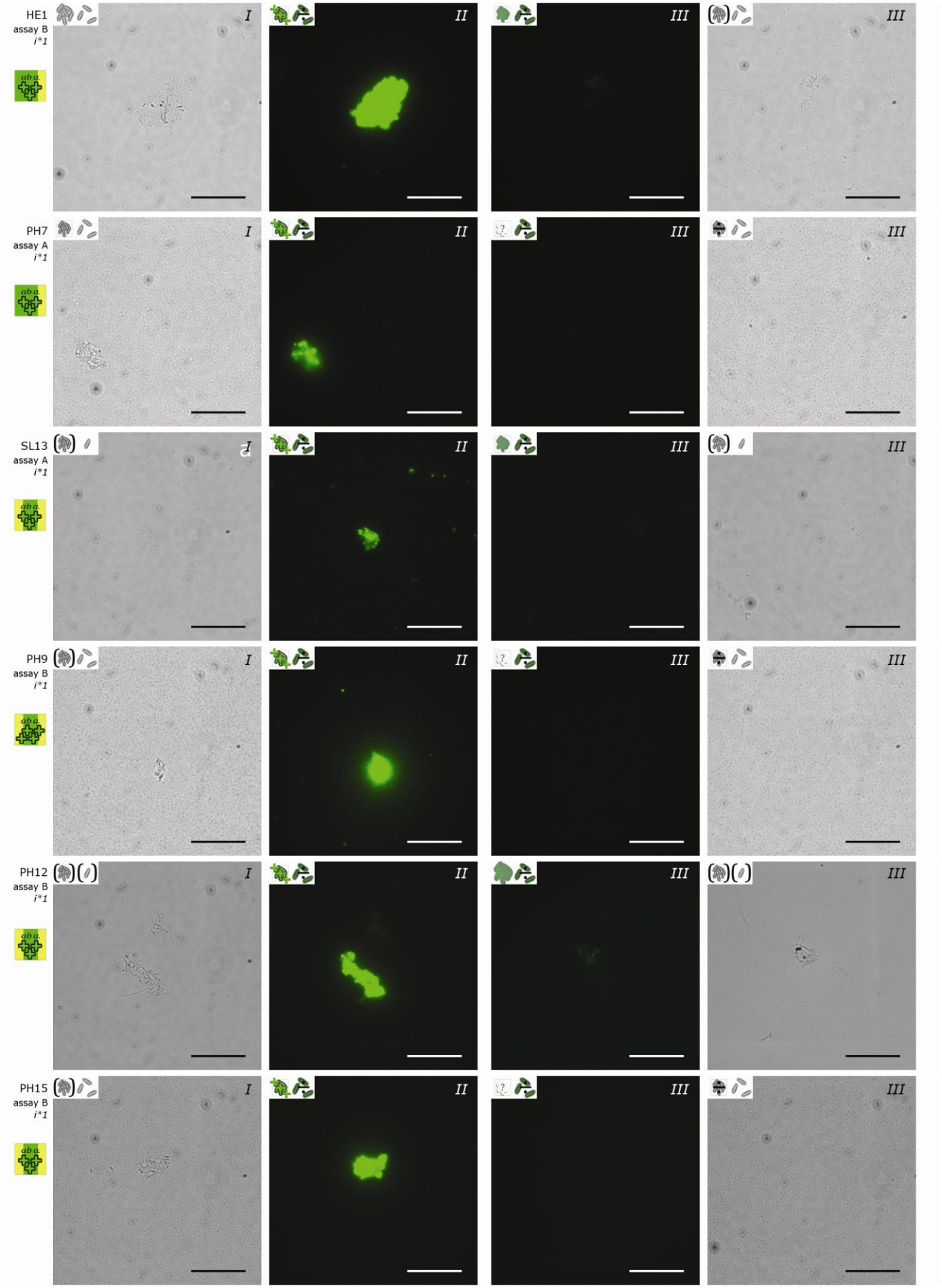
HE1
assay B
i*1
I
II
III
III
PH7
assay A
i*1
I
II
III
III
SL13
assay A
i*1
I
II
III
III
PH9
assay B
i*1
I
II
III
III
PH12
assay B
i*1
I
II
III
III
PH15
assay B
i*1
I
II
III
III

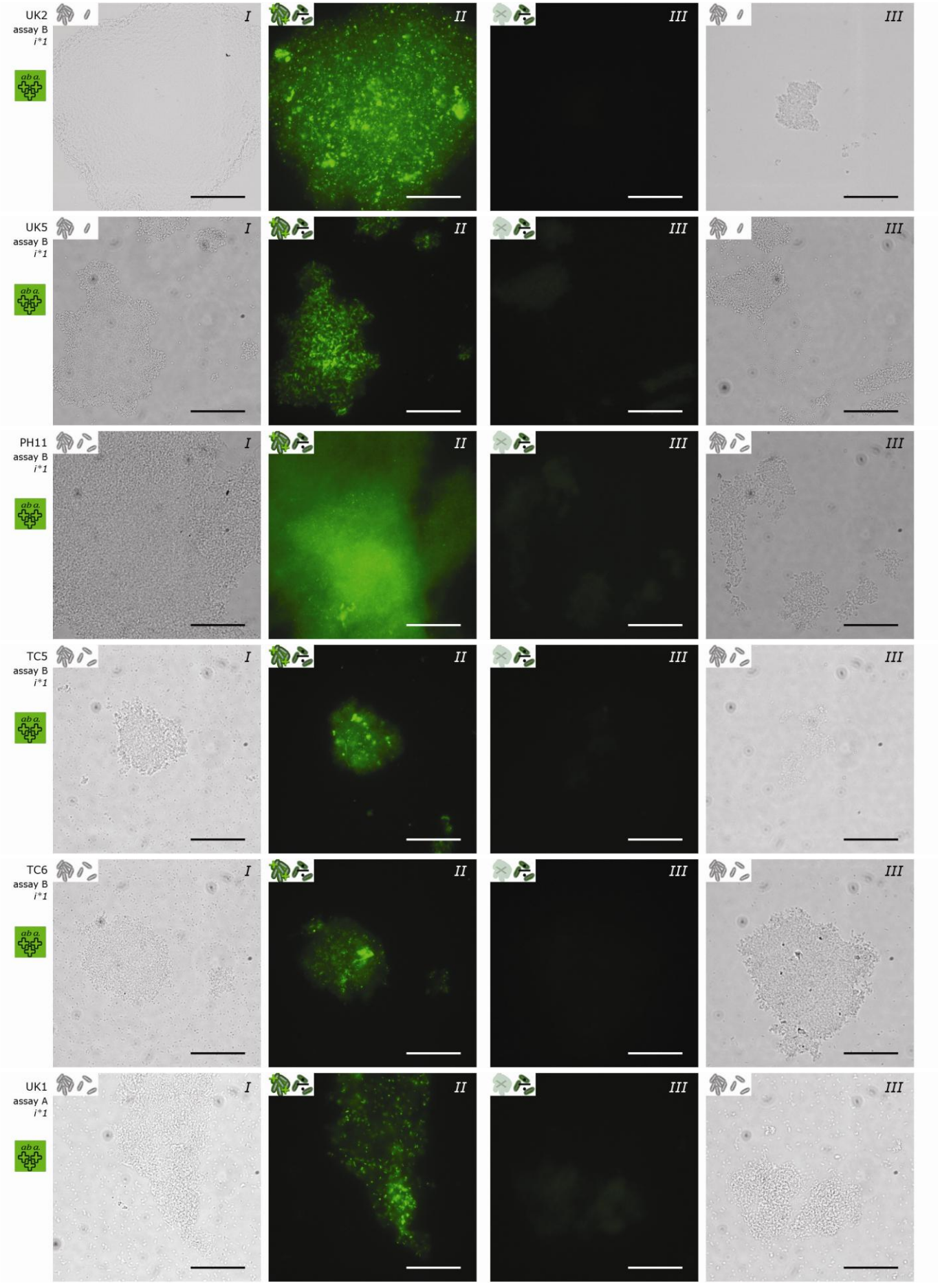
UK2
assay B
i*1
I
II
III
III
UK5
assay B
i*1
I
II
III
III
PH11
assay B
i*1
I
II
III
III
TC5
assay B
i*1
I
II
III
III
TC6
assay B
i*1
I
II
III
III
UK1
assay A
i*1
I
II
III
III

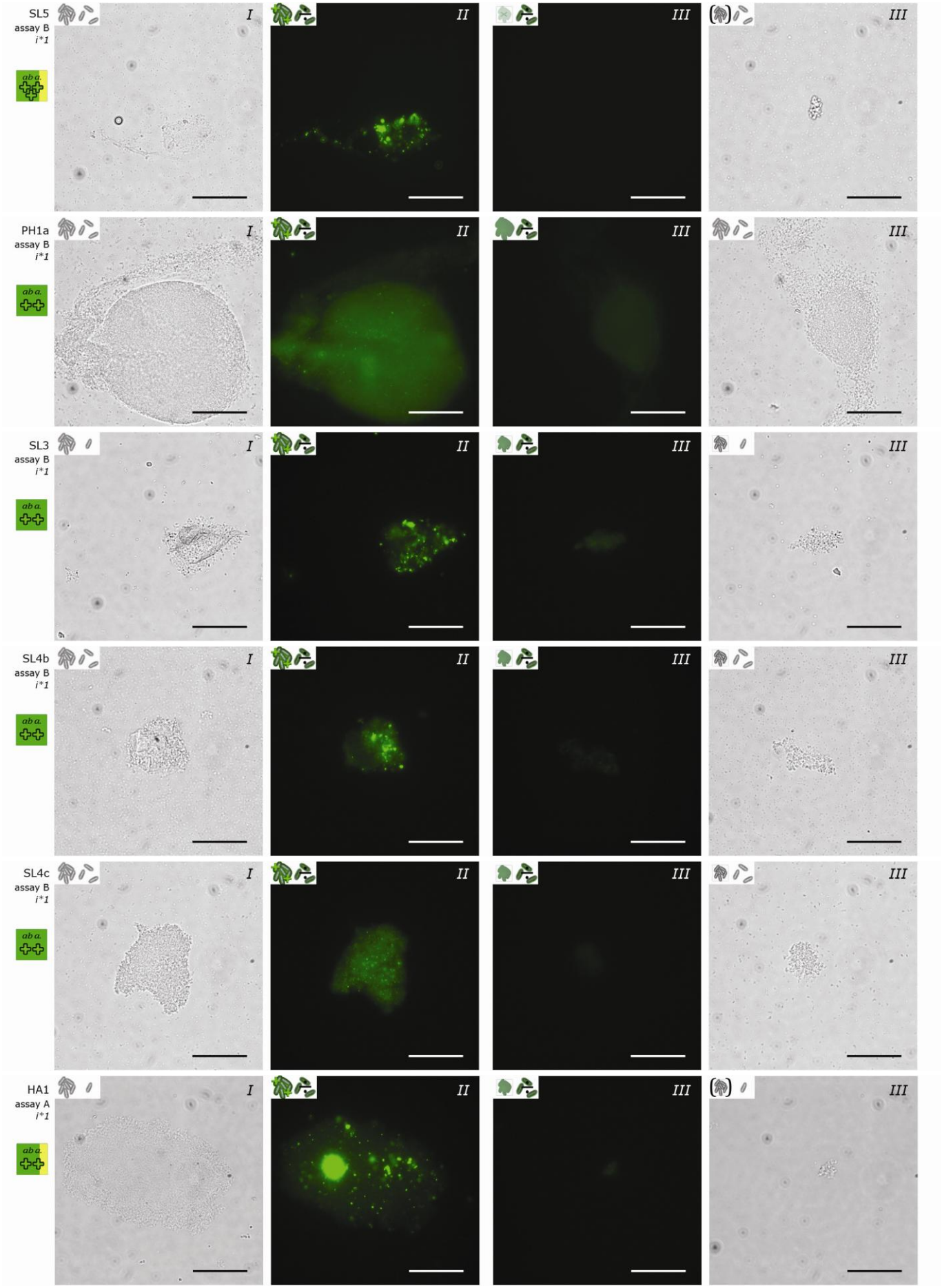
SL5
assay B
i*1
aba.
I
II
III
III
PH1a
assay B
i*1
aba.
I
II
III
III
SL3
assay B
i*1
aba.
I
II
III
III
SL4b
assay B
i*1
aba.
I
II
III
III
SL4c
assay B
i*1
aba.
I
II
III
III
HA1
assay A
i*1
aba.
I
II
III
III

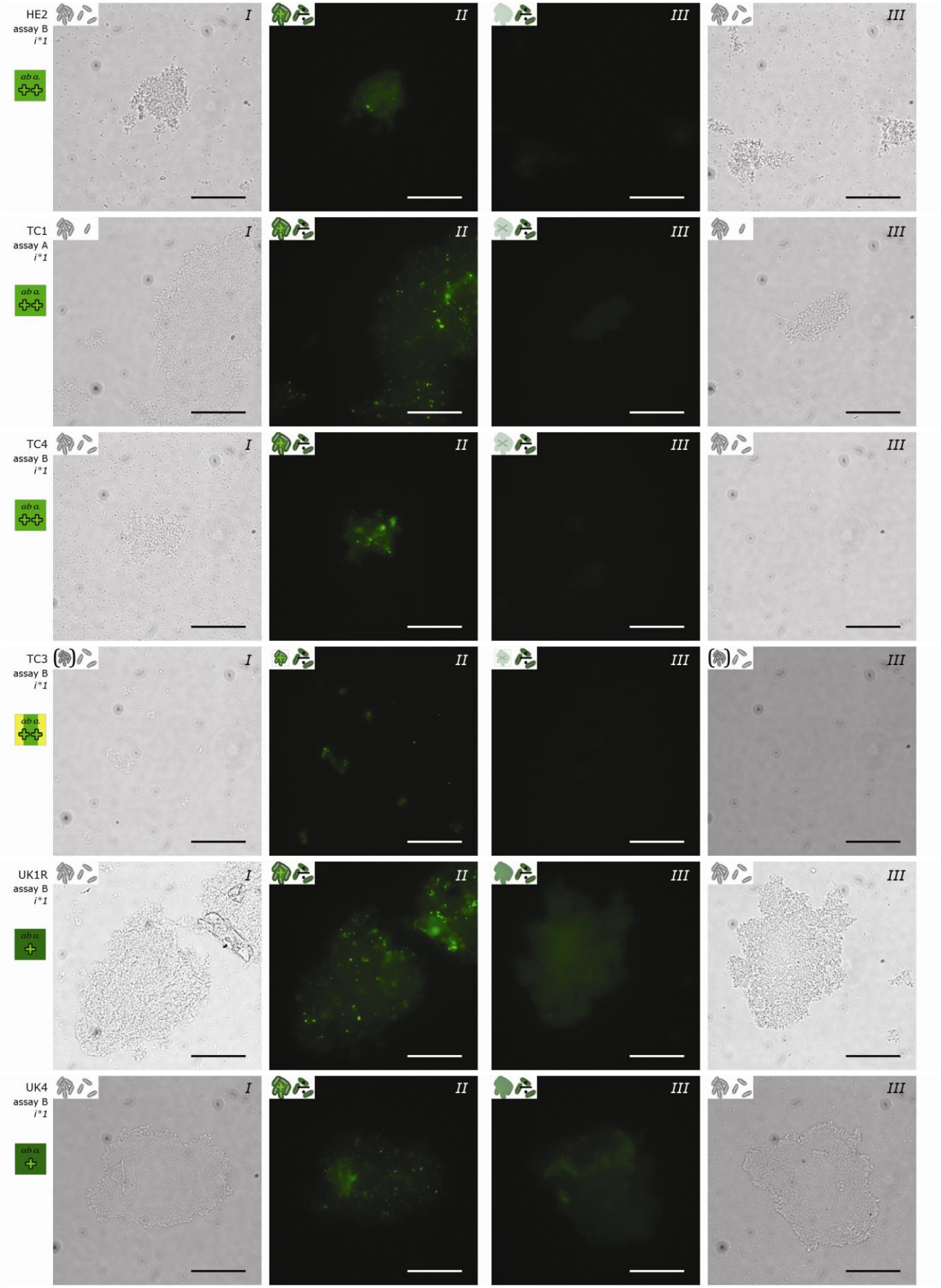
HE2
assay B
i*1
ab a.
I
II
III
III
TC1
assay A
i*1
ab a.
I
II
III
III
TC4
assay B
i*1
ab a.
I
II
III
III
TC3
assay B
i*1
ab a.
I
II
III
III
UK1R
assay B
i*1
ab a.
I
II
III
III
UK4
assay B
i*1
ab a.
I
II
III
III

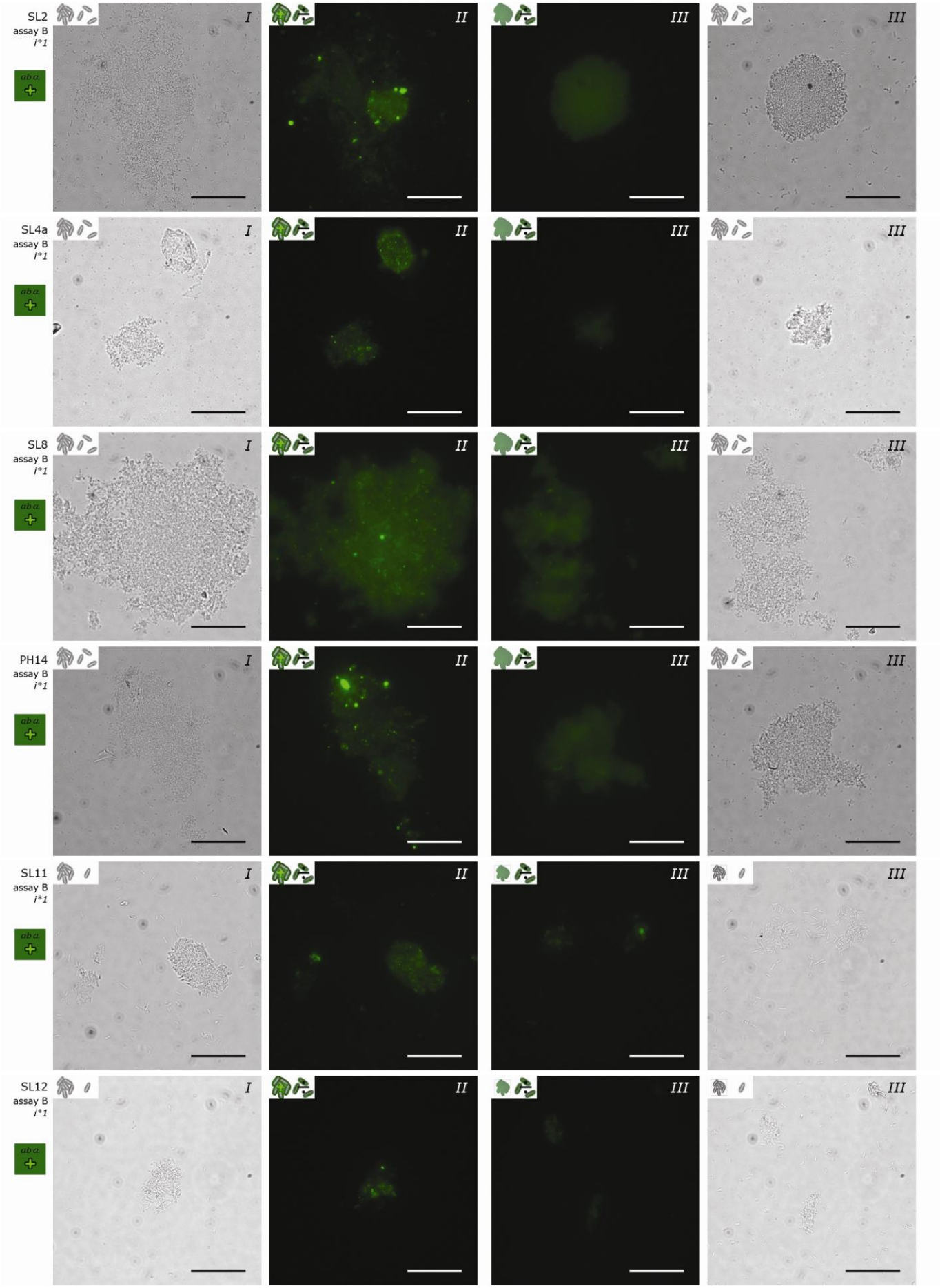
SL2
assay B
i*1
aba
+
I
II
III
III
SL4a
assay B
i*1
aba
+
I
II
III
III
SL8
assay B
i*1
aba
+
I
II
III
III
PH14
assay B
i*1
aba
+
I
II
III
III
SL11
assay B
i*1
aba
+
I
II
III
III
SL12
assay B
i*1
aba
+
I
II
III
III

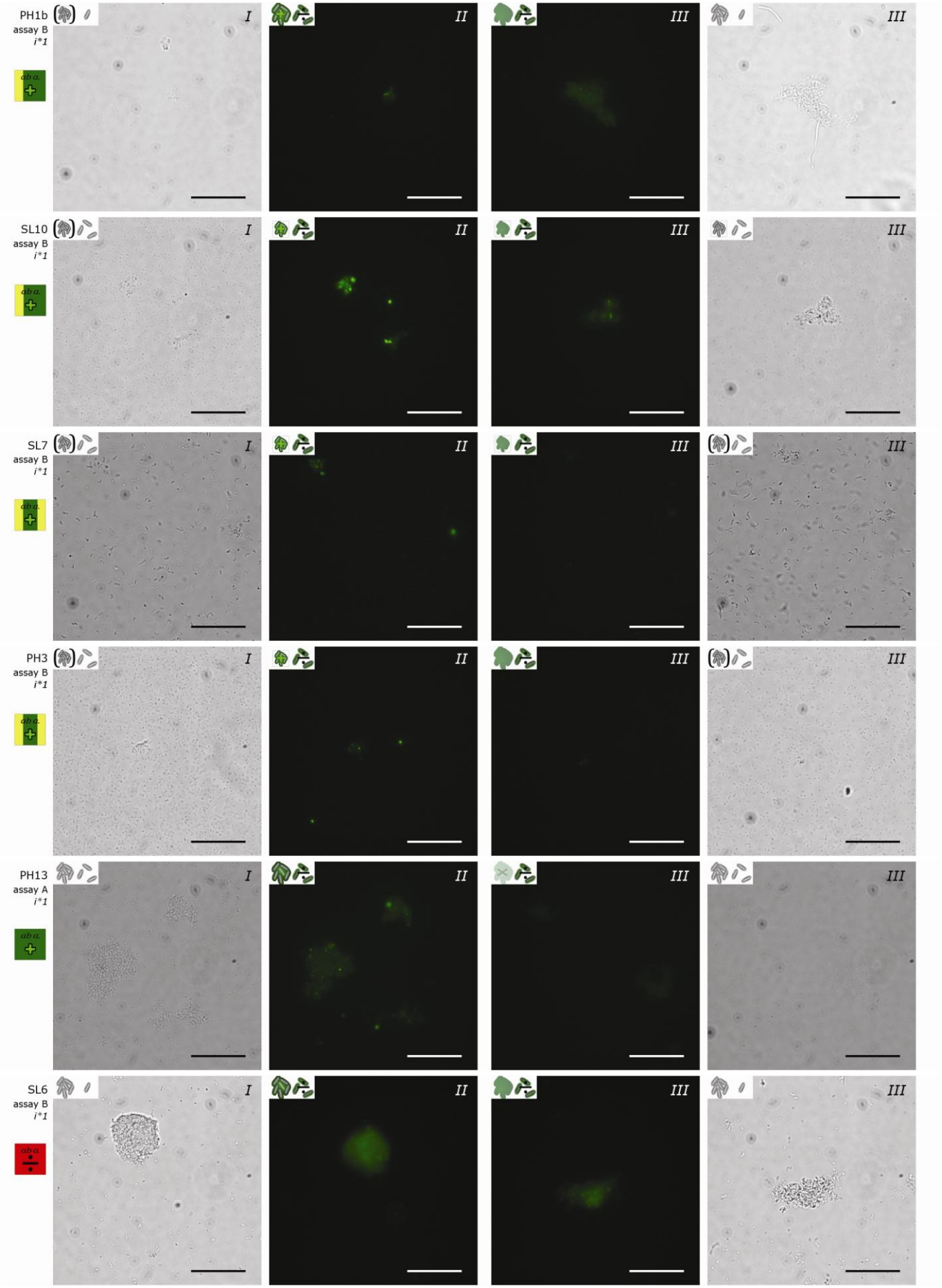
PH1b
assay B
i*1
I
II
III
III
SL10
assay B
i*1
I
II
III
III
SL7
assay B
i*1
I
II
III
III
PH3
assay B
i*1
I
II
III
III
PH13
assay A
i*1
I
II
III
III
SL6
assay B
i*1
I
II
III
III

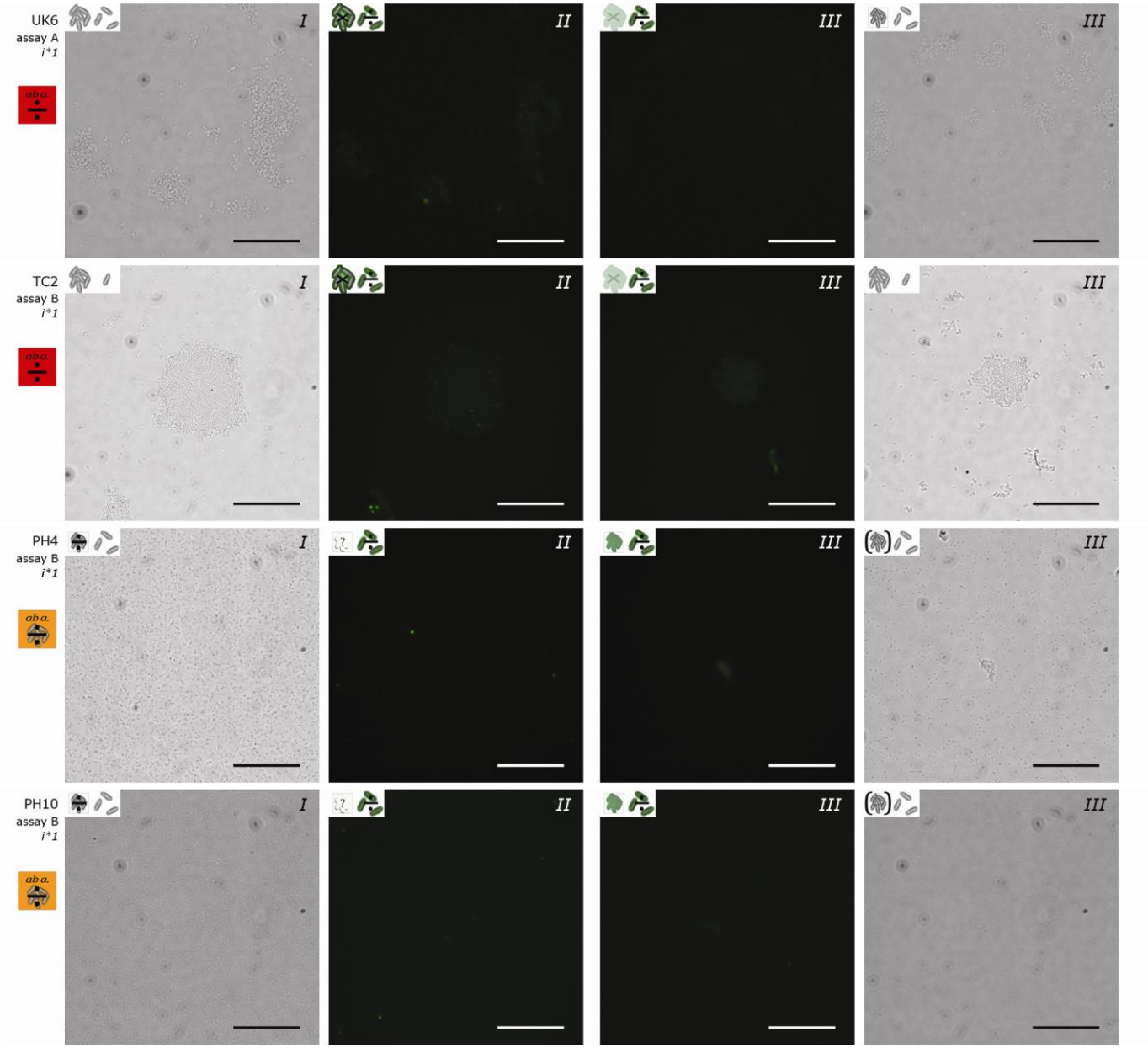

Fig. 11. Immunofluroscense assay on bacteria using WO1 conformational specific antibodies that targets the amyloid epitobe. The degree to which WO1 binds to each bacteria is catogorised for easy comparison. The catogorisation, based on awarding of icons, is explained in Fig. 8. Incubation conditions of bacteria: i*1: 5 days in 10 ml CFA medium (50 ml greiner tube), i*2: 5 days in 10 ml CFA medium with antibotics (50 ml greiner tube), i*3: 2 days in 10 ml CFA medium with antibotics, i*4: 5 days in 20 ml TSB medium (50 ml erli er meyer flask), i*5: 5 days in 10 ml TSB medium (50 ml greiner tube), i*6: unknown.

Appendix B

SDS-PAGE of ±FA pre-threated *p_FuBA*

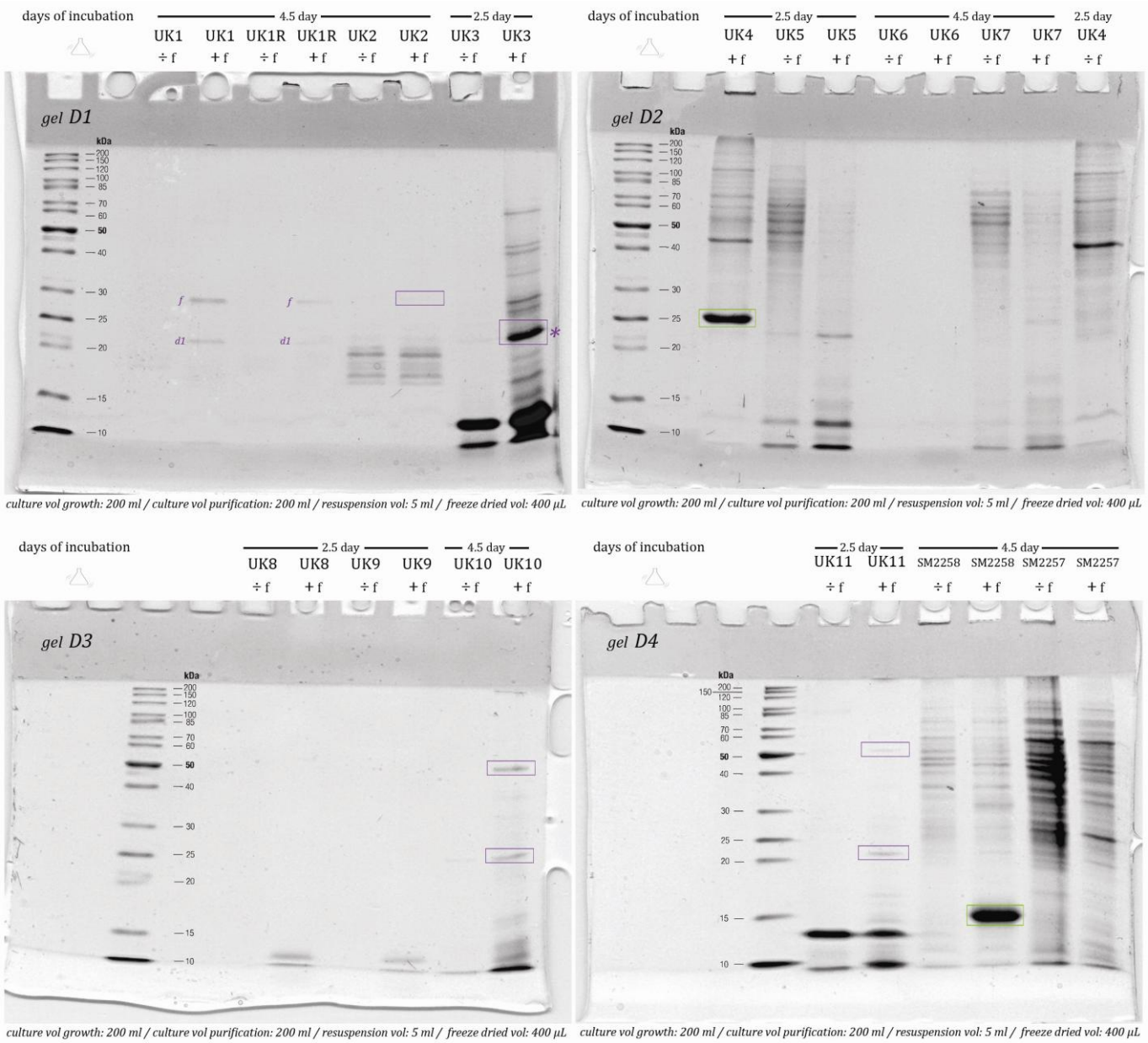

Fig. 12. SDS-PAGE of +/÷ FA pre-threated FuBA purified from UK1-UK11.

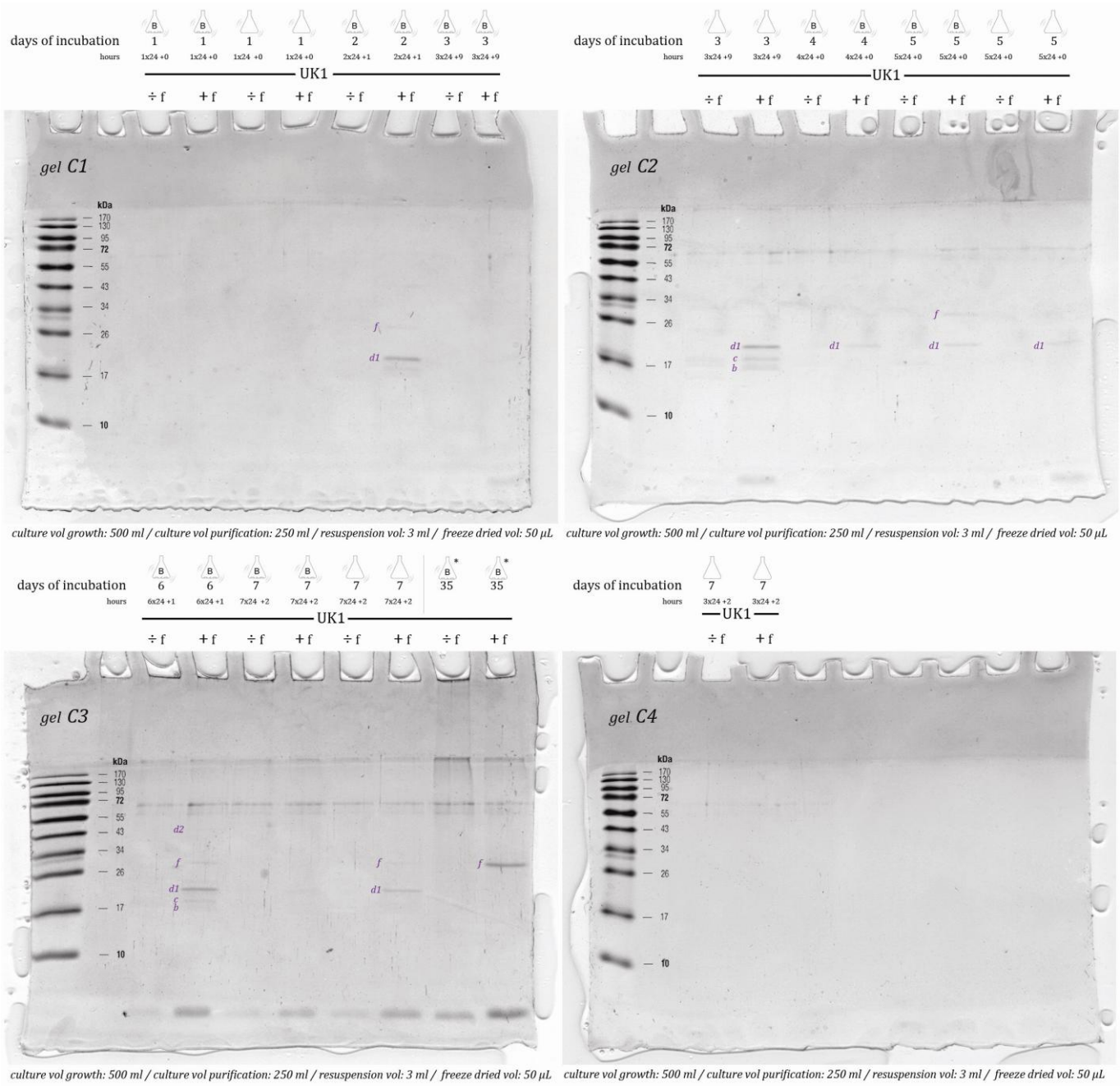

Fig. 13. SDS-PAGE of +/÷ FA pre-threated FuBA purified from UK1 after 1-7 days of incubation in erlienmyer flask with and without baffeles at 26°C and 200rpm. The UK1 cultures were all inocoluated at 0 hours from a starter culture after growth at 26°C and 200rpm for 3 days, at which time the culture could be homogenised without flocs uevently distrubted in suspension. *Gel C4*: UK1 was incubated at room temperature for 7 days with no shaking. Gel C3 lane 1 and 2 from the right: * marks a culture that were inoculated directly from a 44% glycerole UK1 stock, incubated at 26°C and 200rpm for 10 days, and then placed at room temperature wiht no shaking for 25 days until harvest. FuBA was purifeid using 8× enzyme mix.

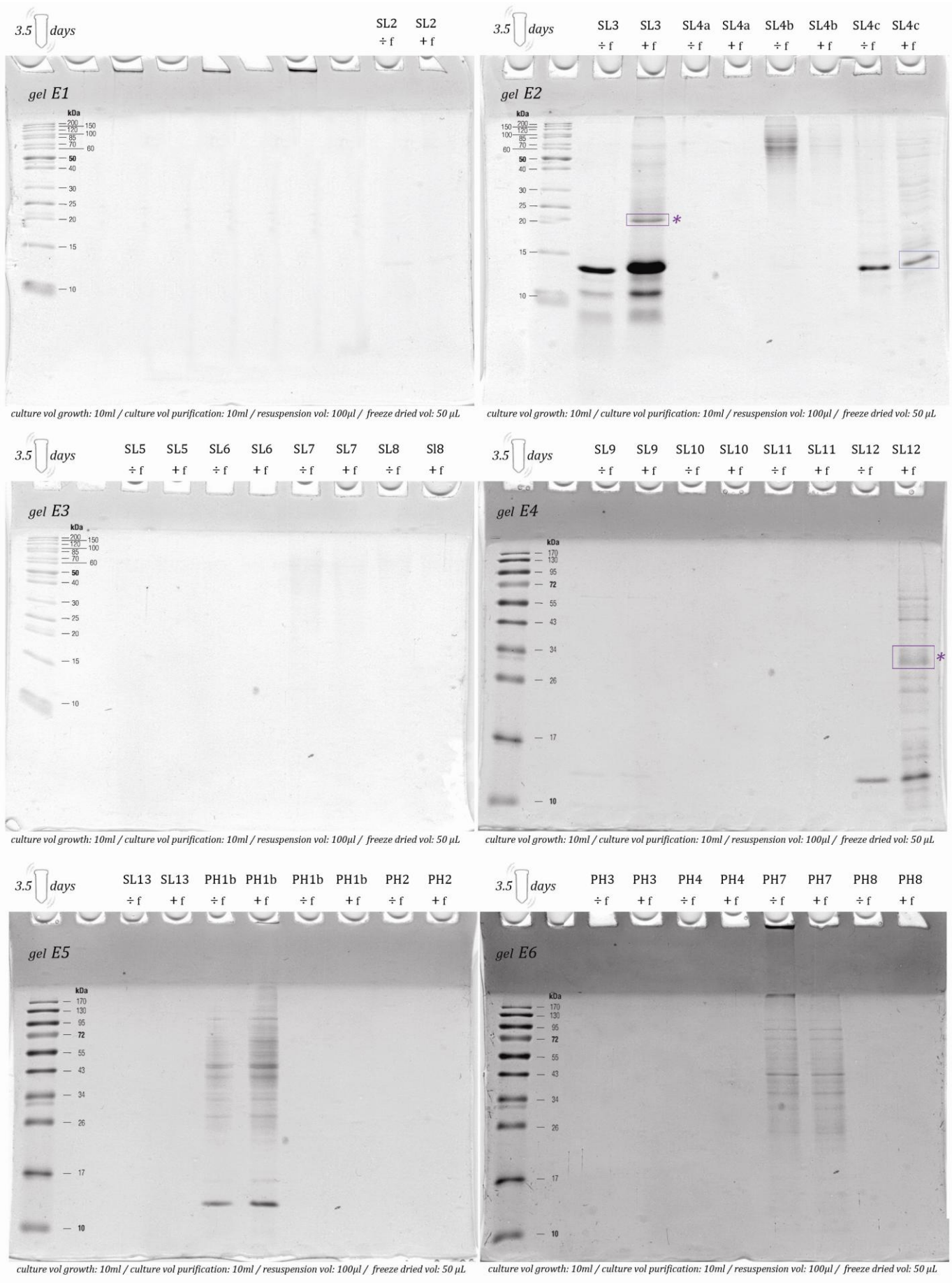

Fig. 14 SDS-PAGE of +/÷ FA pre-threated FuBA. The bacterial isolates were incubated in 10 ml CFA medium at 26°C and 200rpm for 3.5 days prior to FuBA purification.

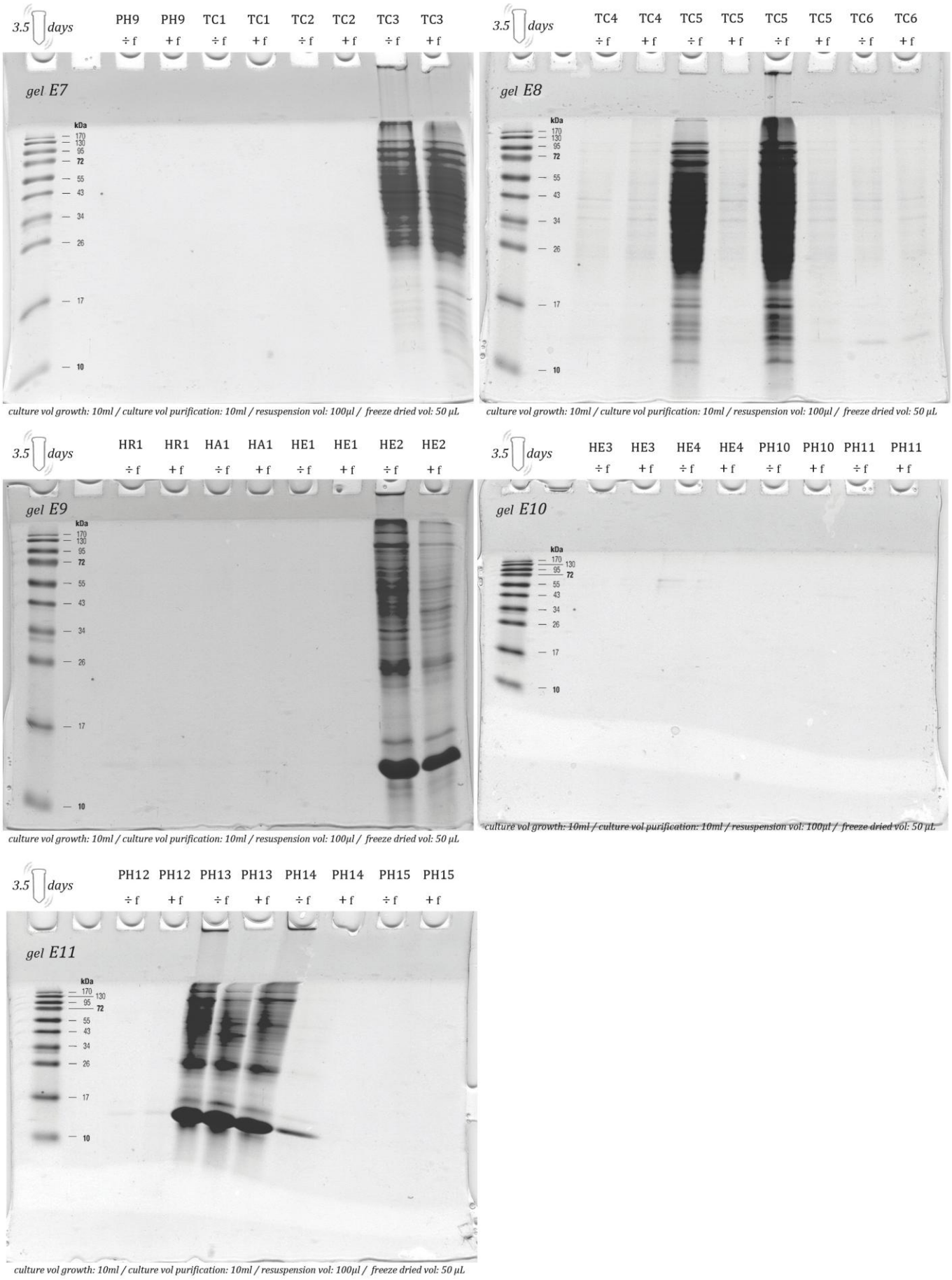

Fig. 15. SDS-PAGE of +/÷ FA pre-threated FuBA. The bacterial isolates were incubated in 10 ml CFA medium at 26°C and 200rpm for 3.5 days prior to FuBA purification.

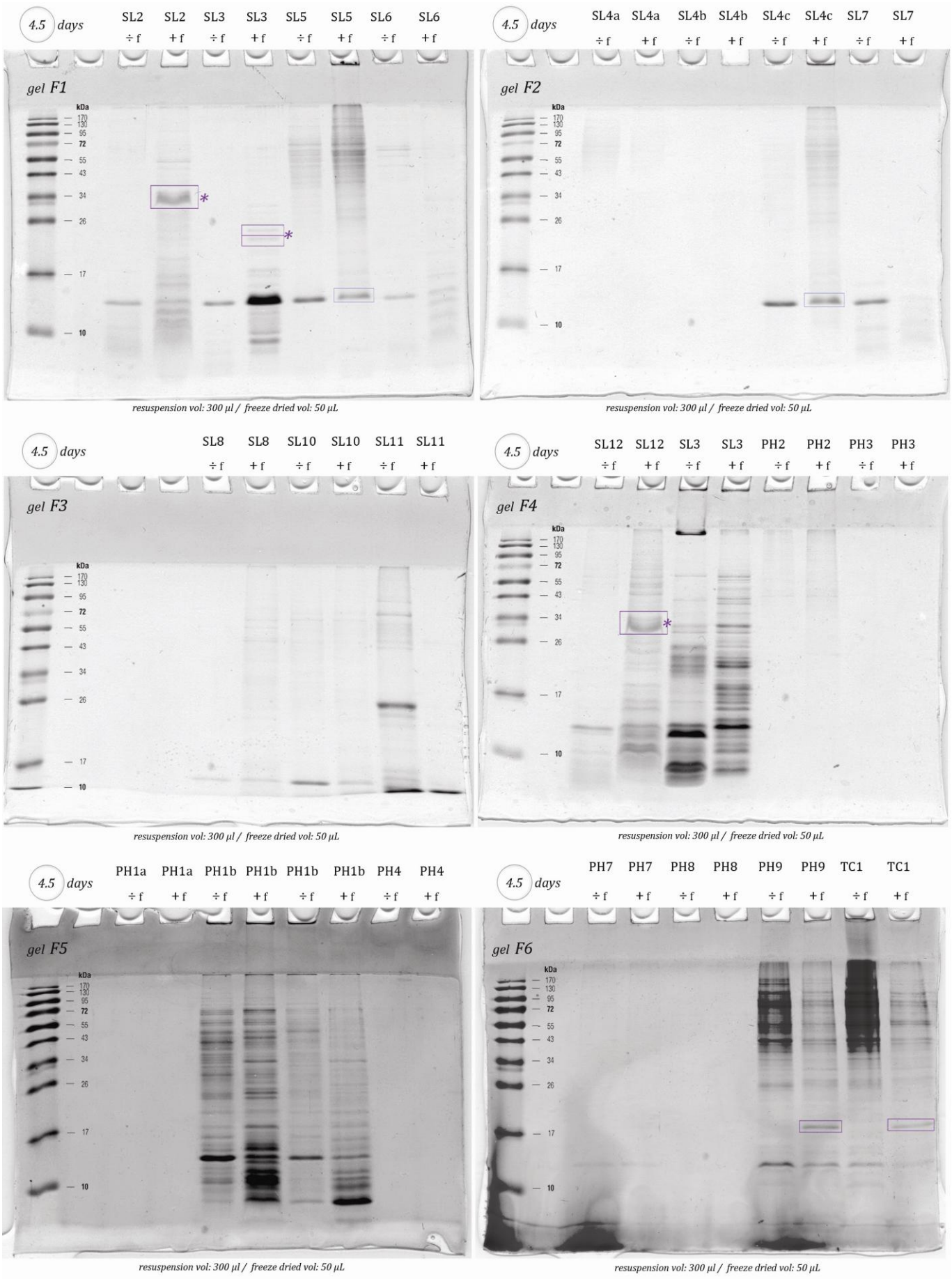

Fig. 16. SDS-PAGE of +/÷ FA pre-threated FuBA. The bacterial isolates were grown on agar plates at 26°C for 4.5 days prior to FuBA purification.

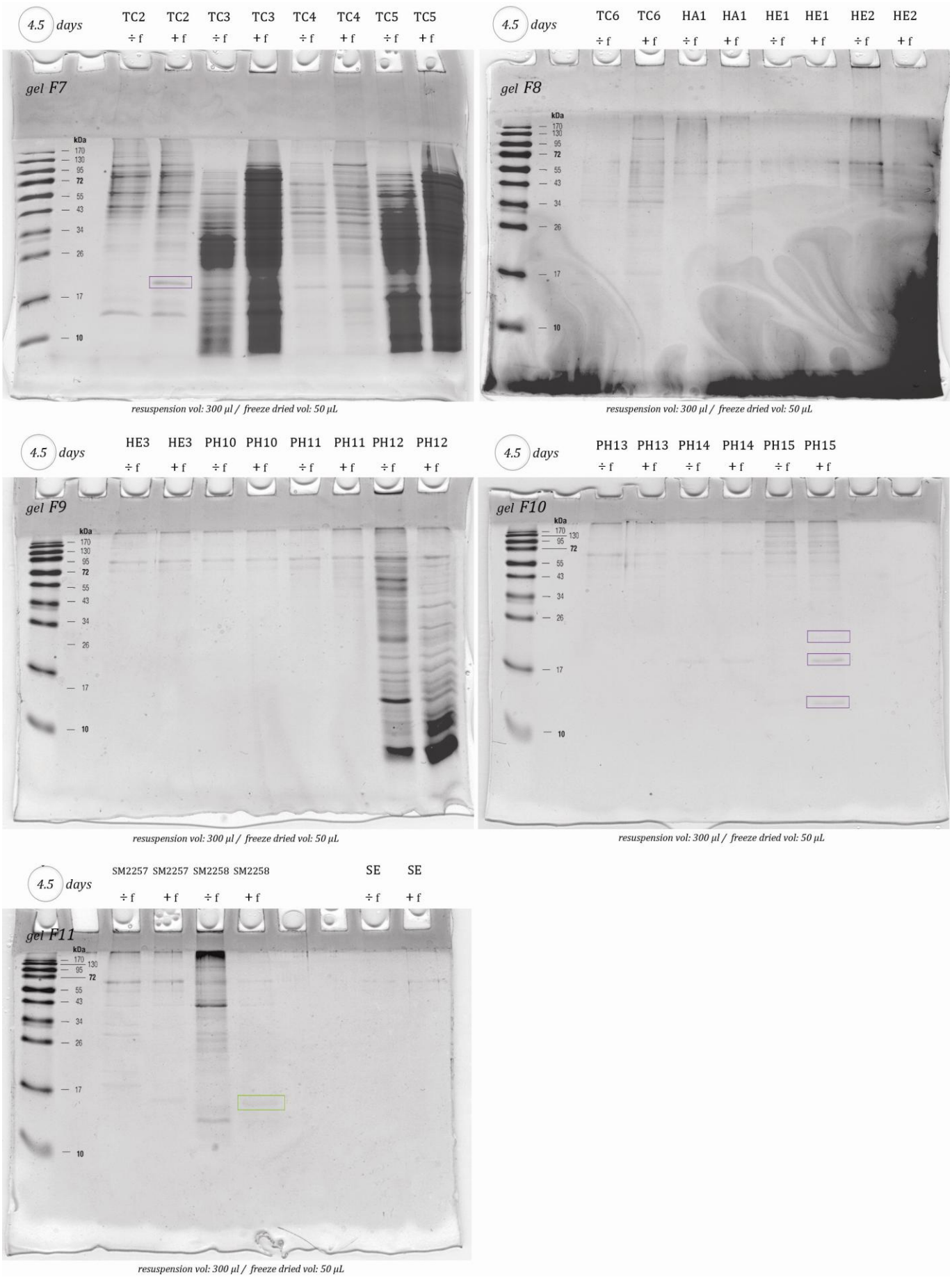

Fig. 17. SDS-PAGE of +/÷ FA pre-threated FuBA. The bacterial isolates were grown on agar plates at 26°C for 4.5 days prior to FuBA purification.

Appendix C

ATR-FTIR of *p_FUBA*

ATR-FTIR was used to detect secondary structure elements in *p_FuBA*. To identify absorption peaks in each interferogram the local minima of the second derivative are plotted on the graph using the matlab function peakdet. The FTIR interferograms can be observed below, and are categorised as given in Table 4:

Table 4. categorisation-system of ATR-FTIR spectra of *p_FUBA*

		Maximum itensity of amide I band		
		AU > 0.3	0.3 ≤ AU ≤ 1.5	AU < 1.5
	Color of figure header bar			
	Intensity range on y-axis of infeogram	[0:1]	[0:0.3]	[0:0.2]
	Peakdet δ-value	0.005	0.00014	-
Maximum intensity of absorption band at 1611-1630 cm^{-1} ($A_{amyloid}$) VS. maximum intensity of absorption band > 1630 cm^{-1} ($A_{\beta\text{-sheet}}$)	$A_{\beta\text{-sheet}} << A_{amyloid}$	1	1	÷A
	$A_{\beta\text{-sheet}}) < A_{amyloid}$	2	2	÷A
	$A_{\beta\text{-sheet}}) \approx A_{amyloid}$ (one peak with two components)	3	3	÷A
	$A_{\beta\text{-sheet}}) > A_{amyloid}$	4	4	÷A
	$A_{\beta\text{-sheet}})$ ~~$A_{amyloid}$~~	÷	÷	÷A

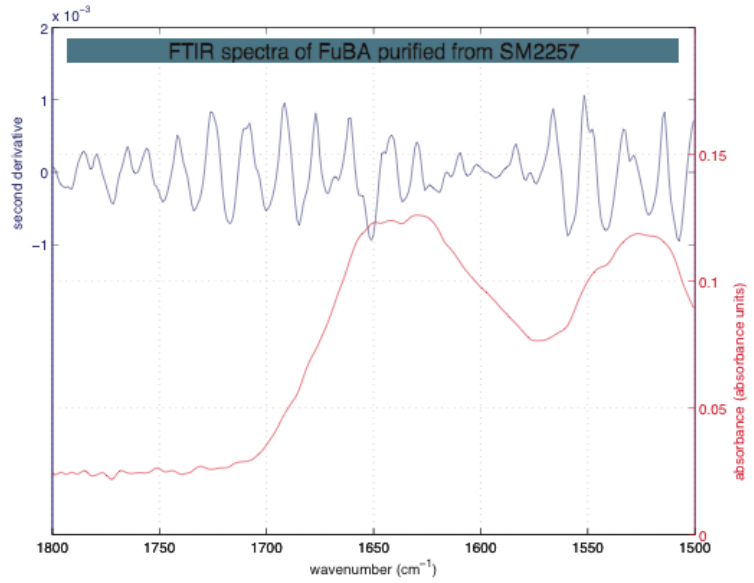
FTIR spectra of FuBA purified from SM2257
second derivative
absorbance (absorbance units)
wavenumber (cm^{-1})

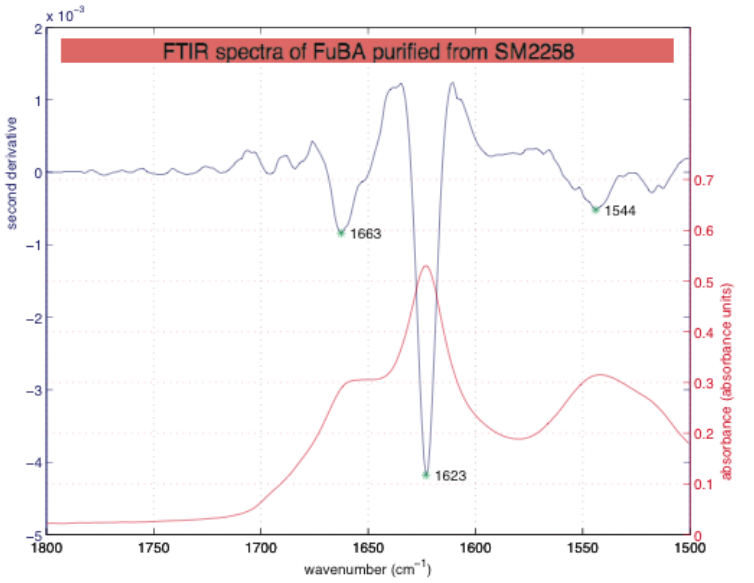
FTIR spectra of FuBA purified from SM2258
1663
1544
1623
second derivative
absorbance (absorbance units)
wavenumber (cm^{-1})

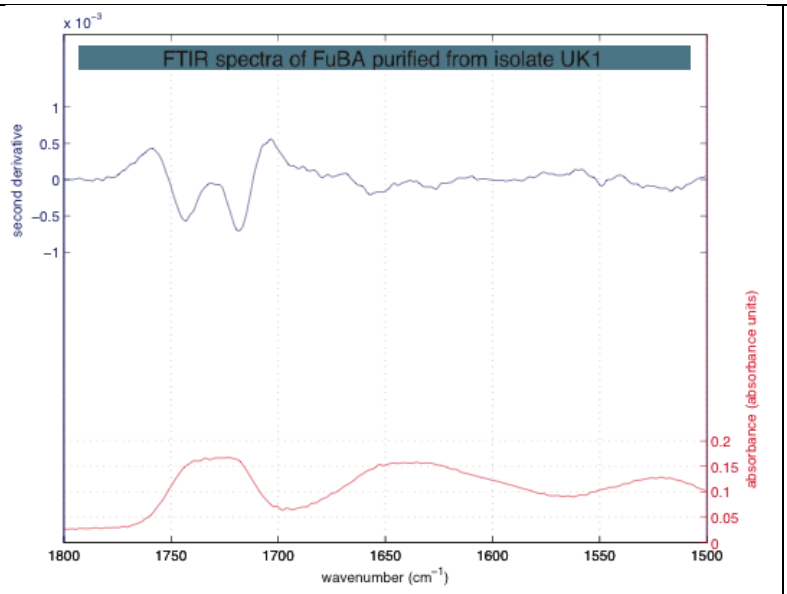
FTIR spectra of FuBA purified from isolate UK1
second derivative
absorbance (absorbance units)
wavenumber (cm^{-1})

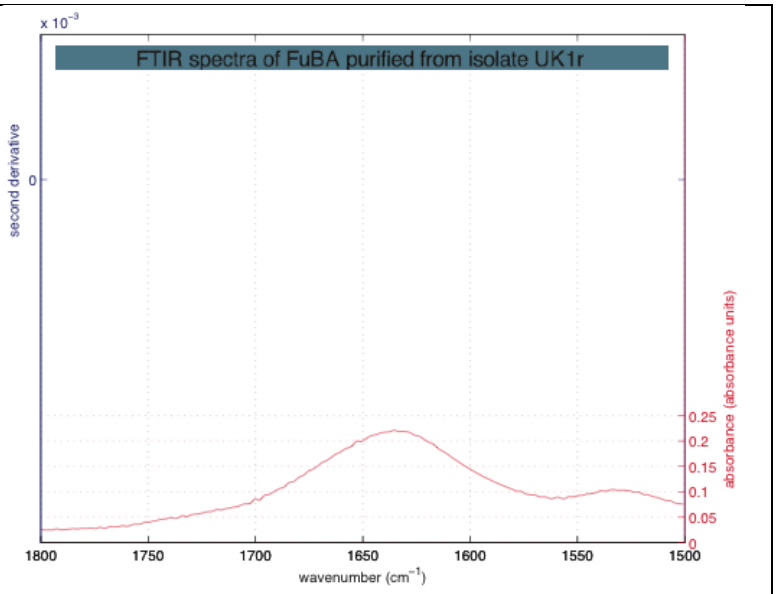
FTIR spectra of FuBA purified from isolate UK1r
second derivative
absorbance (absorbance units)
wavenumber (cm^{-1})

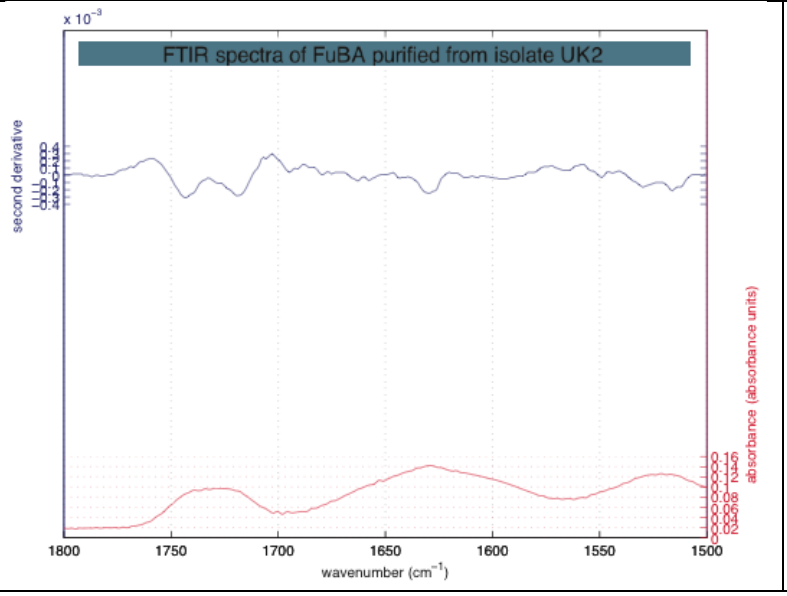
FTIR spectra of FuBA purified from isolate UK2
second derivative
absorbance (absorbance units)
wavenumber (cm^{-1})

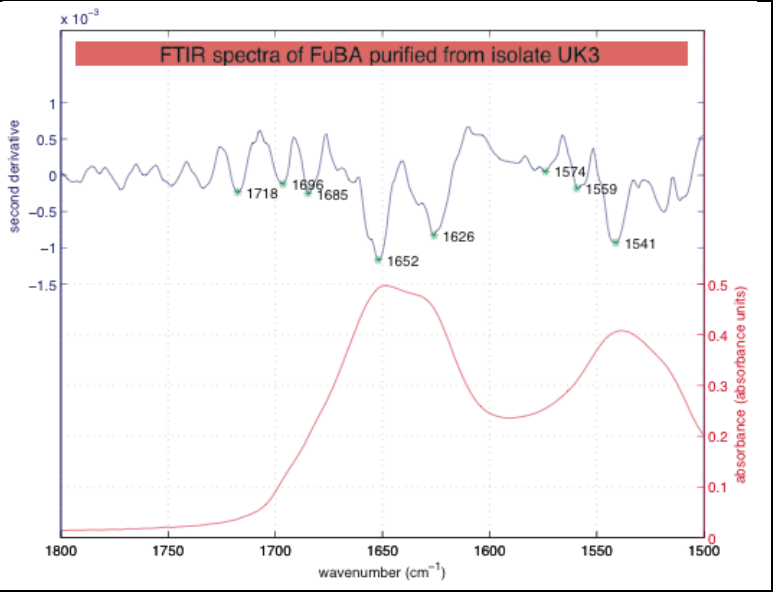
FTIR spectra of FuBA purified from isolate UK3
1718
1696
1685
1652
1626
1574
1559
1541
second derivative
absorbance (absorbance units)
wavenumber (cm^{-1})

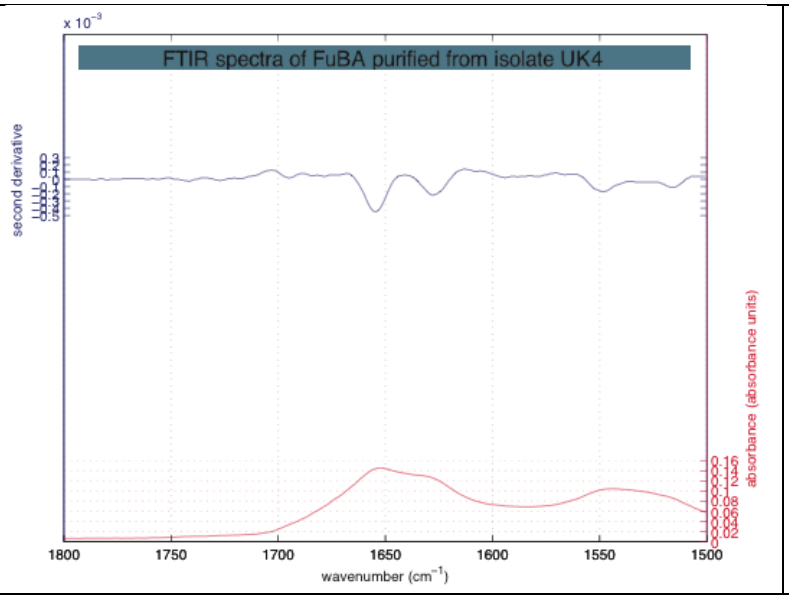
FTIR spectra of FuBA purified from isolate UK4
x 10^-3
second derivative
absorbance (absorbance units)
wavenumber (cm^-1)
1800
1750
1700
1650
1600
1550
1500

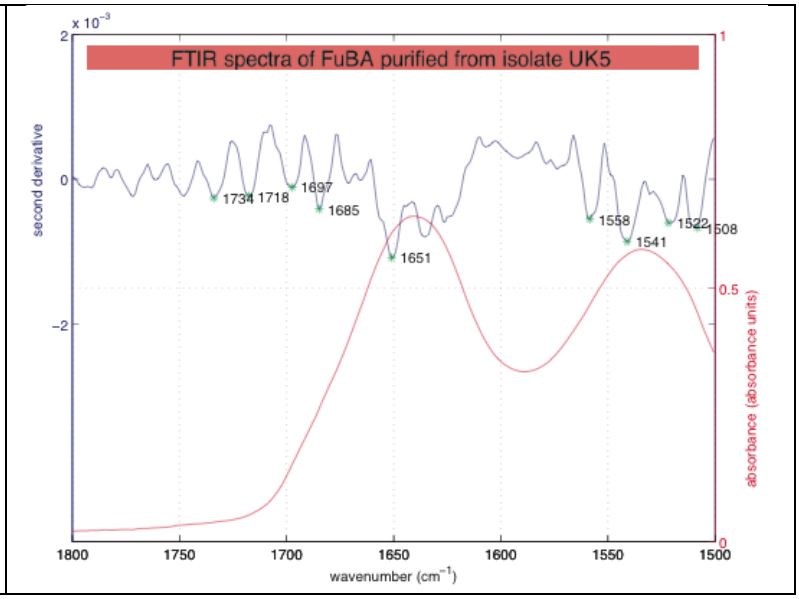
FTIR spectra of FuBA purified from isolate UK5
x 10^-3
second derivative
absorbance (absorbance units)
wavenumber (cm^-1)
1734
1718
1697
1685
1651
1558
1541
1522
1508
1800
1750
1700
1650
1600
1550
1500

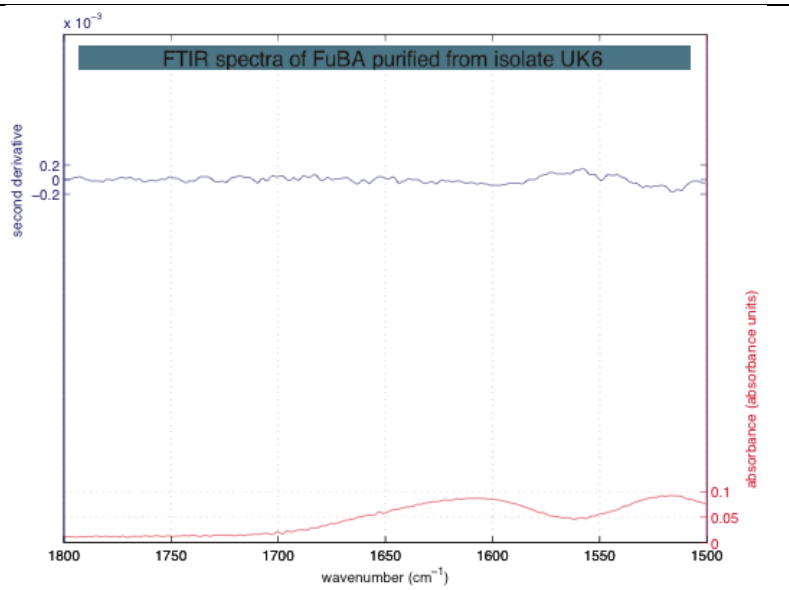
FTIR spectra of FuBA purified from isolate UK6
x 10^-3
second derivative
absorbance (absorbance units)
wavenumber (cm^-1)
1800
1750
1700
1650
1600
1550
1500

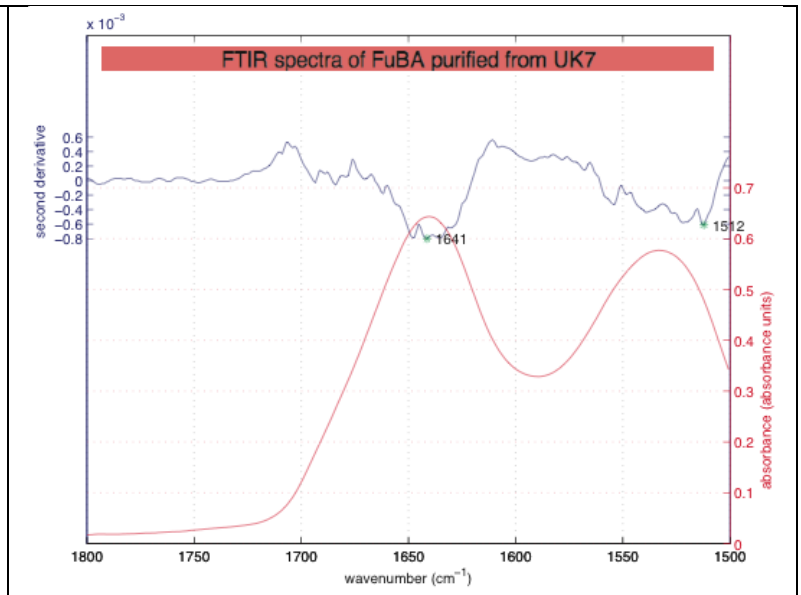
FTIR spectra of FuBA purified from UK7
x 10^-3
second derivative
absorbance (absorbance units)
wavenumber (cm^-1)
1641
1512
1800
1750
1700
1650
1600
1550
1500

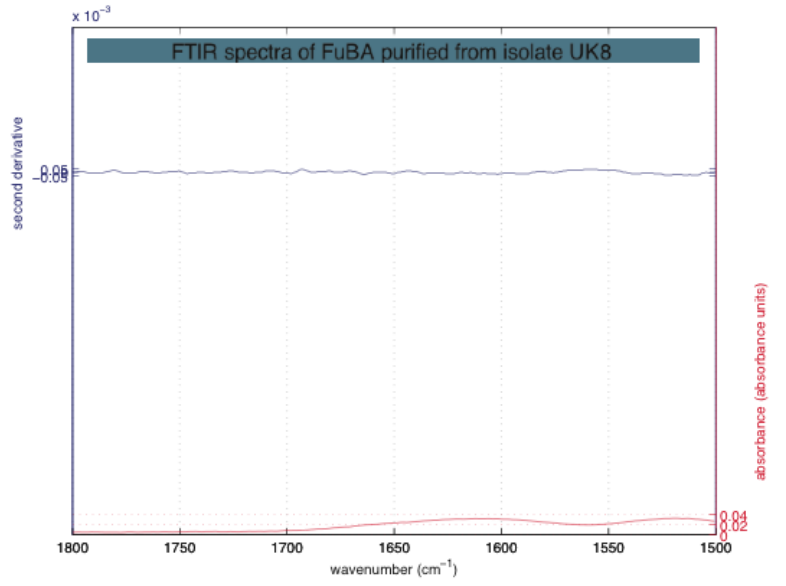
FTIR spectra of FuBA purified from isolate UK8
x 10^-3
second derivative
absorbance (absorbance units)
wavenumber (cm^-1)
1800
1750
1700
1650
1600
1550
1500

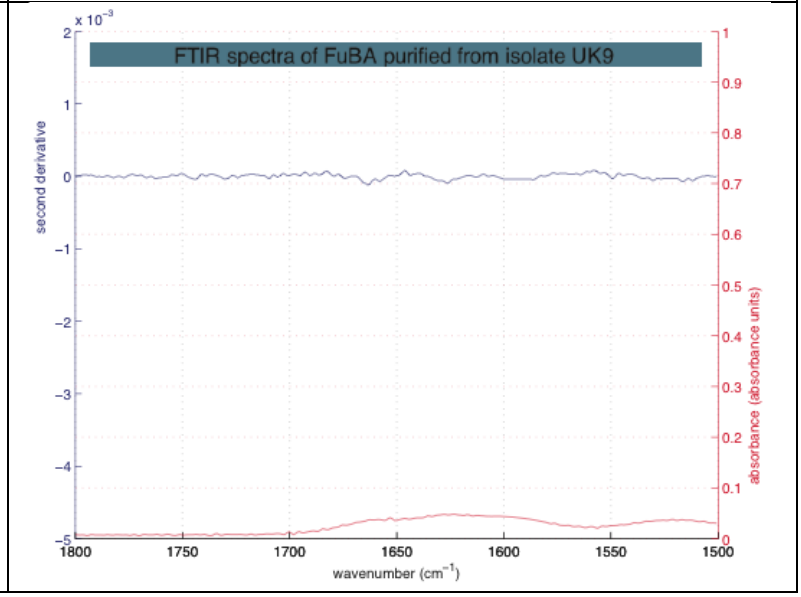
FTIR spectra of FuBA purified from isolate UK9
x 10^-3
second derivative
absorbance (absorbance units)
wavenumber (cm^-1)
1800
1750
1700
1650
1600
1550
1500

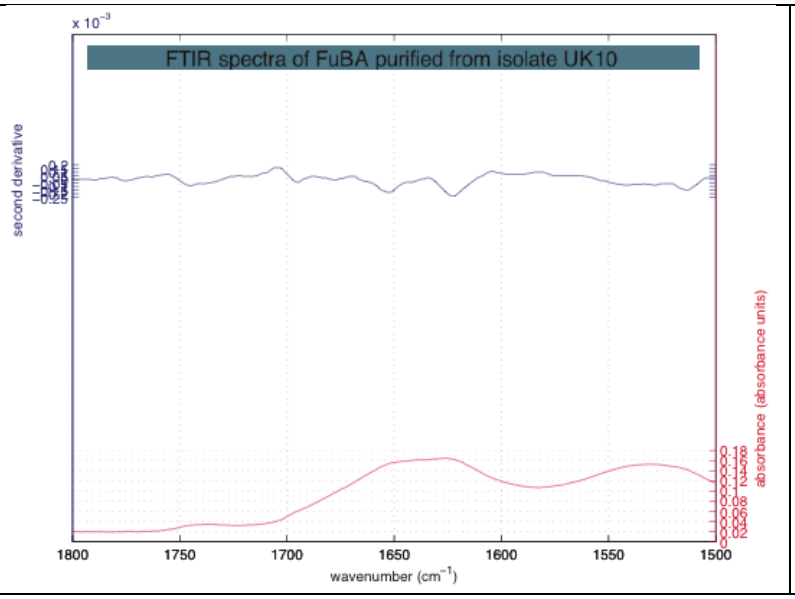
FTIR spectra of FuBA purified from isolate UK10
second derivative
absorbance (absorbance units)
wavenumber (cm^{-1})

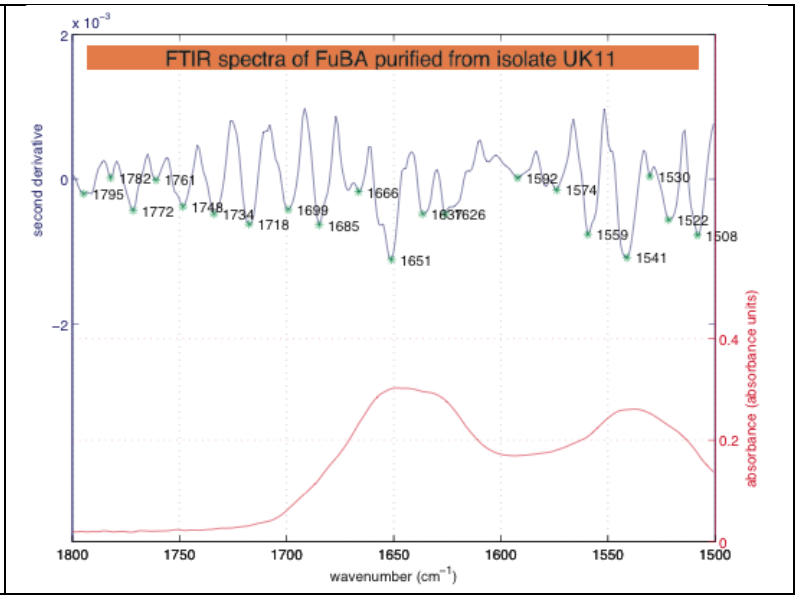
FTIR spectra of FuBA purified from isolate UK11
1795
1782
1772
1761
1748
1734
1718
1699
1685
1666
1651
1637
1626
1592
1574
1559
1541
1530
1522
1508
second derivative
absorbance (absorbance units)
wavenumber (cm^{-1})

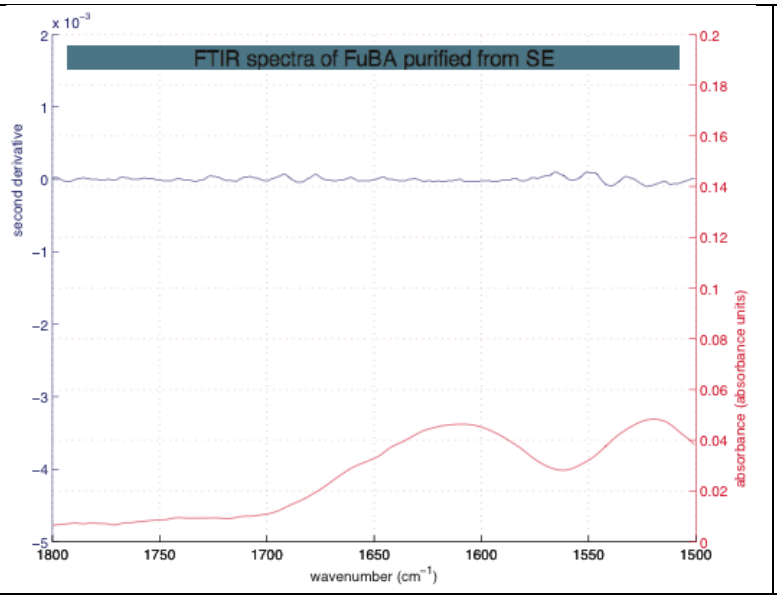
FTIR spectra of FuBA purified from SE
second derivative
absorbance (absorbance units)
wavenumber (cm^{-1})

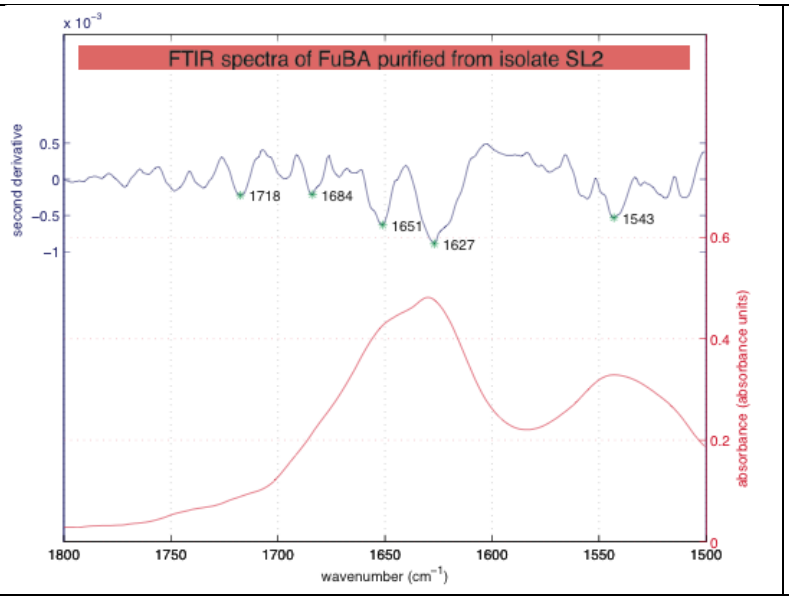
FTIR spectra of FuBA purified from isolate SL2
1718
1684
1651
1627
1543
second derivative
absorbance (absorbance units)
wavenumber (cm^{-1})

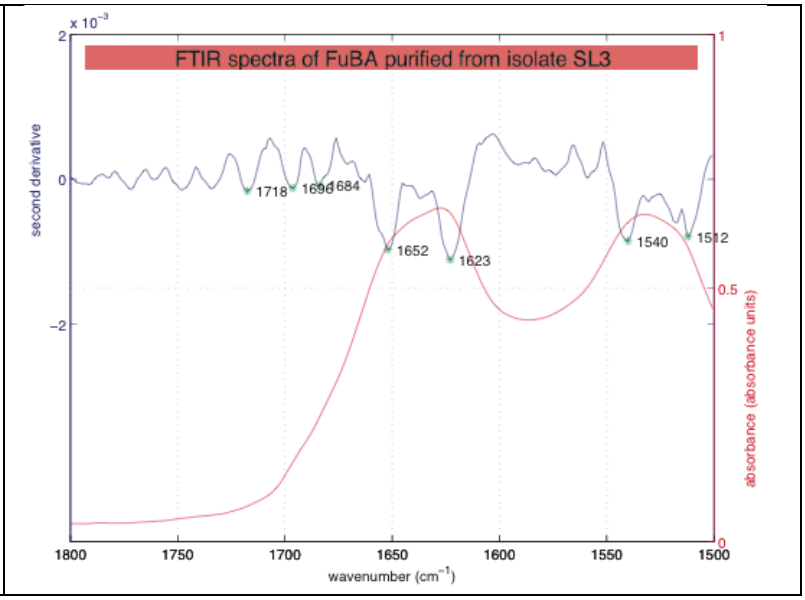
FTIR spectra of FuBA purified from isolate SL3
1718
1696
1684
1652
1623
1540
1512
second derivative
absorbance (absorbance units)
wavenumber (cm^{-1})

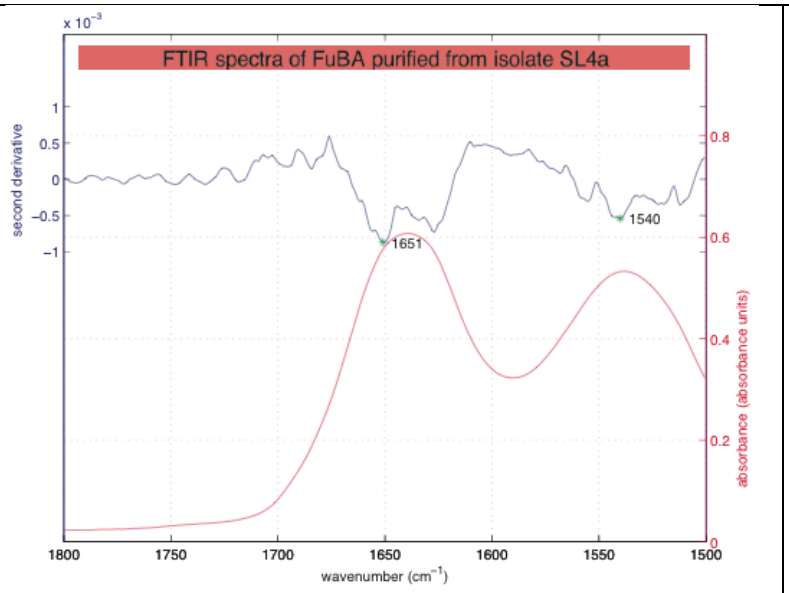
FTIR spectra of FuBA purified from isolate SL4a
x 10^-3
second derivative
absorbance (absorbance units)
wavenumber (cm^-1)
1651
1540

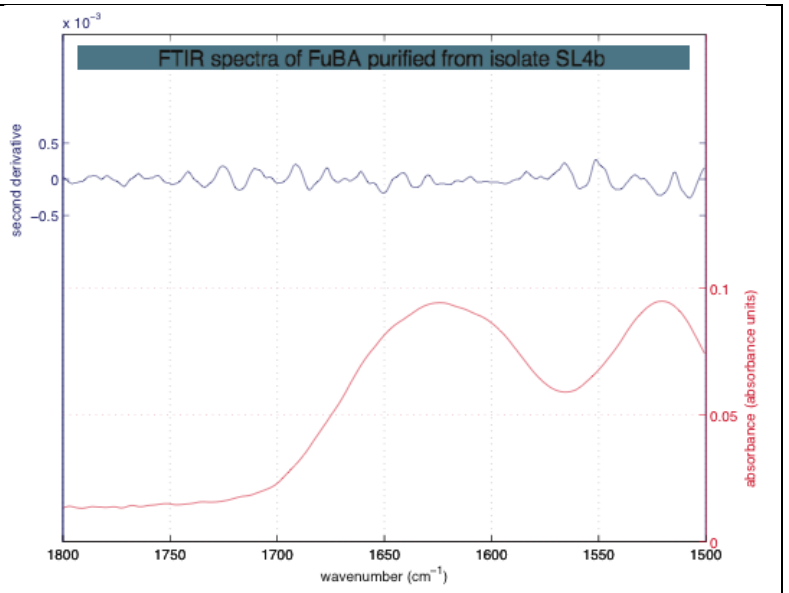
FTIR spectra of FuBA purified from isolate SL4b
x 10^-3
second derivative
absorbance (absorbance units)
wavenumber (cm^-1)

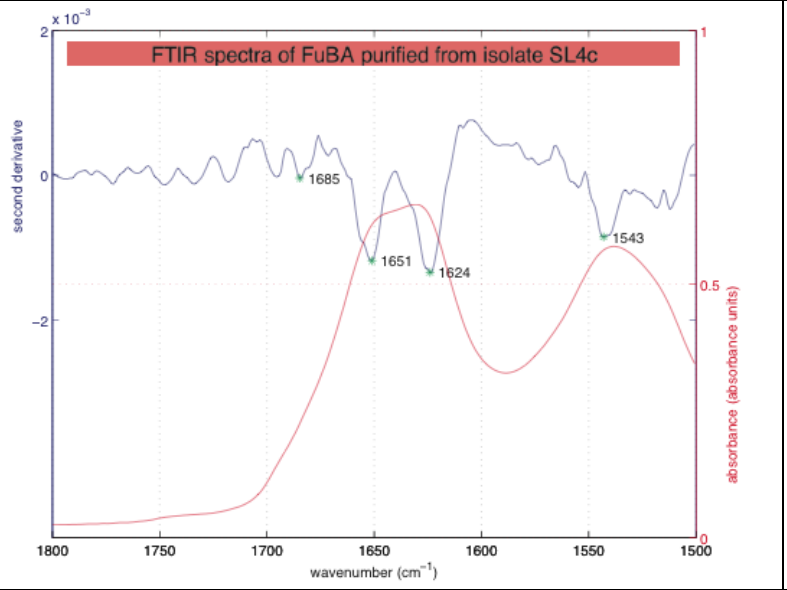
FTIR spectra of FuBA purified from isolate SL4c
x 10^-3
second derivative
absorbance (absorbance units)
wavenumber (cm^-1)
1685
1651
1624
1543

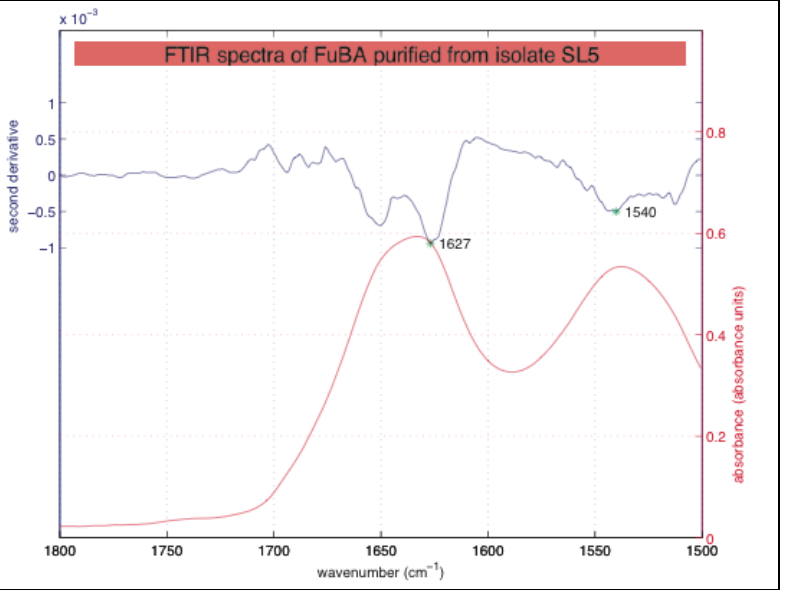
FTIR spectra of FuBA purified from isolate SL5
x 10^-3
second derivative
absorbance (absorbance units)
wavenumber (cm^-1)
1627
1540

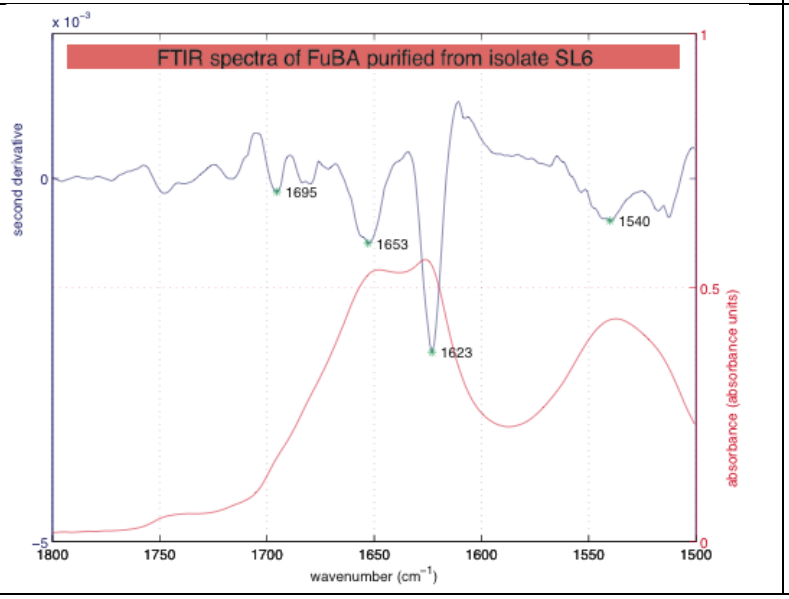
FTIR spectra of FuBA purified from isolate SL6
x 10^-3
second derivative
absorbance (absorbance units)
wavenumber (cm^-1)
1695
1653
1623
1540

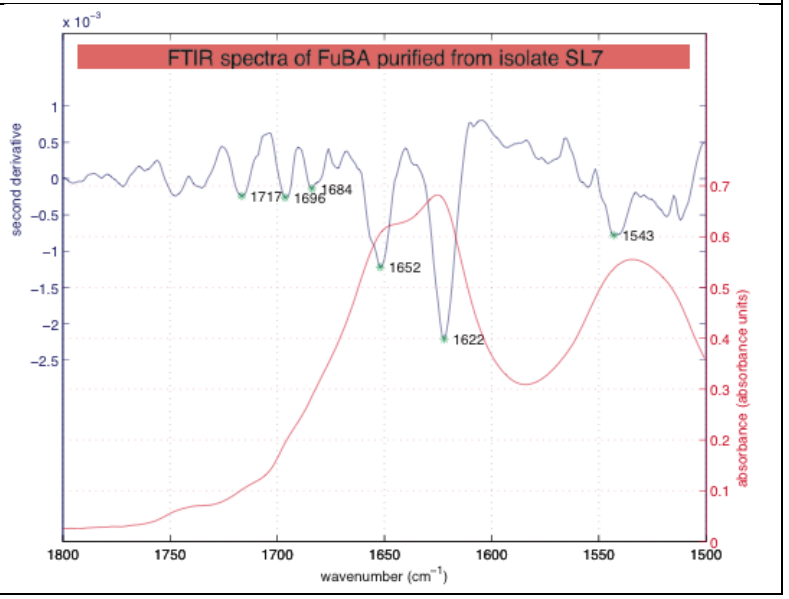
FTIR spectra of FuBA purified from isolate SL7
x 10^-3
second derivative
absorbance (absorbance units)
wavenumber (cm^-1)
1717
1696
1684
1652
1622
1543

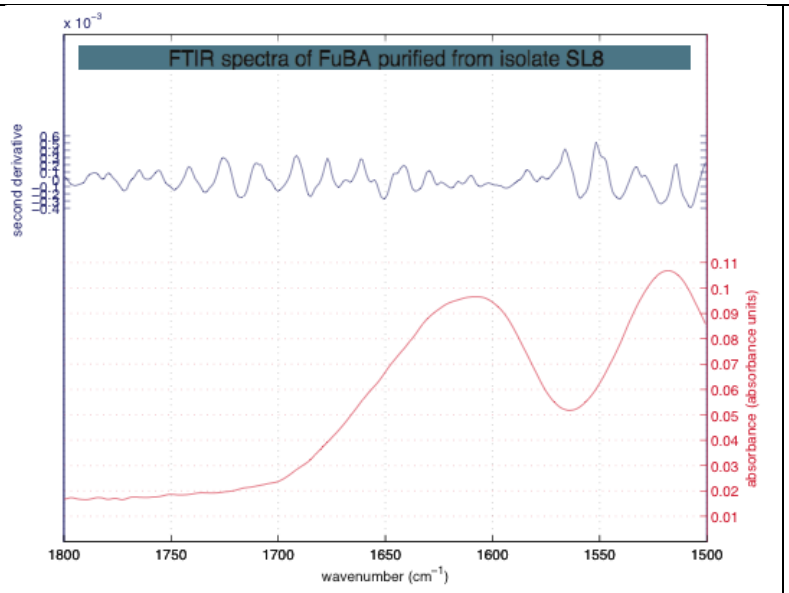
FTIR spectra of FuBA purified from isolate SL8
second derivative
absorbance (absorbance units)
wavenumber (cm^{-1})

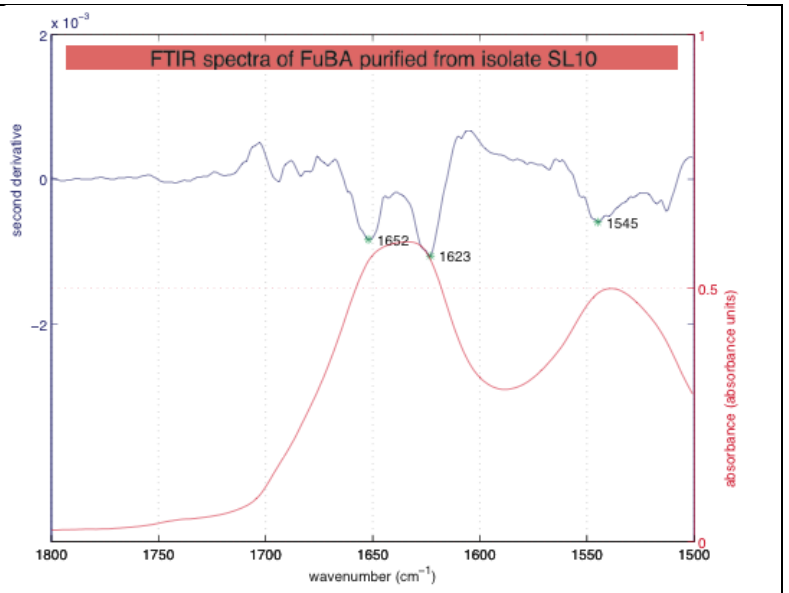
FTIR spectra of FuBA purified from isolate SL10
1652
1623
1545
second derivative
absorbance (absorbance units)
wavenumber (cm^{-1})

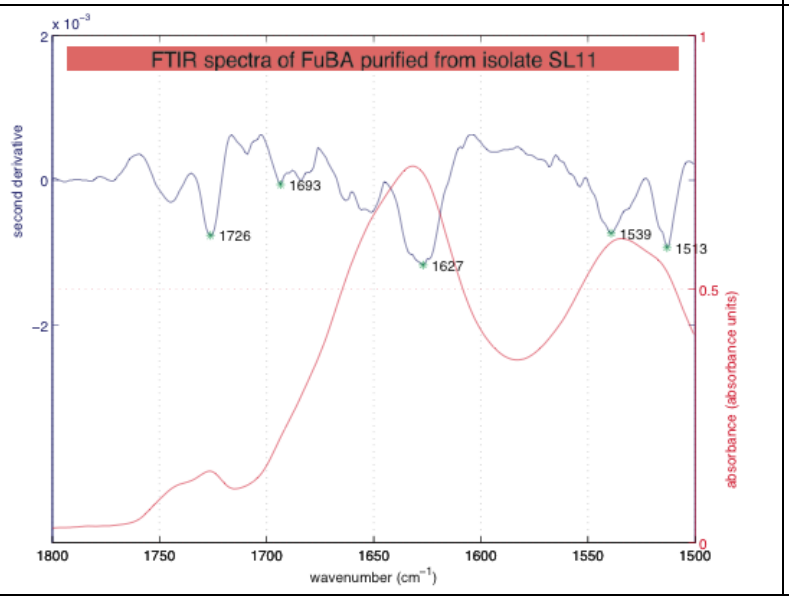
FTIR spectra of FuBA purified from isolate SL11
1726
1693
1627
1539
1513
second derivative
absorbance (absorbance units)
wavenumber (cm^{-1})

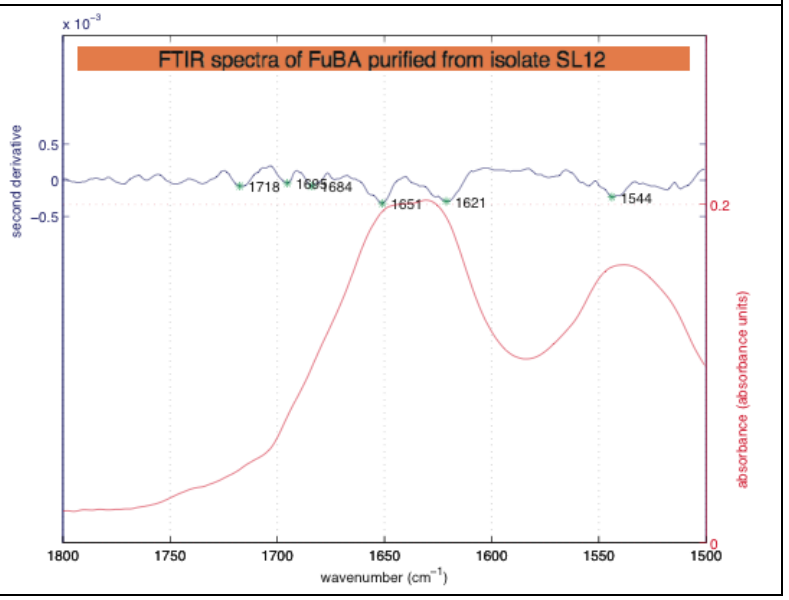
FTIR spectra of FuBA purified from isolate SL12
1718
1695
1684
1651
1621
1544
second derivative
absorbance (absorbance units)
wavenumber (cm^{-1})

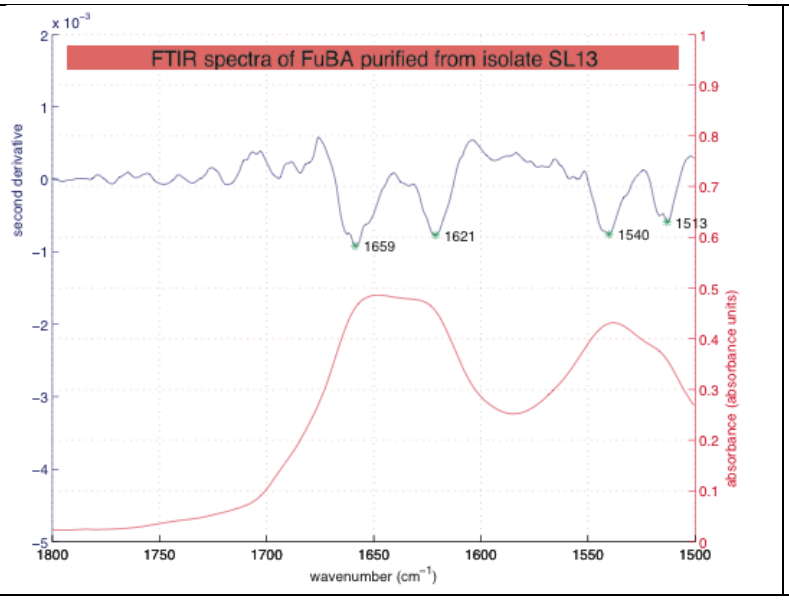
FTIR spectra of FuBA purified from isolate SL13
1659
1621
1540
1513
second derivative
absorbance (absorbance units)
wavenumber (cm^{-1})

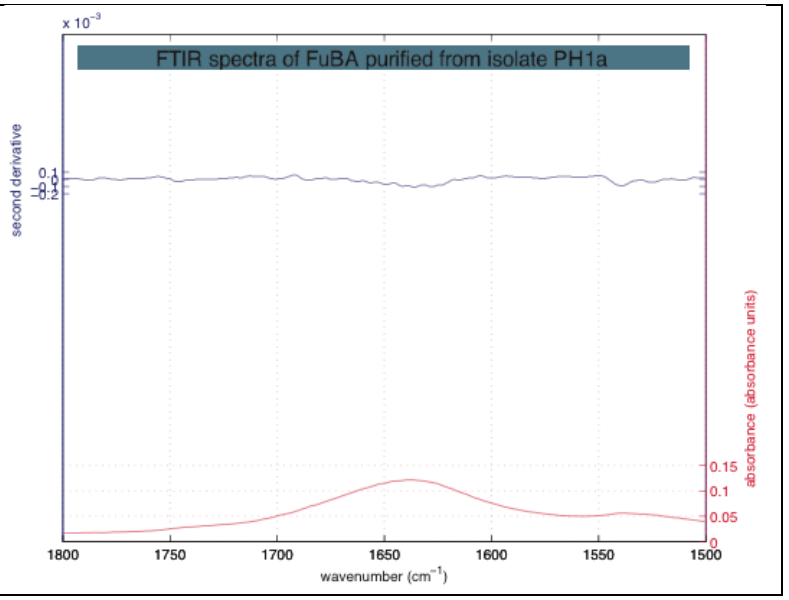
FTIR spectra of FuBA purified from isolate PH1a
second derivative
absorbance (absorbance units)
wavenumber (cm^{-1})

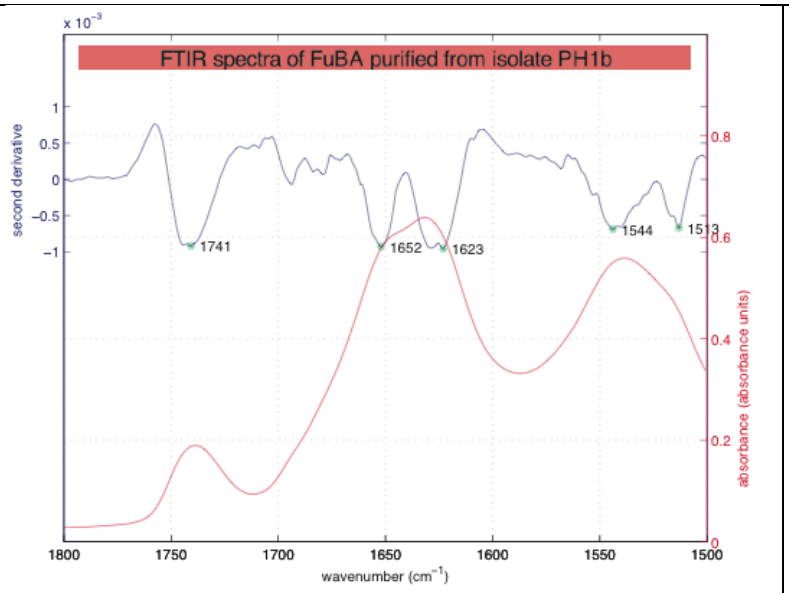
FTIR spectra of FuBA purified from isolate PH1b
x 10^-3
second derivative
absorbance (absorbance units)
wavenumber (cm^-1)
1741
1652
1623
1544
1513

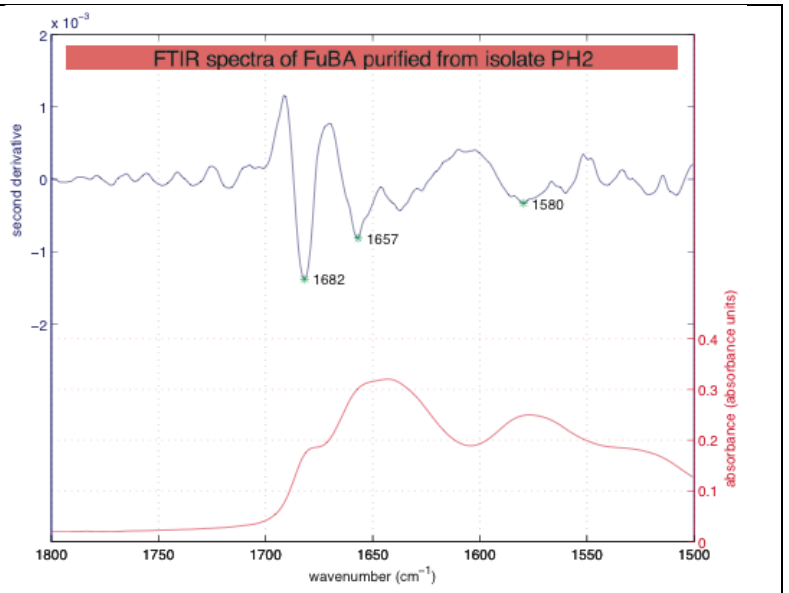
FTIR spectra of FuBA purified from isolate PH2
x 10^-3
second derivative
absorbance (absorbance units)
wavenumber (cm^-1)
1682
1657
1580

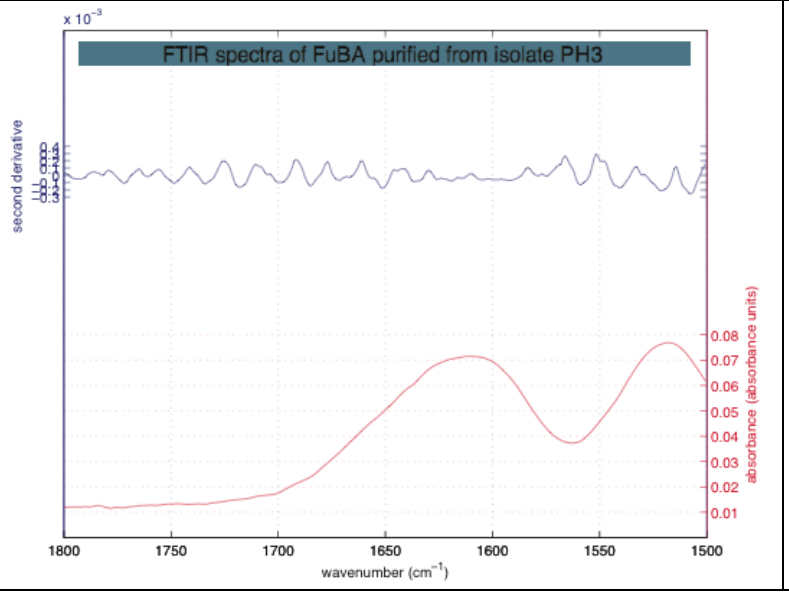
FTIR spectra of FuBA purified from isolate PH3
x 10^-3
second derivative
absorbance (absorbance units)
wavenumber (cm^-1)

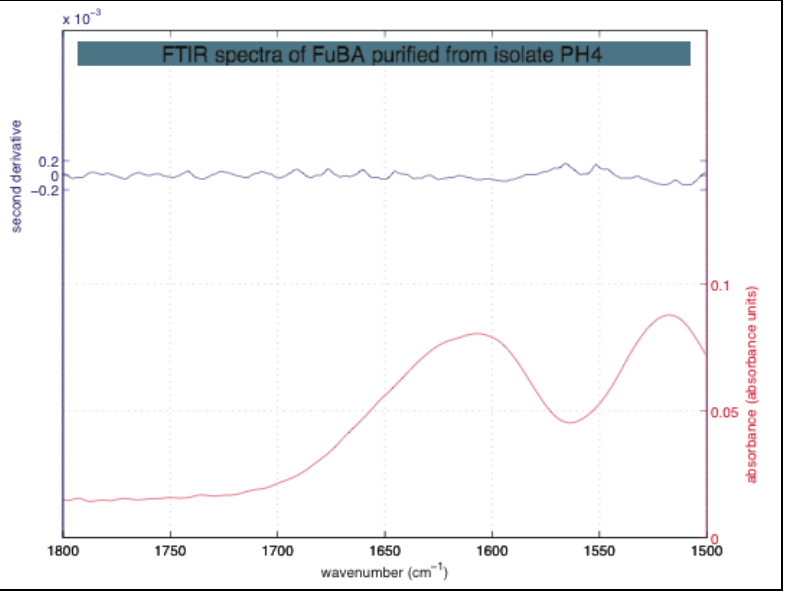
FTIR spectra of FuBA purified from isolate PH4
x 10^-3
second derivative
absorbance (absorbance units)
wavenumber (cm^-1)

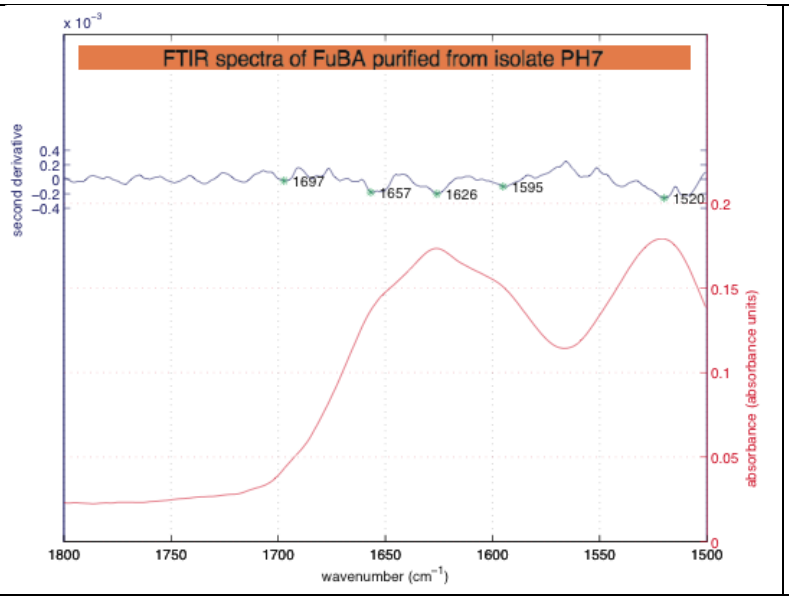
FTIR spectra of FuBA purified from isolate PH7
x 10^-3
second derivative
absorbance (absorbance units)
wavenumber (cm^-1)
1697
1657
1626
1595
1520

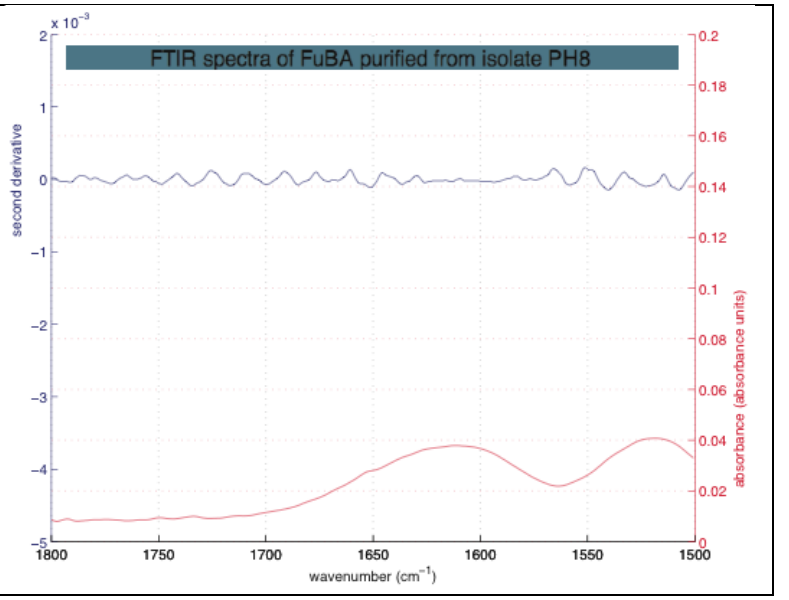
FTIR spectra of FuBA purified from isolate PH8
x 10^-3
second derivative
absorbance (absorbance units)
wavenumber (cm^-1)

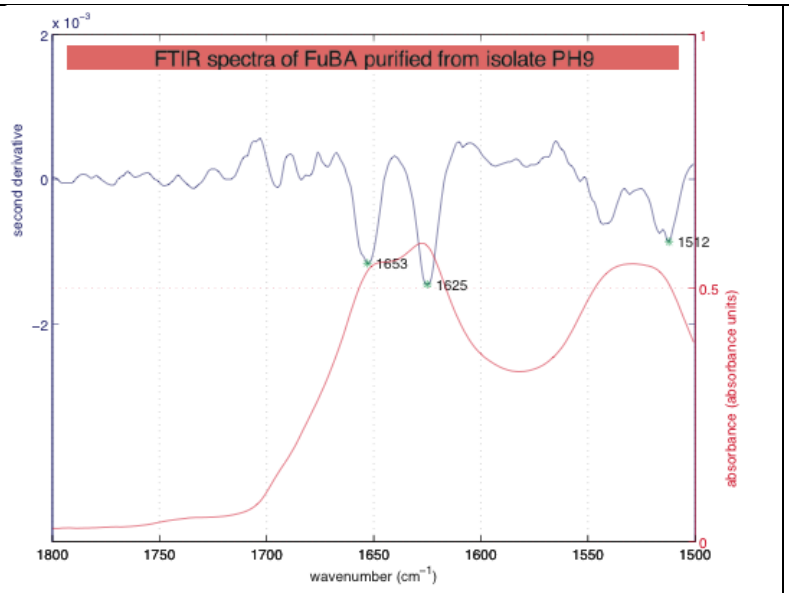
FTIR spectra of FuBA purified from isolate PH9
x 10^-3
second derivative
absorbance (absorbance units)
wavenumber (cm^-1)
1653
1625
1512

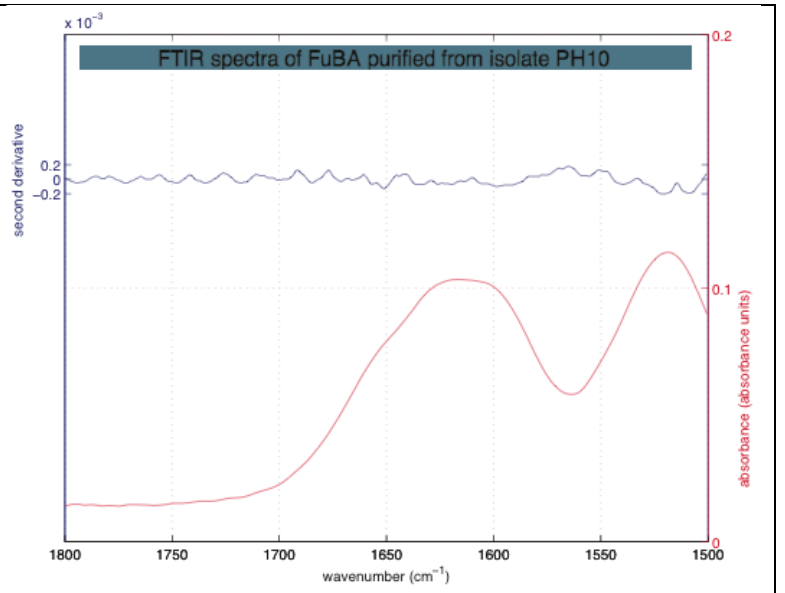
FTIR spectra of FuBA purified from isolate PH10
x 10^-3
second derivative
absorbance (absorbance units)
wavenumber (cm^-1)

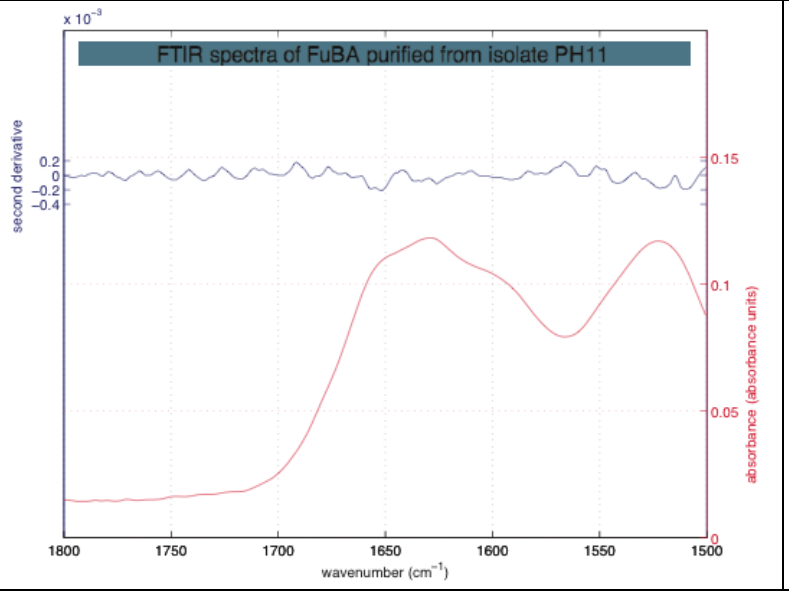
FTIR spectra of FuBA purified from isolate PH11
x 10^-3
second derivative
absorbance (absorbance units)
wavenumber (cm^-1)

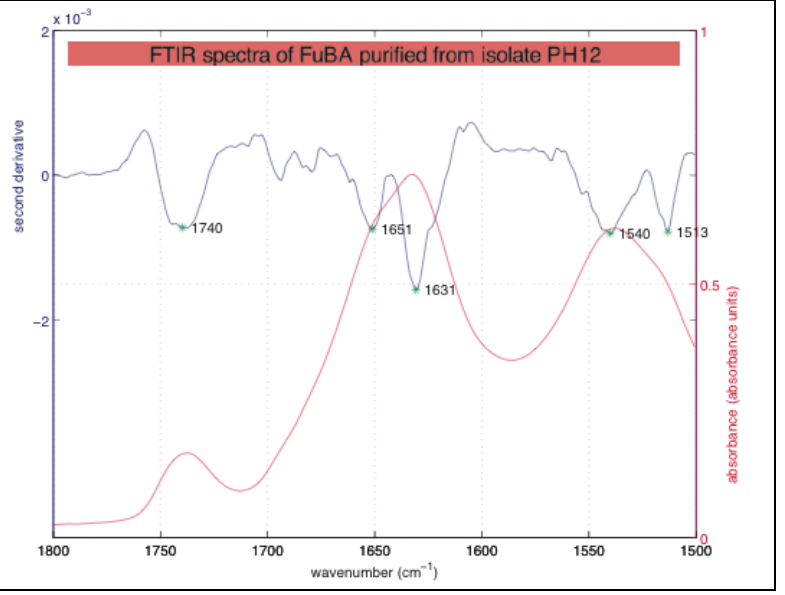
FTIR spectra of FuBA purified from isolate PH12
x 10^-3
second derivative
absorbance (absorbance units)
wavenumber (cm^-1)
1740
1651
1631
1540
1513

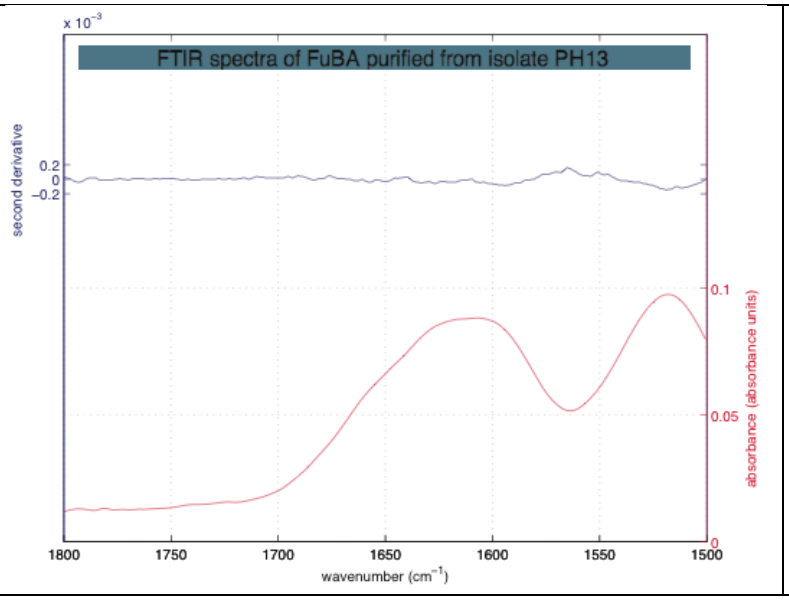
FTIR spectra of FuBA purified from isolate PH13
x 10^-3
second derivative
absorbance (absorbance units)
wavenumber (cm^-1)

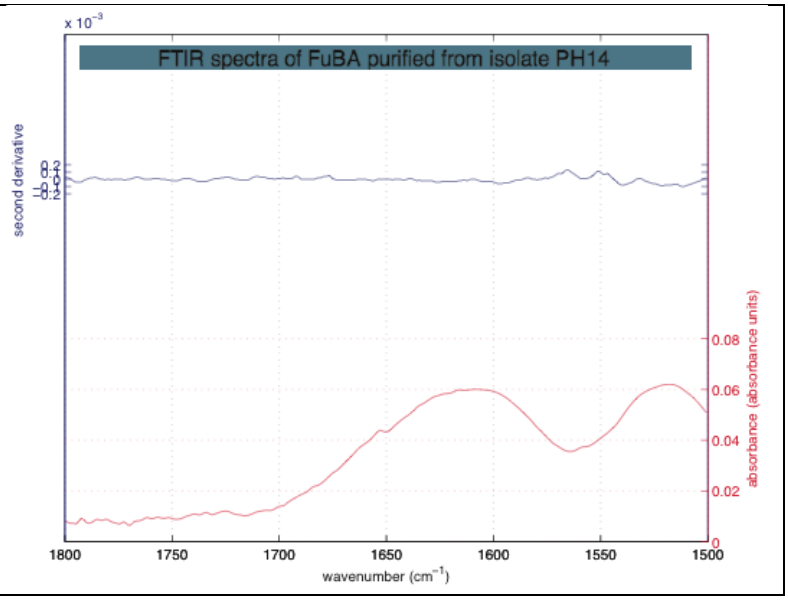
FTIR spectra of FuBA purified from isolate PH14
x 10^-3
second derivative
absorbance (absorbance units)
wavenumber (cm^-1)

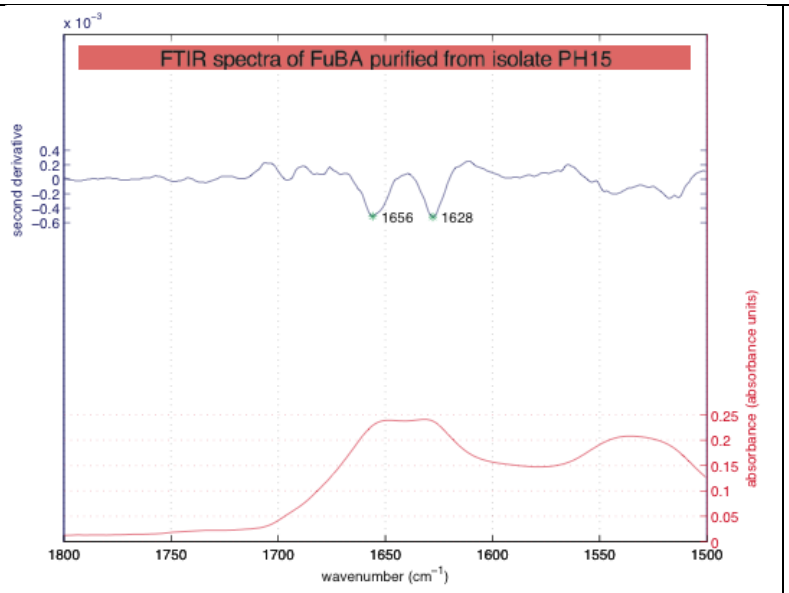
FTIR spectra of FuBA purified from isolate PH15
x 10^-3
second derivative
absorbance (absorbance units)
wavenumber (cm^-1)
1656
1628

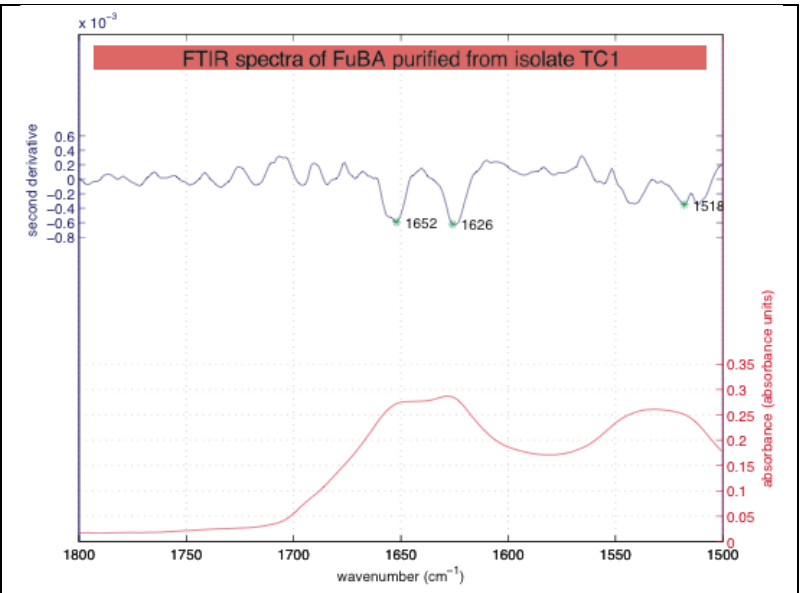
FTIR spectra of FuBA purified from isolate TC1
x 10^-3
second derivative
absorbance (absorbance units)
wavenumber (cm^-1)
1652
1626
1518

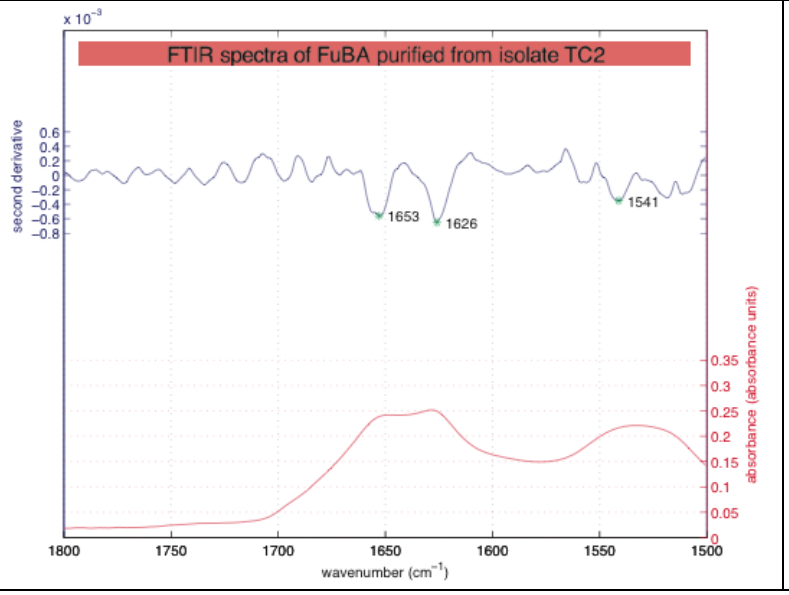
FTIR spectra of FuBA purified from isolate TC2
x 10^-3
second derivative
absorbance (absorbance units)
wavenumber (cm^-1)
1653
1626
1541

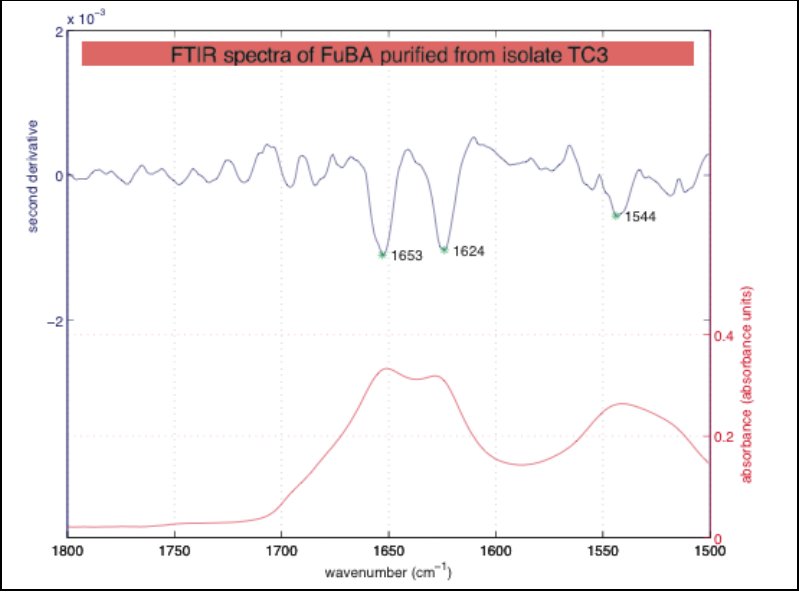
FTIR spectra of FuBA purified from isolate TC3
x 10^-3
second derivative
absorbance (absorbance units)
wavenumber (cm^-1)
1653
1624
1544

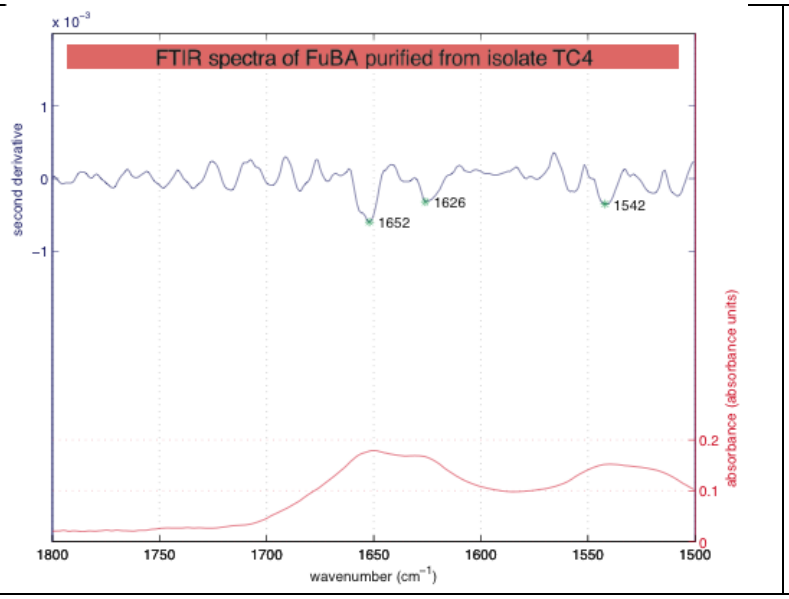
FTIR spectra of FuBA purified from isolate TC4
x 10^-3
second derivative
absorbance (absorbance units)
wavenumber (cm^-1)
1652
1626
1542

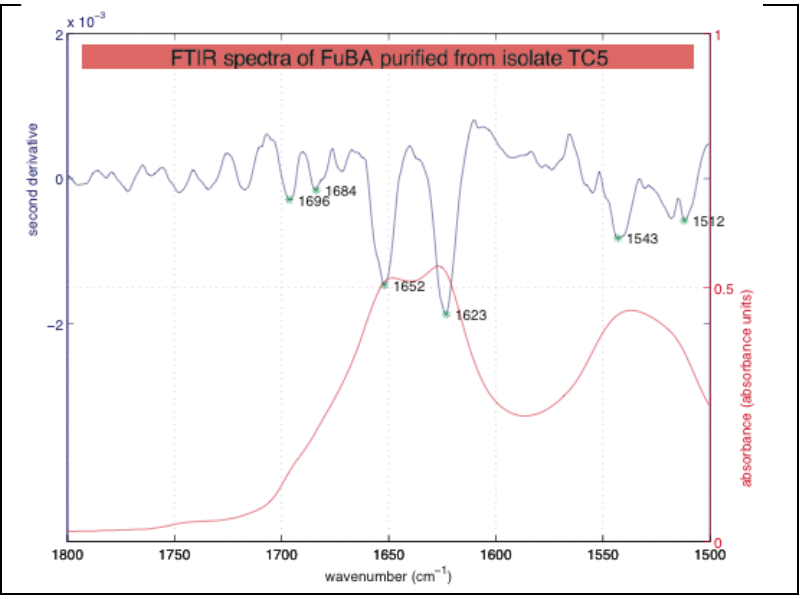
FTIR spectra of FuBA purified from isolate TC5
x 10^-3
second derivative
absorbance (absorbance units)
wavenumber (cm^-1)
1696
1684
1652
1623
1543
1512

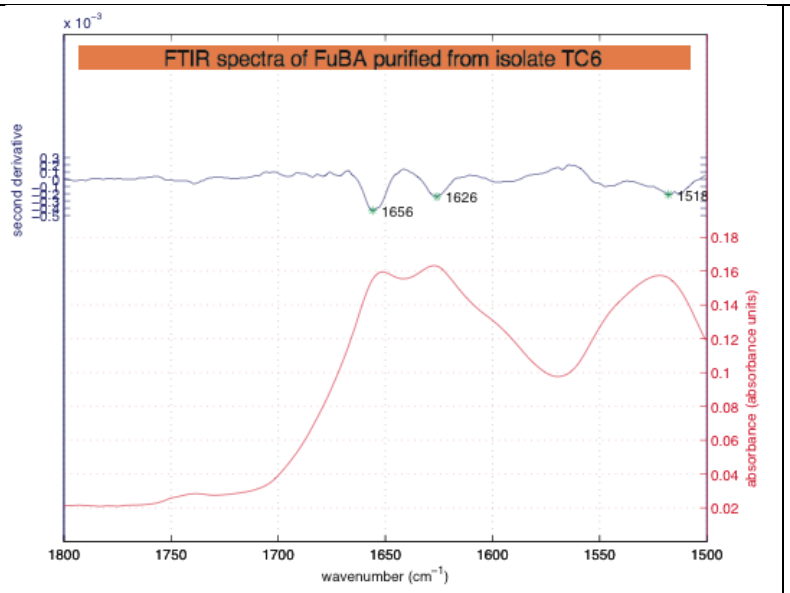

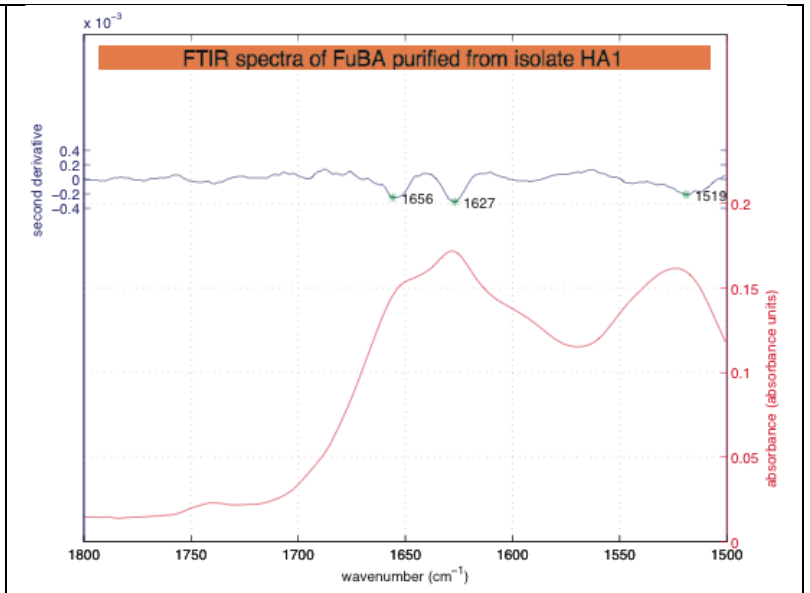

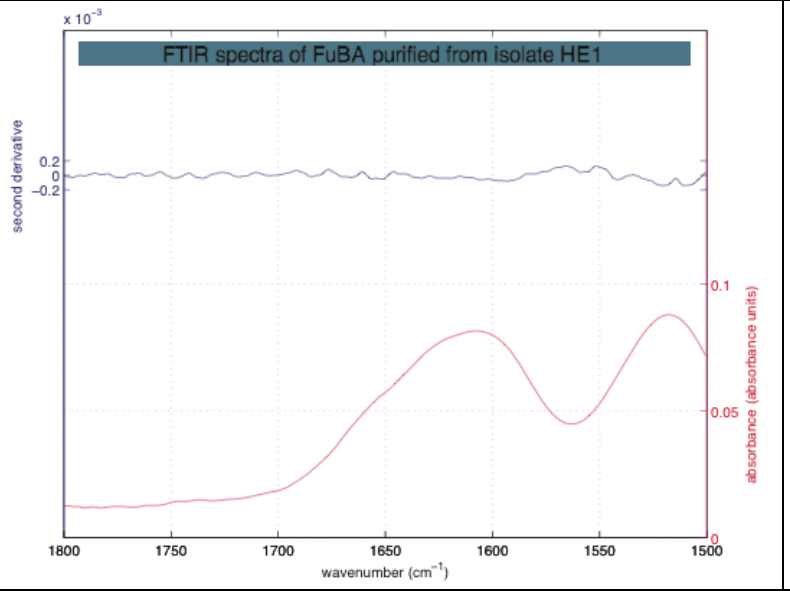

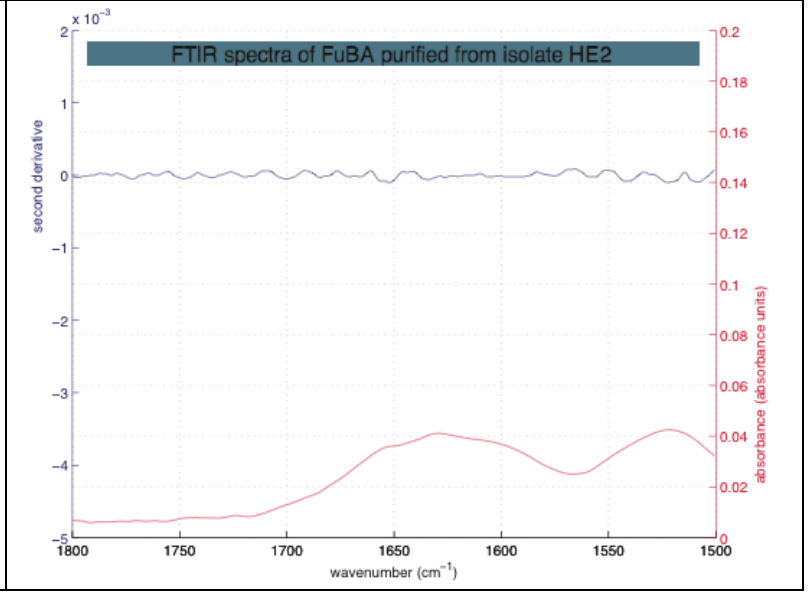

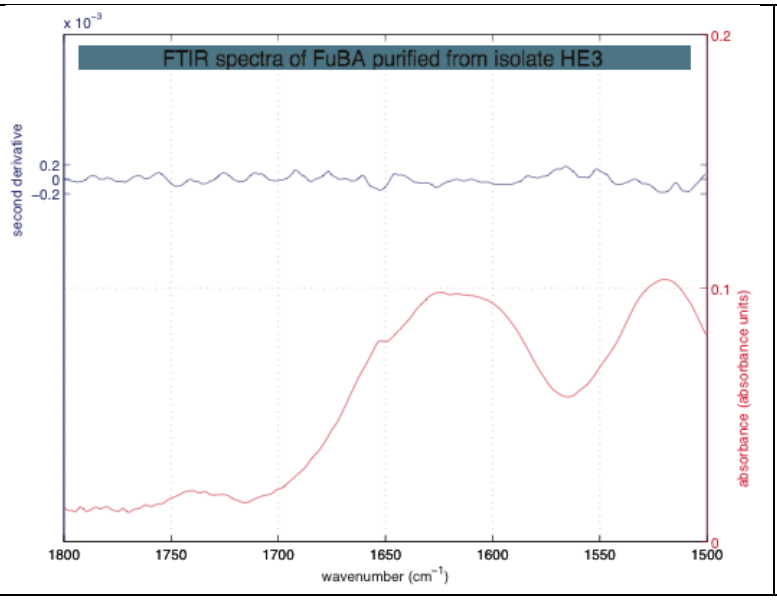

Fig. 18. Amide I region of the FTIR spectra of FuBA. The bacteria were grown on agar plates at 26°C for 4.5 days prior to FuBA purification. For SM2258 the absorbance peak position are found from local minima of the second dirivative, graphed in blue.

Bibliography

Alteri, C. et al., 2007. Mycobacterium tuberculosis produces pili during human infection. *PROCEEDINGS OF THE NATIONAL ACADEMY OF SCIENCES OF THE UNITED STATES OF*, 104(12), 5145-5150.

Arcos-Hernandez, M.V. et al., 2010. Rapid quantification of intracellular PHA using infrared spectroscopy: an application in mixed cultures. *Journal of Biotechnology*, 150(3), 372-379.

Austin, J. et al., 1998. Thin aggregative fimbriae enhance Salmonella enteritidis biofilm formation. *FEMS MICROBIOLOGY LETTERS*, 162(2), 295-301.

Bøgh-Sørensen, L., 2003. *Food preservation techniques*, Woodhead Publishing.

Cerf, E. et al., 2009. Antiparallel β-sheet: a signature structure of the oligomeric amyloid β-peptide. *Biochemical Journal*, 421(3), 415-423.

Chapman, M.R. et al., 2002. Role of Escherichia coli Curli Operons in Directing Amyloid Fiber Formation. *Science*, 295(5556), 851-855.

CHASSY, B. & GIUFFRIDA, A., 1980. METHOD FOR THE LYSIS OF GRAM-POSITIVE, ASPOROGENOUS BACTERIA WITH LYSOZYME. *APPLIED AND ENVIRONMENTAL MICROBIOLOGY*, 39(1), 153-158.

Cheatum, C.M., Tokmakoff, A. & Knoester, J., 2004. Signatures of β-sheet secondary structures in linear and two-dimensional infrared spectroscopy. *The Journal of Chemical Physics*, 120(17), 8201.

Claessen, D. et al., 2003. A novel class of secreted hydrophobic proteins is involved in aerial hyphae formation in Streptomyces coelicolor by forming amyloid-like fibrils. *GENES & DEVELOPMENT*, 17(14), 1714-1726.

COLLINSON, S. et al., 1991. PURIFICATION AND CHARACTERIZATION OF THIN, AGGREGATIVE FIMBRIAE FROM SALMONELLA-ENTERITIDIS. *JOURNAL OF BACTERIOLOGY*, 173(15), 4773-4781.

COLLINSON, S. et al., 1992. THIN AGGREGATIVE FIMBRIAE FROM DIARRHEAGENIC ESCHERICHIA-COLI. *JOURNAL OF BACTERIOLOGY*, 174(13), 4490-4495.

Costerton, J., Montanaro, L. & Arciola, C., 2005. Biofilm in implant infections: Its production and regulation. *INTERNATIONAL JOURNAL OF ARTIFICIAL ORGANS*, 28(11), 1062-1068.

Deckers, D. et al., 2004. Periplasmic lysozyme inhibitor contributes to lysozyme resistance in Escherichia coli. *CELLULAR AND MOLECULAR LIFE SCIENCES*, 61(10), 1229-1237.

Dueholm, M.S. et al., 2010. Functional amyloid in Pseudomonas. *Molecular Microbiology*, no-no.

Dueholm, M. et al., 2010. Functional amyloid in Pseudomonas. *MOLECULAR MICROBIOLOGY*, 77(4), 1009-1020.

Ezaki, T. & Suzuki, S., 1982. Achromopeptidase for lysis of anaerobic gram-positive cocci. *Journal of Clinical Microbiology*, 16(5), 844.

Fraser, P. et al., 1991. pH-dependent structural transitions of Alzheimer amyloid peptides. *Biophysical Journal*, 60(5), 1190-1201.

Gibson, H. et al., 1999. Effectiveness of cleaning techniques used in the food industry in terms of the removal of bacterial biofilms. *JOURNAL OF APPLIED MICROBIOLOGY*, 87(1), 41-48.

Gophna, U. et al., 2001. Curli fibers mediate internalization of Escherichia coli by eukaryotic cells. *INFECTION AND IMMUNITY*, 69(4), 2659-2665.

Gothwal, R.K. et al., 2007. Extraction of bulk DNA from Thar Desert soils for optimization of PCR-DGGE based microbial community analysis. *Electronic Journal of Biotechnology*, 10(3), 0-0.

Hammar, M. et al., 1995. Expression of two csg operons is required for production of fibronectin- and Congo red-binding curli polymers in Escherichia coli K-12. *MOLECULAR MICROBIOLOGY*, 18(4), 661-670.

Hammer, N., Schmidt, J. & Chapman, M., 2007. The curli nucleator protein, CsgB, contains an amyloidogenic domain that directs CsgA polymerization. *PROCEEDINGS OF THE NATIONAL ACADEMY OF SCIENCES OF THE UNITED STATES OF*, 104(30), 12494-12499.

Hammer, N. et al., 2008. Amyloids: Friend or foe? *JOURNAL OF ALZHEIMERS DISEASE*, 13(4), 407-419.

Hebert, L. et al., 2007. Enterococcus faecalis constitutes an unusual bacterial model in lysozyme resistance. *INFECTION AND IMMUNITY*, 75(11), 5390-5398.

Hori, R. & Sugiyama, J., 2003. A combined FT-IR microscopy and principal component analysis on softwood cell walls. *Carbohydrate Polymers*, 52(4), 449–453.

Hrncic, R. et al., 2000. Antibody-mediated resolution of light chain-associated amyloid deposits. *AMERICAN JOURNAL OF PATHOLOGY*, 157(4), 1239-1246.

Jackson, M. & Mantsch, H.H., 1995. The Use and Misuse of FTIR Spectroscopy in the Determination of Protein Structure. *Critical Reviews in Biochemistry and Molecular Biology*, 30(2), 95-120.

Jain, A. et al., 2007. Biofilms - A microbial life perspective: A critical review. *CRITICAL REVIEWS IN THERAPEUTIC DRUG CARRIER SYSTEMS*, 24(5), 393-443.

Jordal, P.B. et al., 2009. Widespread Abundance of Functional Bacterial Amyloid in Mycolata and Other Gram-Positive Bacteria. *Appl. Environ. Microbiol.*, 75(12), 4101-4110.

Kamnev, A., 2008. FTIR spectroscopic studies of bacterial cellular responses to environmental factors, plant-bacterial interactions and signalling. *SPECTROSCOPY-AN INTERNATIONAL JOURNAL*, 22(2-3), 83-95.

Kichise, T., Taguchi, S. & Doi, Y., 2002. Enhanced accumulation and changed monomer composition in polyhydroxyalkanoate (PHA) copolyester by in vitro evolution of Aeromonas caviae PHA synthase.

APPLIED AND ENVIRONMENTAL MICROBIOLOGY, 68(5), 2411-2419.

Kjellerup, B. et al., 2005. Microbial diversity in biofilms from corroding heating systems. *BIOFOULING*, 21(1), 19-29.

Kragelund, C. et al., 2007. Identity, abundance and ecophysiology of filamentous Chloroflexi species present in activated sludge treatment plants. *FEMS microbiology ecology*, 59(3), 671–682.

Laemmli, U.K., 1970. Cleavage of structural proteins during the assembly of the head of bacteriophage T4. *Nature*, 227(5259), 680-685.

Larsen, P. et al., 2008. Amyloid-like adhesins produced by floc-forming and filamentous bacteria in activated sludge. *APPLIED AND ENVIRONMENTAL MICROBIOLOGY*, 74(5), 1517-1526.

Larsen, P. et al., 2007. Amyloid adhesins are abundant in natural biofilms. *Environmental Microbiology*, 9(12), 3077-3090.

Legal, J.M., Manfait, M. & Theophanides, T., 1991. Applications of FTIR spectroscopy in structural studies of cells and bacteria. *Journal of Molecular Structure*, 242, 397-407.

Lens, P., Stoodley, P. & Mahony, T., 2003. *Biofilms in medicine, industry and environmental biotechnology: characteristics, analysis and control*, IWA Publishing.

López de la Paz, M. et al., 2002. De novo designed peptide-based amyloid fibrils. *Proceedings of the National Academy of Sciences of the United States of America*, 99(25), 16052 -16057.

Nilsson, M.R., 2004. Techniques to study amyloid fibril formation in vitro. *Methods*, 34(1), 151-160.

O'Nuallain, B. & Wetzel, R., 2002. Conformational Abs recognizing a generic amyloid fibril epitope. *PROCEEDINGS OF THE NATIONAL ACADEMY OF SCIENCES OF THE UNITED STATES OF*, 99(3), 1485-1490.

Olsen, A., Jonsson, A. & Normark, S., 1989. Fibronectin binding mediated by a novel class of surface organelles on Escherichia coll. *Nature*, 338(6217), 652-655.

Otzen, D. & Nielsen, P., 2008. We find them here, we find them there: Functional bacterial amyloid. *Cellular and Molecular Life Sciences*, 65(6), 910-927.

Otzen, D.E., 2002. Protein Unfolding in Detergents: Effect of Micelle Structure, Ionic Strength, pH, and Temperature. *Biophysical Journal*, 83(4), 2219-2230.

PACKER, E., INGRAHAM, J. & SCHER, S., 1965. FACTORS AFFECTING RATE OF KILLING OF ESCHERICHIA COLI BY REPEATED FREEZING AND THAWING. *JOURNAL OF BACTERIOLOGY*, 89(3), 718-&.

Prigent-Combaret, C. et al., 2001. Complex regulatory network controls initial adhesion and biofilm formation in Escherichia coli via regulation of the csgD gene. *JOURNAL OF BACTERIOLOGY*, 183(24), 7213-7223.

Prigent-Combaret, C. et al., 1999. Abiotic Surface Sensing and Biofilm-Dependent Regulation of Gene Expression in Escherichia coli. *J. Bacteriol.*, 181(19), 5993-6002.

Reddy, S. et al., 2008. Isolation of bacteria producing polyhydroxyalkanoates (PHA) from municipal sewage sludge. *WORLD JOURNAL OF MICROBIOLOGY & BIOTECHNOLOGY*, 24(12), 2949-2955.

Romero, D. et al., 2010. Amyloid fibers provide structural integrity to Bacillus subtilis biofilms. *Proceedings of the National Academy of Sciences*, 107(5), 2230-2234.

Ryu, J. & Beuchat, L., 2005. Biofilm formation by Escherichia coli O157 : H7 on stainless steel: Effect of exopolysaccharide and curli production on its resistance to chlorine. *APPLIED AND ENVIRONMENTAL MICROBIOLOGY*, 71(1), 247-254.

Schaudinn, C. et al., 2007. Bacterial biofilms, other structures seen as mainstream concepts. *MICROBE-AMERICAN SOCIETY FOR MICROBIOLOGY*, 2(5), 231.

Shewmaker, F. et al., 2009. The Functional Curli Amyloid Is Not Based on In-register Parallel β-Sheet Structure. , 284(37), 25065-25076.

Silverstein, A. et al., 2006. Biofilm formation on clinically noninfected penile prostheses. *JOURNAL OF UROLOGY*, 176(3), 1008-1011.

Sleight, S., Wigginton, N. & Lenski, R., 2006. Increased susceptibility to repeated freeze-thaw cycles in Escherichia coli following long-term evolution in a benign environment. *BMC EVOLUTIONARY BIOLOGY*, 6. Available at: http://apps.isiknowledge.com.zorac.aub.aau.dk/full_record.do?product=WOS&search_mode=GeneralSearch&qid=1&SID=S128IB2gOp5J1GhL9A8&page=1&doc=1 [Accessed December 2, 2010].

Uversky & Longhi, S., 2009. *Instrumental Analysis of Intrinsically Disordered Proteins: Assessing Structure and Conformation*, Wiley-Interscience.

Vidal, O. et al., 1998. Isolation of an Escherichia coli K-12 mutant strain able to form biofilms on inert surfaces: Involvement of a new ompR allele that increases curli expression. *JOURNAL OF BACTERIOLOGY*, 180(9), 2442-2449.

White, A.P. et al., 2001. Structure and characterization of AgfB from salmonella enteritidis thin aggregative fimbriae. *Journal of Molecular Biology*, 311(4), 735-749.

Xu, J. et al., 2002. In situ FTIR study on melting and crystallization of polyhydroxyalkanoates. *Polymer*, 43(25), 6893–6899.

Zandomeneghi, G. et al., 2004. FTIR reveals structural differences between native beta-sheet proteins and amyloid fibrils. *PROTEIN SCIENCE*, 13(12), 3314-3321.

Zandomeneghi, G. et al., 2004. FTIR reveals structural differences between native β-sheet proteins and amyloid fibrils. *Protein Science*, 13(12), 3314-3321.